

DEVELOPMENT OF PERMANENT CHEMICAL HYDROGEL FILMS BASED ON
CHITOSAN AND CARBOXY METHYL CELLULOSE FOR MOISTURE ABSORBING
PACKAGING FILMS



by
Hatice Semizer Aksoy

Submitted to Graduate School of Natural and Applied Sciences
in Partial Fulfillment of the Requirements
for the Degree of Doctor of Philosophy in
Chemical Engineering

Yeditepe University
2017

DEVELOPMENT OF PERMANENT CHEMICAL HYDROGEL FILMS BASED ON
CHITOSAN AND CARBOXY METHYL CELLULOSE FOR MOISTURE ABSORBING
PACKAGING FILMS

APPROVED BY:

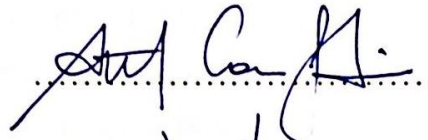
Assist. Prof. Dr. Erde Can
(Thesis Supervisor)



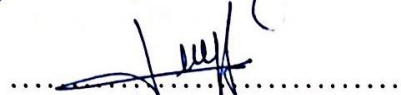
Dr. İbrahim Sani Özdemir
(Thesis Co-supervisor)



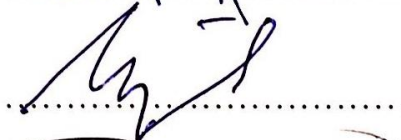
Prof. Dr. Atif Can Seydim



Prof. Dr. Duygu Avcı Semiz



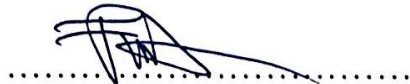
Prof. Dr. Mustafa Özilgen



Prof. Dr. Süheyla Uzman



Assist. Prof. Dr. Funda Oğuz



DATE OF APPROVAL:/...../2017

ACKNOWLEDGEMENTS

I would like to express my gratitude to my advisor Assist. Prof. Dr. Erde CAN for her guidance, technical support and helpful feedback during my dissertation. I would like to thank to my co-advisor Dr. İbrahim Sani ÖZDEMİR for his encouragement, technical and intellectual support throughout the toughest times during my dissertation.

I am very thankful to Assoc. Prof. Dr. Erdal ERTAŞ and Dr. Ferda SEYHAN, Dr. Mesude Banu BAHAR and Dr. Aytunga ARIK KİBAR from TUBITAK Marmara Research Center for their support during my studies.

I am deeply thankful to my dear family and my dear friends. Special thanks to my mother Aliye, my father Mithat and my sister Yelda for their support from so far away distances.

At last but not least, I express my endless appreciation to my husband Mesut AKSOY for his love, patient, support and encouragement at every time when I sink into despair and enlightening my way during this very long journey with his optimism.

ABSTRACT

DEVELOPMENT OF PERMANENT CHEMICAL HYDROGEL FILMS BASED ON CHITOSAN AND CARBOXY METHYL CELLULOSE FOR MOISTURE ABSORBING PACKAGING FILMS

Food waste is one of the world's most important problems. In medium and in high income countries, the highest amount of food waste occurs at household level. Dry foods, fresh fruits and vegetables are among the most wasted food products at household level. The main aim of this study is to develop biopolymer based chemical permanent hydrogel films which can be used as a moisture absorber/regulator in food packaging systems with an ultimate goal to prolong the shelf-life of products. In the first part of the study, semi-interpenetrating polymer network (Semi-IPNs) hydrogel films based on genipin crosslinked-chitosan (Ch) and sodium carboxymethyl cellulose (CMC) were prepared by solution-casting method. Swelling degree, thermal and mechanical properties, physical and chemical interactions within network of hydrogel films were characterized and the effect of addition of genipin on biodegradability of hydrogel films in compost environment was tested. Genipin cross-linking increased the tensile modulus, strength and thermal stability of the hydrogel films although decreased the swelling degree of the hydrogel films in water and reduced the biodegradation rate. The results indicated that the developed hydrogel films have a great potential for food packaging applications. In the second part of the study, hydrogel films were applied in food packaging systems and their efficacy in prolonging the secondary shelf-life of Turkish coffee, mushroom (*Agaricus bisporus*) and broccoli florets (*Brassica oleracea*) was investigated and performance of hydrogel films on absorbing/regulating the excessive moisture inside packaging atmosphere was studied. Sensorial quality, relative humidity within packaging atmosphere were followed for Turkish coffee stored at both room and refrigerator temperature and moisture loss behavior, microbial load, color and texture of the mushrooms and broccoli florets stored at 5°C and 25°C were analyzed. The results showed that hydrogel films can be effectively used as auxiliary packaging materials for regulating inside the packaging of high moisture containing foods which can help prolonging their shelf-life upon temperature fluctuations.

ÖZET

NEM TUTUCU AMBALAJ FİLMİ OLARAK KİTOZAN ve KARBOKSİMETİL SELÜLOZ BAZLI DAYANIKLI HİDROJEL FİLM GELİŞTİRİLMESİ

Gıda atıkları dünyanın en önemli sorunlarından biridir. Orta ve yüksek gelirli ülkelerde, en fazla gıda atıkları, gıda zinciri boyunca evsel tüketim aşamasında gerçekleşir. Evsel tüketim aşamasında en çok israf edilen gıda ürünleri kuru yiyecekler, taze meyve ve sebzelerdir. Bu araştırmanın temel amacı, ürünlerin raf ömrünü uzatmak üzere gıda ambalaj sistemlerinde nem tutucu / düzenleyici olarak kullanılabilen biyopolimer esaslı kimyasal sürekli hidrojel filmler geliştirmektir. Çalışmanın ilk bölümünde, çözelti dökme yöntemi ile genipin çapraz bağlı-çitozan (Ch) ve sodyum karboksimetil selüloz (NaCMC) bazlı yarı-interpenetre polimer ağı (Semi-IPNs) yapıda hidrojel filmleri hazırlandı. Şişme ve çözünme derecesi, termal ve mekanik özellikler, gelişmiş hidrojel film ağ yapısı içindeki fiziksel ve kimyasal etkileşimler karakterize edildi. Ek olarak, çapraz bağlayıcı olarak genipin eklenmesinin kitozan / CMC hidrojel filmlerinin kompost ortamında biyobozunurluğu üzerine etkisi analiz edildi. Genipin ile çapraz bağlama, sudaki hidrojel filmlerin şişme derecesinin ve biyobozunma hızının azalmasına neden olmuşken; hidrojel filmlerin gerilme modülünü, mukavemet ve termal kararlılığını arttırmıştır. Sonuçlar, kitozan ve karboksimetil selüloz esaslı geliştirilmiş hidrojel filmlerin gıda ambalajlama uygulamaları için büyük bir potansiyele sahip olduğunu ortaya koymuştur. Çalışmanın ikinci bölümünde, hidrojel filmler Türk kahvesi, mantar (*Agaricus bisporus*) ve brokoli çiçekleri (*Brassica oleracea*) üzerine uygulandı ve orta raf ömrünü uzatmada etkinlikleri araştırılıp, hidrojel filmlerin emici / ambalaj atmosferindeki aşırı nemi regüle etmesi üzerine çalışıldı. Türk kahvesi için duyu kalite, bağıl nem, ambalaj atmosferi, nem kaybı davranışları, mikrobiyal yük, mantar ve brokoli çiçeklerinin renkleri ve dokuları analiz edildi. Sonuçlar, hidrojel filmlerin, sıcaklık dalgalanmaları nedeniyle ürün üzerinde oluşabilecek su kondenzasyonunu engelleyip raf ömrünü uzatmaya yardımcı olabileceğini ve yüksek nem içeren gıdalardaki aşırı nemi regüle etmede yardımcı ambalajlama malzemesi olarak etkin bir şekilde kullanılabileceğini gösterdi.

TABLE OF CONTENTS

ACKNOWLEDGEMENTS.....	III
ABSTRACT.....	IV
ÖZET	V
LIST OF FIGURES	X
LIST OF TABLES.....	Xv
LIST OF SYMBOLS/ABBREVIATIONS.....	XVI
1. INTRODUCTION.....	1
2. THEORETICAL BACKGROUND	4
2.1. POLYMERS	4
2.1.1. Polymer Classification Based on Origin.....	4
2.1.2. Polymer Classification Based on Monomer Composition.....	5
2.1.3. Polymer Classification Based on Polymer Architecture.....	6
2.1.4. Polymer Classification Based on Reaction to Temperature	7
2.1.5. Thermal Transitions in Polymers.....	7
2.1.6. Mechanical Properties of Polymers	8
2.2. HYDROGELS.....	10
2.2.1. Classification of Hydrogels	10
2.2.2. Biopolymers for Forming Hydrogels.....	11
2.2.3. Chitosan	13
2.2.4. Sodium CarboxyMethyl Cellulose.....	15
2.2.5. Complexes of Chitosan and Sodium CarboxyMethyl Cellulose	16
2.3. FOOD WASTE	17
2.4. FOOD PACKAGING	18
2.4.1. Role of packaging	18
2.4.2. Types of food packaging materials and technologies.....	19
3. AIM OF THESIS.....	25
4. MATERIALS AND METHODS	27
4.1. CHEMICALS.....	27
4.1.1. Chemicals Used in Titration Experiments	27

4.1.2.	Chemicals Used in Preparation of Hydrogel Films	27
4.1.3.	Chemicals Used in Biodegradation Tests	27
4.1.4.	Chemicals Used in Packaging for High Moisture Foods.....	28
4.1.5.	Chemicals Used in Microbiological Tests	28
4.1.6.	Foods used in shelf-life studies.....	28
4.2.	METHODS	28
4.2.1.	Fourier Transform Infrared Spectroscopy (FT-IR).....	29
4.2.2.	Differential Scanning Calorimetry (DSC)	30
4.2.3.	Dynamic Mechanical Analysis (DMA)	31
4.2.4.	Thermal Gravimetric Analysis (TGA).....	31
4.2.5.	Biodegradability Tests	32
4.2.6.	Statistical Analysis.....	33
5.	EXPERIMENTAL STUDY	34
5.1.	TITRATION EXPERIMENTS FOR DETERMINATION OF THE OPTIMUM CMC / CH RATIO	34
5.2.	FILM PREPARATION.....	34
5.2.1.	Preparation of physical hydrogel films	34
5.2.2.	Preparation of chemically cross-linked hydrogel films	35
5.2.3.	Crosslinking evidences of hydrogel films	36
5.2.4.	Determination of swelling degree of the hydrogel films in water	36
5.3.	FT-IR SPECTROSCOPY	37
5.4.	DIFFERENTIAL SCANNING CALORIMETRY (DSC).....	37
5.5.	DYNAMIC MECHANICAL ANALYSIS (DMA)	37
5.6.	THERMAL GRAVIMETRIC ANALYSIS (TGA).....	37
5.7.	TENSILE TESTS.....	38
5.8.	BIODEGRADABILITY TESTS	38
5.8.1.	Total organic carbon analysis	38
5.8.2.	Preparation of controlled compost and sea sand.....	38
5.8.3.	Biodegradation Test by Microbial Oxidative Degradation Analyzer based on ISO 14885-2	40
5.9.	APPLICATIONS OF HYDROGELS IN FOOD PACKAGING	43
5.9.1.	Packaging for moisture sensitive dry foods: The case of Turkish coffee	43

5.9.2. Packaging for high moisture foods: The case of mushroom and broccoli.....	45
6. CHARACTERIZATION OF CHITOSAN-CARBOXYMETHYL CELLULOSE HYDROGEL FILMS AND THEIR PROPERTIES.....	52
6.1. DETERMINATION OF THE OPTIMUM CMC / CH RATIO	52
6.2. STRUCTURAL CHARACTERIZATION OF THE HYDROGEL FILMS BY FT-IR SPECTROSCOPY	53
6.3. CROSSLINKING EVIDENCES OF HYDROGEL FILMS	55
6.4. SWELLING DEGREE OF HYDROGEL FILMS IN WATER	56
6.5. DIFFERENTIAL SCANNING CALORIMETRIC (DSC) ANALYSIS.....	58
6.6. DYNAMIC MECHANICAL ANALYSIS (DMA)	59
6.7. THERMAL GRAVIMETRIC ANALYSIS (TGA).....	62
6.8. TENSILE TESTS.....	63
6.9. BIODEGRADABILITY	65
7. APPLICATIONS OF CHITOSAN-CARBOXYMETHYL CELLULOSE HYDROGEL FILMS IN FOOD PACKAGING	68
7.1. PACKAGING FOR MOISTURE SENSITIVE DRY FOODS: THE CASE OF TURKISH COFFEE.....	68
7.1.1. Relative Humidity.....	68
7.1.2. Sensorial Quality	69
7.2. PACKAGING FOR HIGH MOISTURE FOODS: THE CASE OF MUSHROOM AND BROCCOLI.....	74
7.2.1. Moisture loss behavior of mushrooms and broccoli florets.....	74
7.2.2. Moisture gain behavior of the cross-linked Ch-CMC hydrogel (Gnp-1)	77
7.2.3. Humidity regulation by the hydrogel (Gnp1) in package headspace at constant temperature	79
7.2.4. Humidity regulation with the hydrogel film (Gnp1) in package headspace at fluctuating temperatures	86
8. CONCLUSIONS AND RECOMMENDATIONS FOR FUTURE WORK	98
8.1. CONCLUSIONS.....	98
8.2. RECOMMENDATIONS FOR FUTURE WORK.....	100
REFERENCES	102

APPENDIX A.....118

APPENDIX B.....122

APPENDIX C.....126

APPENDIX D.....130

APPENDIX E.....132

APPENDIX F.....134

APPENDIX G.....129



LIST OF FIGURES

Figure 2.1. Ethylene (monomer) and polyethylene structure	5
Figure 2.2. Copolymer classification in terms of monomer arrangements.....	6
Figure 2.3. Representation of the stress-strain behaviour of plastics	9
Figure 2.4. Schematic of hydrogel classification	11
Figure 2.5. Chemical structure of chitosan	14
Figure 2.6. Chemical structure of sodium carboxymethyl cellulose	15
Figure 2.7. Physical interaction between chitosan and sodium carboxymethylcellulose	16
Figure 3.1. Representation of the Semi-IPN hydrogel structure	26
Figure 4.1. Schematic illustration of the FT-IR system	29
Figure 4.2. Schematic illustration of DSC system	30
Figure 4.3. Schematic illustration of a TGA system	32
Figure 4.4. Schematic of a MODA apparatus	33
Figure 5.1. Initial sizes of uncross-linked and genipin cross-linked hydrogel films	41
Figure 5.2. Uncross-linked, cross-linked hydrogel samples and cellulose powder in compost initially	41

Figure 5.3. Microbial oxidative degradation analyzer apparatus with samples.....	42
Figure 5.4. Lid of the metal cans with integrated hydrogel films, control coffee sample and coffee package with hydrogel film	45
Figure 5.5. Mushroom and broccoli placed in desiccator with desired RH and T	47
Figure 5.6. Hydrogel film and silica gels placed in dessicator with desired RH and T.....	48
Figure 5.7. Experimental set-up for humidity regulation experiments.....	49
Figure 5.8. Illustration of CIE L a b color space	51
Figure 6.1. Potentiometric and conductimetric titration curves for the titration of Ch (HCl) solution with CMC solution.....	53
Figure 6.2. FT-IR spectra of chitosan, Na-CMC, physical and chemical hydrogel films ...	55
Figure 6.3. Hydrogel film samples with ratios of genipin/chitosan of Gnp05, Gnp1, Gnp2 and Gnp3, w/w from left to right	56
Figure 6.4. Swelling degrees (%) of uncross-linked and cross-linked hydrogel films as a function of time.....	58
Figure 6.5. DSC thermograms for uncross-linked and cross-linked hydrogel films	59
Figure 6.6. Storage modulus (E') and tan delta variation with temperature for uncross-linked and cross-linked hydrogel films.....	61
Figure 6.7. TGA curves for uncross-linked and cross-linked hydrogel films	62
Figure 6.8. Tensile test results of uncross-linked and cross-linked hydrogel films presented in column graphs.....	64

Figure 6.9. Test materials in compost after 45 days uncross-linked film and genipin-crosslinked film.....	66
Figure 6.10. Cumulative CO ₂ evolution percentage biodegradation during 45 days.....	67
Figure 7.1. Relative humidity vs storage time plots of Turkish coffee at 5 °C and 25 °C ..	68
Figure 7.2. Odor parameters used in sensory evaluation	71
Figure 7.3. Aroma flavor parameters used in sensory evaluation	73
Figure 7.4. The change in the sensory scores for overall liking parameters for the coffees as a function of storage time.	74
Figure 7.5. Moisture loss of mushrooms within all the combinations of temperature and RH.	75
Figure 7.6. Moisture loss of broccoli florets within all the combinations of temperature and % RH.....	76
Figure 7.7. Changes in mass of mushrooms (W, mg) over time.	76
Figure 7.8. Changes in mass of broccoli (W, mg) over time	77
Figure 7.9. Moisture absorption behaviors of the Ch-CMC hydrogel film (Gnp1) and silica gel at different RH and temperatures.	78
Figure 7.10. The experimental set-up showing the mushrooms in control box with silica gel and hydrogel at the beginning and at the end of the storage at 5 °C	80
Figure 7.11. Headspace % RH and temperature versus storage time curves, measured in packages of mushrooms stored at 5 °C.....	81

Figure 7.12. The experimental set-up showing the mushrooms in control box with silica gel and hydrogel at the beginning and at the end of the storage at 25 °C	82
Figure 7.13. Headspace % RH and temperature versus storage time curves measured in packages of mushrooms stored at 25 °C.....	83
Figure 7.14. The experimental set-up showing the broccoli florets in control box with silica gel and hydrogel at the beginning and at the end of the storage at 5 °C.....	84
Figure 7.15. Headspace % RH and temperature versus storage time curves measured in packages of broccoli florets stored at 5 °C.	84
Figure 7.16. The experimental set-up showing the broccoli florets in control box with silica gel and hydrogel at the beginning and at the end of the storage at 25 °C.....	85
Figure 7.17. Headspace % RH and temperature versus storage time curves measured in packages of broccoli florets stored at 25 °C.	86
Figure 7.18. Headspace % RH and temperature versus storage time curves measured in the packages of mushrooms stored for 24 hours under fluctuating temperature regime.....	88
Figure 7.19. Appearance of the gills and the cap of mushrooms exposed to fluctuating temperatures after 1 day.....	89
Figure 7.20. Firmness values of the mushrooms exposed to fluctuating temperatures at the end of 24 hours	90
Figure 7.21. CIE L*a*b* color parameter values of the mushrooms exposed to fluctuating temperatures at the end of 24 hours	91
Figure 7.22. The total aerobic bacteria (TBC), yeast and mold load of the mushrooms exposed to fluctuating temperatures at the end of 24 hours..	92

Figure 7.23. Headspace % RH and temperature versus storage time curves measured in the packages of broccoli florets stored for 24 hours under fluctuating temperature regime	94
Figure 7.24. Appearance of broccoli florets exposed to fluctuating temperatures initially, in control package after 1 day in hydrogel package after 1 day	94
Figure 7.25. Firmness values of the broccoli florets exposed to fluctuating temperatures at the end of 24 hours.....	96
Figure 7.26. CIE L*a*b* color parameter values of the broccoli florets exposed to fluctuating temperatures at the end of 24 hours.	96
Figure 7.27. The total aerobic bacteria (TBC), yeast and mold load of the broccoli florets exposed to fluctuating temperatures at the end of 24 hours.	97

LIST OF TABLES

Table 5.1. Designations of prepared hydrogel films.....	35
Table 5.2. Properties of controlled compost.....	40
Table 5.3. Descriptors and definitions used by the trained sensory panel to describe the sensory properties of the Turkish coffee samples.....	44
Table 6.1. The swelling degree (%) of the hydrogel films in water at equilibrium after 210 minutes	58
Table 6.2. Storage modulus values at 25 °C and Tg values of hydrogel films as determined from DMA	61

LIST OF SYMBOLS/ABBREVIATIONS

C	Carbon
CO ₂	Carbon dioxide
C ₂ H ₄	Ethylene
CaO	Calcium oxide
E'	Storage modulus
E''	Loss modulus
HCl	Hydrochloric acid
H ₂ O ₂	Hydrogen peroxide
m ₁	Mass of empty holders
m ₂	Initial mass of holders with dry compost
m ₃	Mass of holders with saturated compost after vacuum filtration
m ₄	Mass of holders with dried compost at 105°C
M	Weight of sample at each time interval
M _i	Initial weight of each sample
M _w	Molecular weight
N	Nitrogen
O ₂	Oxygen
P	Phosphate
t	Time
T	Temperature
T _g	Glass transition temperature
W _i	Weight of the sample before swelling
W _s	Weight of the sample after swelling
ε	Strain
σ	Stress
AgNPs	Silver nanoparticles
Ch	Chitosan

CMC	Sodium carboxymethyl cellulose
CVS	Computer vision system
DMA	Dynamic mechanical analysis
DNA	Deoxyribonucleic acid
DRBC	Dichloran Rose Bengal Chloramphenicol
DSC	Differential scanning calorimetry
EB	Elongation at break
FAO	Food and Agriculture Organization of the United Nations
FT-IR	Fourier Transform Infrared Spectroscopy
Gnp	Genipin
GSE	Grapefruit seed extract
HA	Hyaluronic acid
HRP	Horseradish peroxidase
IEP	Isoelectric point
IPNs	Interpenetrating polymeric networks
MAP	Modified Atmosphere Packaging
MODA	Microbial Degradation Oxidative Analyzer
MRD	Maximum Recovery Diluent
NMR	Nuclear Magnetic Resonance
PCA	Plate Count Agar
PECs	Polyelectrolyte complexes
PNIPA	poly(N-isopropylacrylamide)
PPO	Polyphenol oxidase
PVA	Polyvinyl acetate
RH	Relative Humidity
Semi-IPNs	Semi- Interpenetrating polymeric networks
SIK	Swedish Institute for Food and Biotechnology
TBC	Total aerobic bacteria
TEOS	Tetraethoxy silane
TGA	Thermal gravimetric analysis
TM	Tensile modulus
TOC	Total organic carbon
TS	Tensile strength

TTI	Time-temperature indicators
TÜİK	Türkiye İstatistik Kurumu
WHC	Water Holding Capacity
XRD	X-Ray Diffraction



1. INTRODUCTION

Food waste is one of the world's most important problems. In medium and in high income countries, the highest amount of food waste occurs at household level all along the food chain [1]. Major part of these wastes is due to improper handling of foods which could not be consumed at once. Dry foods and fresh fruits and vegetables are among the most wasted food products at household level.

Due to their sensitivity to moisture, dry foods such as Turkish coffee, instant coffee, biscuits, nuts etc. are generally packed with packaging materials which have low permeability to oxygen and water vapor. As long as the package integrity is kept intact dry foods are generally considered as long shelf-life foods. However, as soon as the package is opened they get spoiled due to agglomeration, softening and/or loss of aroma as a result of increased moisture content. The increase in moisture content further triggers oxidative reactions which lead to the development of off-flavors and rancid taste. To absorb and/or control the excess moisture inside the food package, sachets containing silica gel, molecular sieves, calcium oxide (CaO) and natural clays (e.g. montmorillonite) are used such as MINIPAX®, STRIPPAX®, Desipak®, Sorb-it® etc. [2]. However, sachets can be accidentally consumed by infants. Besides, integration of these sachets inside the package is not practical due to their size and volume. Therefore the usage of these sachets in food industry is rather limited. As a result, packaging systems which can absorb the ingress moisture is needed in order to avoid the moisture uptake and related spoilage reactions in dry foods during multiple serving at home.

Different from other food products fresh fruits and vegetables are living organisms since major metabolic reactions continue even after harvest. The energy needed to fuel the metabolic activity is supplied from sugars and organic acids via respiration. Therefore, in order to keep produces fresh for longer periods the respiration rate should be slowed down. By this way the energy reserves which are limited with the amount present at harvest will be consumed for longer periods. However, the freshness of the fruits and vegetables also depend on the relative humidity of the surrounding atmosphere. Most of the fruits and vegetables contain high amount of water (75-95 %) and when the relative humidity of the surrounding atmosphere is lower than the moisture of the fruits and vegetables they tend to loose

moisture. As a result, they shriveled which negatively affect the consumer appeal. Therefore, for the preservation of fruit and vegetables the common strategy applied is to keep them at low temperature and high humidity environment. For this purpose fruit and vegetables are transported and stored at low temperatures all along the supply chain and packed with permeable packaging materials in order to limit moisture loss. However, during the supply chain at several points' cold chain can be interrupted and fruit and vegetables are exposed to high temperatures. These fluctuations in temperatures may result in water condensation on the inner surface of the package and on the product itself. This situation increases the risk of microbial spoilage as well. Since fruit and vegetables are in contact with soil and organic fertilizers in the field they are usually highly contaminated with soil born spoilage bacteria and fungi. Therefore, water condensation on the product and possible nutrient leakage from the injured fruit and vegetables provides spoilage microorganisms with favorable growth conditions. As a result, these microorganisms can rapidly proliferate and deteriorate the fruit and vegetable. Therefore in fruit and vegetable preservation the humidity inside the package should be controlled at an optimum level in order to compromise between condensation and wilting. In current practice, packaging materials which have macro or micro perforations are used for humidity control inside the fruit and vegetable packages. However, if not optimized well, there still exist a risk of humidity build up which can lead to condensation or, inversely, excessive moisture loss which can result in shriveling of the produce. In a recent application Rux et al., (2016) incorporated water absorbing salts into plastic trays with an ultimate aim of regulating the humidity inside the package. In this quoted study authors were successful in maintaining optimum relative humidity levels inside tomato packaging without giving rise to water condensation or excessive wilting of the produces [3].

Chitosan is a linear polysaccharide derived from deacetylation of chitin. It is one of the mostly used biopolymers in hydrogel preparation. Chitin, poly (β -(1-4)-N-acetyl-D-glucosamine), is known as the second abundant biopolymer in nature after cellulose. Chitosan has a wide range of application areas such as medical, environmental, agricultural, food, drug, and cosmetic fields due to its hydrophilic nature, antimicrobial properties, biodegradability and biocompatibility [4]. These properties make chitosan quite attractive and preferable material in hydrogel preparation. Carboxymethyl cellulose (CMC) is a derivative of cellulose which is also known as the most abundant biopolymer in nature. It is a significant natural biopolymer with which chitosan based hydrogels are prepared.

Availability, and high hydrophilicity make the usage of these two biopolymers together attractive. Genipin is a natural crosslinking agent which has a good ability to crosslink primary amino groups of chitosan and proteins. Genipin is commonly used in just East Asia countries such as Japan and Korea for food and medicinal ingredient. Some studies showed that it has less cytotoxicity compared to the glutaraldehyde which is one of the mostly used agent to crosslink chitosan [5,6]. Sung et al. have reported a study on cytotoxicity evaluation of genipin for biological tissue and concluded that cytotoxicity of genipin was dramatically lower than glutaraldehyde [6]. These qualities make genipin very attractive to be used as a cross linker in food packaging applications.

In order to overcome the above mentioned risks associated to conventional packaging materials for dry and high moisture containing foods, hydrogel films based on natural and biodegradable polymers having capability to absorb moisture seems as an alternative packaging system. Thus, in this study, semi-interpenetrating polymer network (Semi-IPNs) hydrogel films based on genipin crosslinked-chitosan (Ch) and sodium carboxymethyl cellulose (CMC) will be prepared by solution-casting method. Swelling degree, thermal and mechanical properties, physical and chemical interactions within network of developed hydrogel films will be characterized and their applications in packaging of Turkish coffee, mushroom (*Agaricus bisporus*) and broccoli florets (*Brassica oleracea*) will be investigated. In this system, the crosslinked chitosan network structure will result in a permanent, stable hydrogel and will improve the mechanical and thermal resistance of the final hydrogel films and CMC will also increase the water absorbing capacity of the developed semi-interpenetrating polymer network hydrogel films due to its hydrophilic nature. In addition, the packaging system is also expected to be safe for both human health and environment.

2. THEORETICAL BACKGROUND

2.1. POLYMERS

Poly and *mers* have meanings of *many* and *parts* in ancient Greek words, respectively. A polymer is known as a long chain molecule which is represented by a large number of repeating units. These repeating units are connected to each other by covalent bonds. In literature, polymers can be classified based on some different criteria. Generally used classification parameters to characterize polymers are their origin, monomer composition, polymer architecture and reaction to temperature [7].

2.1.1. Polymer Classification Based on Origin

2.1.1.1. *Natural Polymers*

Polymers found in plants or animals are called as natural polymers or biopolymers. Natural polymers are derived from sources available in nature. They can be extracted from plants or derived from shells or skeleton of animals. Polyschaccarides, proteins, nucleic acids are known as natural polymers. Cellulose, chitin, shellac, starch, silk, woll, proteins, deoxyribonucleic acid (DNA), gelatin are very common examples of natural polymers [7].

2.1.1.2. *Synthetic Polymers*

Synthetic polymers are known as man-made polymers. These kind of polymers are synthesized by using different polymerization techniques. Plastics, synthetic rubber or synthetic fibers are the widely used synthetic polymers. Nylon, polyethylene, polypropylene, polystyrene, polyvinyl chloride, bakelite are common examples of synthetic polymers [7].

2.1.2. Polymer Classification Based on Monomer Composition

2.1.2.1. Homopolymers

Mono and *mers* have meanings of *one* and *parts* in ancient Greek words, respectively. Monomers are the main building blocks of polymers. Monomer units can be linked to each other via polymerization to form polymers. Polymers are synthesized by polymerization of a single monomeric repeating unit are called homopolymers. Homopolymers has only one type of repeating unit in their chains. As an example, polyethylene is a homopolymer derived from polymerization of two or more “ethylene” monomeric units [7,8].

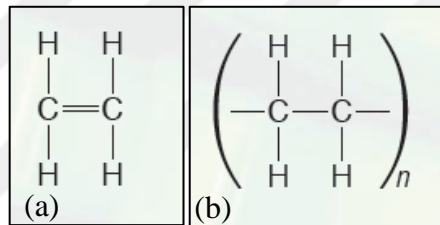


Figure 2.1. (a) Ethylene (monomer) and (b) polyethylene structure [8]

2.1.2.2. Copolymers

Polymers synthesized by polymerization of two different monomeric repeating units are called copolymers. In copolymers, two different type of repeating units are joined in the same polymer chain. Copolymers are classified in terms of the monomer arrangement in the polymer chain. In alternating copolymers, two monomers are arranged in alternating sequence. In block copolymers, each type of monomer is grouped together and two segments of pure homosequences are consisted. When monomers are arranged randomly, copolymers are called as random copolymers. In graft copolymers, polymer side chains of one repeating unit are grafted to another repeating unit on a linear backbone [7,8]. Figure 2.2 depicts the copolymer classification in terms of monomer arrangements.

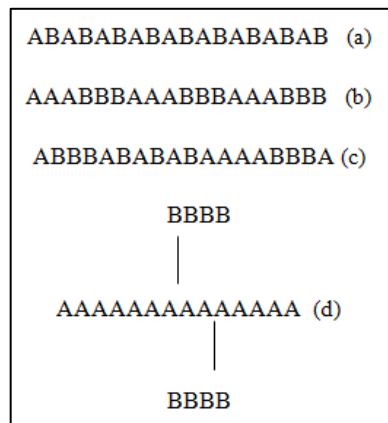


Figure 2.2. A and B are any monomers. (a) Alternating copolymer, (b) Block copolymers, (c) Random copolymer and (d) Graft copolymer [8]

2.1.3. Polymer Classification Based on Polymer Architecture

2.1.3.1. Linear Polymers

In linear polymers, monomeric units are linked to each other to form a linear chain without any branching. Linear polymers are regularly packed and exhibit high density, high tensile strength and high melting point properties. Polyvinyl acetate (PVA), polystyrenes are common examples of linear polymers [9].

2.1.3.2. Branched Polymers

In branched polymers, monomeric units are linked to each other to form a linear chain with side branched chains. Branched polymers are irregularly packed and exhibit lower density, lower tensile strength and lower melting point properties compared to linear polymers. Low density polyethylene and glycogene are examples of branched polymers [9].

2.1.3.3. Crosslinked Polymers

In crosslinked polymers, monomeric units are chemically linked to each other to form a three dimensional network structure. Crosslinked polymers have a higher melting point, and

are harder and more brittle compared to linear and branched polymers. Bakelite, formaldehyde, and epoxy resins are common examples of crosslinked polymers [9].

2.1.4. Polymer Classification Based on Reaction to Temperature

2.1.4.1. Thermoplastics

Thermoplastics are known as thermosoftening plastics which means that they can be thermally processed. Thermoplastics can be melted and made to flow and easily molded in desired shapes when heated. The reheating, recooling and reshaping cycle can be repeated many times without losing their properties. Polypropylene, polyethylene, polyvinylchloride, polystyrene, polyethylenetheraphthalate and polycarbonate are common thermoplastics [7].

2.1.4.2. Thermosets

Thermoset plastics are vulcanized, cured or hardened into desired shapes under temperature and pressure. Vulcanization and curing are chemical processes in which permanent crosslinked bridges are constructed between chains of molecules resulting in a three dimensional network. Thermosetting plastics hold their shape even though heated. Thermoset plastics are more stable and durable than thermoplastics because of crosslinking throughout polymeric chains. Due to its chemical resistance, durability, mechanical strength, hardness and thermal stability, thermoset plastics find a wide range of application areas. Epoxies, phenolic resins and vulcanized rubber are examples of thermosetting polymers widely used in industry [7].

2.1.5. Thermal Transitions in Polymers

2.1.5.1. Crystallization

Crystallization is a process of partial alignment of molecular chains of polymers. Polymers can be cooled from melt, can be exposed to mechanical stretching or solvent evaporation

may be carried out under certain conditions which would result in a regular crystalline structure. Generally, polymers can only produce partially crystalline structures, and therefore are called as semicrystalline. Degree of crystallinity of a polymer can range between 10% and 80% and be evaluated by different techniques such as Nuclear Magnetic Resonance (NMR), X-Ray Diffraction (XRD), Differential Scanning Calorimetry (DSC) etc. There are both so many factors affecting the morphology of crystals and degree of crystallinity of a polymeric material, such as crystallization temperature, polymer type and structure, cooling rate etc. Polymers which show high degree of crystallinity have higher glass transition temperatures, and exhibit higher mechanical strength and brittleness [10].

2.1.5.2. Melting

Melting temperature which is a first order transition temperature is the temperature where phase transition occurs from crystalline state to liquid amorphous state. Around the melting point T_m , chains or side groups on the polymer backbone undergoes short range movements freely. Melting temperature is a specific property for crystalline polymers [10].

2.1.5.3. Glass Transition

Glass transition temperature is the temperature where transition occurs from glassy state to rubbery state. Glass transition temperature (T_g) is a specific property for amorphous polymers. Below T_g , polymers are brittle, hard and stiff. Polymers get more flexible and softer in rubbery state and become subjected to creep, above T_g . T_g of a polymeric material appears below its melting point, T_m [10].

2.1.6. Mechanical Properties of Polymers

Polymers are generally characterized as viscoelastic materials, which exhibit both elastic solid and viscous liquid characteristics. A polymer does not behave like a totally elastic solid or a totally viscous liquid. Polymers show different responses resulting in different deformations under loading [11].

For defining mechanical properties of polymeric materials, there are several important terms that must be defined. Stress (σ) is described as the applied force per unit cross-sectional area of a polymeric material. The measure of the deformation per unit length after the application of stress is called as strain (ϵ). Mechanical properties involve the strength, brittleness, softness, stiffness etc. of a polymeric material.

A stress-strain curve gives very important information about the mechanical behavior of a polymeric material. Tensile strength which is the ability of withstanding of a material to the applied force, is a measure of strength. There are some factors affecting the strength of a polymer. For instance, strength of a material rises with increase in molecular weight, crystallinity and crosslinking. Young's modulus is the measure of stiffness of a polymeric material. It is defined as the ratio of stress to the strain. Increase in Young's modulus rises the rigidity of polymeric material. Elongation at break is the strain at the moment of rupture. It is expressed as percentage change in the length of the material. Elongation at break can be defined as the measure of elasticity of a polymeric material. The general stress strain behavior of different types of polymeric materials are depicted in Figure 2.3.

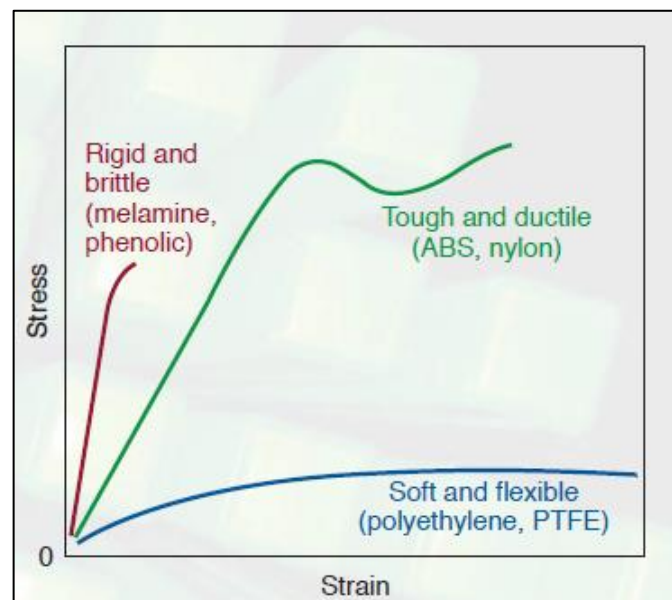


Figure 2.3. Representation of the stress-strain behaviour of plastics [12]

2.2. HYDROGELS

Hydrogels are crosslinked and 3D polymeric networks which can absorb 1000 times greater than their dry weight without disintegrating [13, 14]. Hydrogels can be prepared by using synthetic or natural polymers. The first synthetic hydrogel was synthesized by Czech chemists, Otto Wichterle and Drahoslava to use in contact lens production. Hydrogels are investigated in different research areas because of ability to absorb water, their soft and elastic structure.

Hydrogels receive considerable attentions in biomedical field due to their sensitivity to environmental parameters such as temperature, pH and ionic strength, concentration, electrical field etc. [15]. They have a very wide range of application areas such as controlled drug delivery systems [16], tissue engineering [17], wound healing [18], biosensor [19], and enzyme immobilization [20]. Additionally, hydrogels are preferred as water absorbers [21] and used in controlled fertilizer delivery [22] in agricultural fields. Some applications exist in textile areas to remove heavy metals, inorganic anions, textile dye and metal ions from waste water [23, 24].

2.2.1. Classification of Hydrogels

In literature, hydrogels can be classified based on some different criteria such as their origin, response characteristics, degradability, physical properties, ionic charges or preparation techniques. The other generally used classification parameter to characterize hydrogels is crosslinking.

2.2.1.1. Physical Hydrogels

In physical hydrogels polymeric units can be held together by electrostatic interactions between oppositely charged groups. The network in physical hydrogels consists of molecular entanglements, and / or secondary forces including ionic, hydrogen bonding or hydrophobic interactions. They are also called as reversible hydrogels as a result of disruption caused by changes in physical conditions [25, 26].

2.2.1.2. Chemical Hydrogels

In chemical hydrogels, the networks are held together by covalent bonds. Thus the network is attained by using a cross-linker. The chemical hydrogels are also called as permanent hydrogels.

2.2.1.3. Interpenetrating Polymer Network

There is another polymeric network structure in hydrogels, interpenetrating polymeric networks (IPNs). IPNs are the blends of at least two crosslinked polymeric networks which own their specific properties. Semi-Interpenetrating polymeric networks (Semi-IPNs) include a crosslinked polymeric network and a guest polymer chain [25, 26]. A schematic of hydrogel classification is depicted in Figure 2.4.

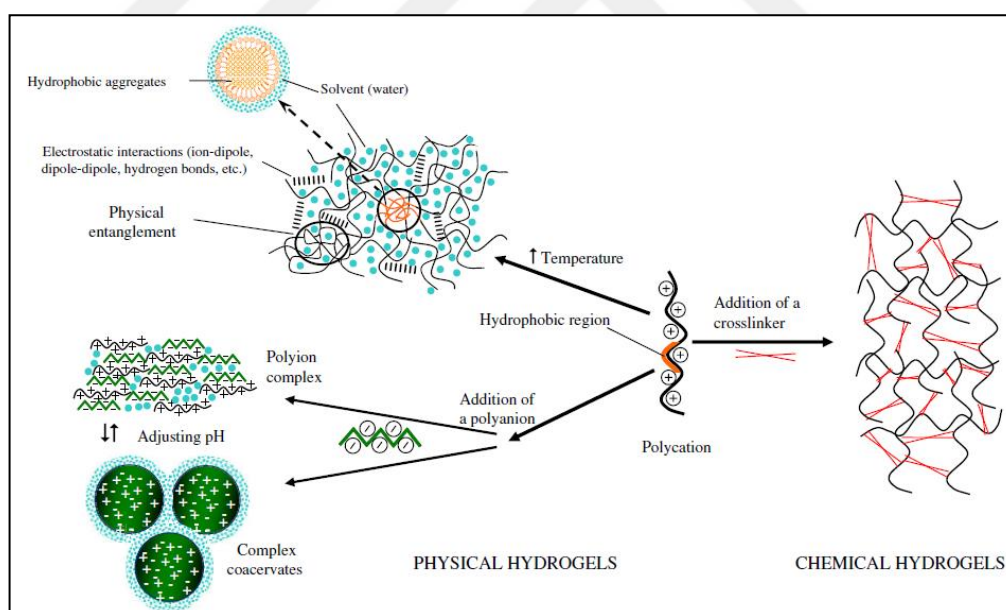


Figure 2.4. Schematic of hydrogel classification [25]

2.2.2. Biopolymers for Forming Hydrogels

Polyelectrolyte complexes (PECs) are formed by interactions between oppositely charged polyelectrolytes in the solution [27]. Polysaccharides and proteins are the mostly widely

used pairs for hydrogel preparation. The electrostatic interaction or repulsion between -COOH group on the polysaccharide and -NH₃⁺, -COOH groups on the protein chain are reversible but strong associations. Besides, interactions between two biopolymers comprises hydrogen and hydrophobic bonds [25]. There are so many parameters which affect the stability of PECs including density of charges, degree of ionization, pH of reaction medium, concentration of polyelectrolytes, distribution of ionic groups, molecular weight, mixing ratio, order of reacting polyelectrolytes etc. [27]. Among polysaccharides, hyaluronic acid, alginate, chitosan and cellulose derivatives and among proteins, alginate, collagen, gelatin and elastine are particularly attractive biopolymers for forming hydrogels which have found extensive applications in biomedical field [28].

Hyaluronic acid (HA) is a linear polysaccharide composed of alternating units of glucuronic acid and N-acetylglucosamine units. HA is one of the major fragments of different tissues of living organisms such as extracellular matrix of skin, cartilage, and the vitreous humor. Due to its biocompatible, biodegradable, non-immunogenic and non-toxic properties, it has a great potential in biomedical applications [29]. HA has carboxyl groups on the backbone which results in the negative charge of HA, thus enables it to get in contact with positively charged ions. Moreover, HA is a very promising material in order to get hydrogels exhibiting required morphology, stiffness and bioactivity [30]. Polyelectrolyte complexes of HA with the positively charged biopolymers have been extensively studied.

One of the mostly preferable polysaccharide based biopolymer used in hydrogel preparation is alginate. Alginate is also a linear and hydrophilic polysaccharide derived from brown seaweeds and brown algae consisting of alternating β -D-mannuronic acid and R-L-guluronic acid units. Alginate has carboxylic acid groups on the backbone which attributes negatively charges, and thus increasing its affinity to positively charged ions to form gels [31, 32].

Moreover, alginate has been demonstrated as a mucoadhesive, biocompatible, nonimmunogenic and easily chemically modified material [29, 33]. Alginate is one of the attractive biopolymers to construct hydrogel systems.

Gelatin is another biopolymer used in preparation of hydrogels among proteins. Gelatin is a biodegradable protein based biopolymer derived from from acidic or basic hydrolysis of collagen. Difference in origin and isolation methods results in two different types of gelatin, cationic gelatin with an isoelectric point (IEP) of 9 (Gelatin A) or anionic gelatin with an

IEP of 5 (Gelatin B) [29]. Due to its unique feature, gelatin is used in a wide variety of applications, ranging from food-related over pharmaceutical and photographic to technical products. In biomedical application gelatin is generally crosslinked by using different crosslinking agents to avoid dissolution at body temperature because it has a solgel transition temperature around 30° C [28]. Gelatin based hydrogels has a wide range of potential application areas within biomedical [25, 34-36] and food packaging industry [37-39].

Pectin is a linear polysaccharide consisting of D-galacturonic acid units linked by α -1,4-glycosidic bond and generally isolated from citrus peels and apple pomace. Pectine is generally prepared with other biopolymers in order to increase its flexibility and reduce its brittleness and rigidity caused from Galacturonate rings in the structure [25, 40].

Other widely used biopolymers to construct hydrogel systems are chitosan and cellulose which will be described in the following sections, below.

2.2.3. Chitosan

Chitosan is a linear polysaccharide derived from deacetylation of chitin. It is one of the mostly used biopolymers in hydrogel preparation. Chitin, poly (β -(1-4)-N-acetyl-D-glucosamine), is known as the second abundant biopolymer in nature after cellulose. Chitin is derived from shells of crustaceans such as shrimps and crabs, skeleton of arthropods, cell walls of yeast and fungi. The structure of chitosan is shown in Figure 2.5. Chitosan derived from chitin has a wide range of application areas such as medical, environmental, agricultural, food, drug, cosmetic fields due to their hydrophilic nature, antimicrobial properties, biodegradability and biocompatibility [41]. These properties make chitosan quite attractive and preferable material in hydrogel preparation. These properties make chitosan quite attractive and preferable material in hydrogel preparation.

There are so many studies showing usage of chitosan in hydrogel preparation with synthetic polymers or natural polymers for usage in different fields. Zu et al. have prepared blend hydrogels of chitosan with poly(vinyl-alcohol) by using glutaraldehyde as a crosslinking agent and nano-insulin was loaded to blend hydrogel for transdermal drug delivery insulin [42]. Nand et al. have prepared semi interpenetrating networks of genipin crosslinked

chitosan hydrogel with poly(vinyl-alcohol) [43]. Khurma et al. have worked on the preparation of semi interpenetrating networks of genipin crosslinked chitosan hydrogel with poly(vinyl pyrrolidone) [44]. In another study, Risbud et al. have investigated semi-IPNs preparation of glutaraldehyde crosslinked chitosan blend hydrogel membrane with poly(vinyl pyrrolidone) resulting in pH sensitive material for antibiotic release system [45]. Lih et al. have reported the enzyme-triggered preparation of chitosan with poly(ethylene glycol) by crosslinking with horseradish peroxidase (HRP) and hydrogen peroxide (H_2O_2) as tissue adhesives [46]. In another study, Islam ann Yasin have prepared a pH sensitive chitosan hydrogel with poly (lactic acid) using a tetraethoxy silane (TEOS) for controlled delivery of an anti-inflammatory agent, dexamethasone [47].

Additionally, there are some studies reporting the preparation of chitosan based hydrogel systems with natural polymers. Martinez-Ruvalcaba et al. have prepared chitosan based hydrogel with addition of xanthan to investigate the viscoelastic properties [48]. Zhong et al. have fabricated the three dimensional chitosan hydrogel with poly (ϵ -caprolactone) for potential usage in tissue engineering application [49]. Yang et al. have prepared carboxymethyl chitosan hydrogel beads with alginate in form of semi-interpenetrating polymeric network structure for drug delivery in intestine [50]. Munjeri et al. have reported a study on hydrogel bead preparation of chitosan and pectine for potential use in drug delivery for colons [51]. Wang et al. have prepared hydrogel films of chitosan with gelatine to absorb excess exudates for wound healing applications [52].

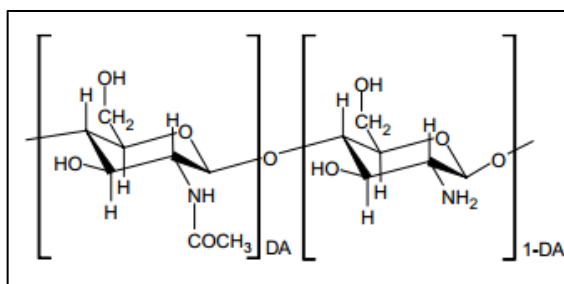


Figure 2.5. Chemical structure of chitosan [53]

2.2.4. Sodium Carboxymethyl Cellulose

Sodium carboxymethyl cellulose (Na-CMC) is a derivative of cellulose and cellulose is also known as the most abundant biopolymer in nature. Availability and abundance of CMC make the use of this natural biopolymer quite attractive in various applications. The structure of sodium carboxymethyl cellulose is shown in Figure 2.6.

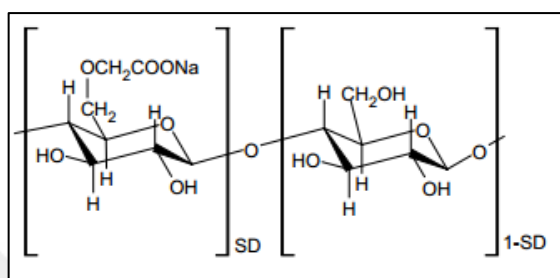


Figure 2.6. Chemical structure of sodium carboxymethyl cellulose [48]

There are so many studies showing usage of carboxymethyl cellulose in hydrogel preparation for various applications. Bajpai et al, have prepared crosslinked carboxymethylcellulose hydrogels with polyacrylamide for controlled release of agrochemicals in agricultural production field [54]. Raafat et al. have investigated γ -rays induced crosslinking synthesis of superabsorbant hydrogels based on carboxymethylcellulose and polyvinylpyrrolidone (PVP) for use in controlled delivery of fertilizers in agricultural field [22]. Gulsonbi et al. have fabricated silver/carboxymethylcellulose-poly(acrylamide) hydrogel nanocomposites for potential use in controlled drug delivery applications [55]. In another study, Asma et al. have reported formation of polyelectrolyte complexes between carboxymethylcellulose and glutaraldehyde crosslinked-gelatin for potential usage in tissue engineering applications [56]. Ma et al. have studied preparation of an intelligent hydrogel system which is pH and temperature sensitive based on carboxymethylcellulose (CMC) and poly(*N*-isopropylacrylamide) (PNIPA) crosslinked by clay and have examined the swelling behavior and mechanical characteristics for potential applications for technological and biomedical application areas [57].

2.2.5. Complexes of Chitosan and Sodium Carboxymethyl Cellulose

Generally, physical hydrogels are prepared using chitosan and CMC due to their polyionic structure. These polyionic complexes are formed as a result of the interaction between the negatively charged carboxyl groups of CMC and positively charged amino groups of chitosan. The interaction scheme can be seen in Figure 2.7.

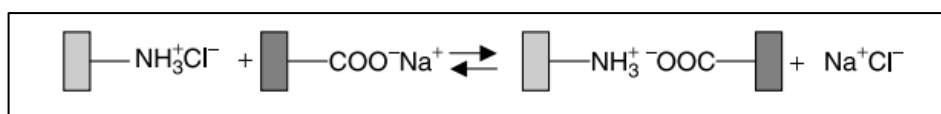


Figure 2.7. Physical interaction between chitosan and sodium carboxymethyl cellulose

There are many studies on physical hydrogels of these two biopolymers. Rosca et al. and Fukuda et al. have investigated the electrostatic interaction and complex formation mechanism between chitosan and CMC in aqueous solution and in solid phase [53]. Chen et al. have prepared freeze-dried Ch/CMC polyelectrolyte complexes for potential uses in pulp tissue regeneration applications [58]. In addition, Zhao et al. have synthesized soluble PECs based on Ch and CMC in aqueous phase and have prepared membranes of these PECs in solid phase for potential applications in the field of membrane separation [59]. In another study, Mitsumata et al. have reported the preparation of a ternary polyelectrolyte complex system based on interaction between Ch, k-carrageenan and CMC and have investigated the swelling characteristics of synthesized gels both in water and alkaline solutions [60]. Moreover, Bigucci et al. have formed a polyelectrolyte complex system based on chitosan and CMC to release an antiseptic against both *G. negative* and *G. positive* bacteria for treatment of vaginal infections [61]. Cerchiara et al. have studied on polyelectrolyte complexation of chitosan and CMC resulting in the form of spray-dried microparticles for colon-specific delivery of an antibiotic [62]. In another study, Lai et al. have prepared a polyelectrolyte complex of chitosan and CMC for usage in encapsulation of drugs in order to extend the drug release for pharmaceutical applications [63]. Additionally, Nakagawa et al. have reported to prepare a ternary cryogel system based on chitosan, CMC and k-carrageenan in order to encapsulate food ingredients with the aim of controlled release [64].

Besides, it is also possible to prepare semi-interpenetrating polymeric networks with chitosan and Na-CMC. In this method, chitosan is cross-linked by a crosslinker and Na-CMC is introduced to this network by ionic interaction. In such a study, Kaihara et al. have reported the usage of genipin crosslinked-chitosan and Na-CMC together in order to prepare a semi-interpenetrating polymeric network and have caged a magnetite inside the polymeric network and polymer-magnetite hybrid nanoparticles have been obtained in order to use them in medical areas such as controlled drug delivery and hyperthermia [65]. In another study, Feng et al. have investigated the semi-interpenetrating polymeric network structure preparation of an amphoteric membrane based on Ch and CMC crosslinked by epichlorohydrin to adsorb or separate proteins for membrane chromatography applications [66]. However, to our knowledge, semi-interpenetrating polymeric networks of chitosan and CMC prepared and characterized for food packaging applications have not been reported.

2.3. FOOD WASTE

Food waste is one of the world's most vital and growing problems. During the last decades, much attention is paid on the waste in foods. According to the final report of the studies implemented by The Swedish Institute for Food and Biotechnology (SIK) on request from the Food and Agriculture Organization of the United Nations (FAO), 1.3 billion tonnes of the food (approx. one-third) produced for human is lost or wasted per year in the worldwide. These food loss and waste occurs in different stages of whole the supply chain which begins from the agricultural production and ends at the domestic consumption. In low-income countries food is lost mostly during early and middle stages of the supply chain (production and transportation stages) rather than the consumption stage. On the other hand, the highest amount of waste occurs at the consumption stage of the food chain at the middle/high-income countries. This means that foods are thrown away in middle- and high-income countries even though the foods are still appropriate for human consumption [1]. It has been also reported that 14.5 % of 251 million municipal solid wastes is composed of food waste in USA [67].

Up to our knowledge, the only study on the domestic waste composition has been performed by Türkiye İstatistik Kurumu (TÜİK) in 1993. According to this study, 1 kg municipal waste appears for each person daily in our country. 0.6 kg per each 1 kg of municipal waste is

composed of domestic waste. Domestic waste includes 64.15 percent of organic waste. It is also estimated that 28.4 million tonnes municipal domestic waste appears per year [68]. In addition to all this major loss, food waste produces green gas emissions by contributing to global warming and climate change. All these data indicates that food waste is a serious and growing problem since the amount of food waste reaches to huge quantities.

There is a lack of knowledge about how packaging affects food waste in households despite of being known as one of the most vital parameters in reducing food waste at household level. Cox et al. and Wrap et al. have reported that some reasons of food waste are related to consumers' shopping preferences such as 'buying too much', "spontaneous purchasing", 'offers to take three and pay for two' and 'multi-packs' [69, 70]. Cox et al. have also noticed that 'food gone past its sell by date' is the main driver of food waste at household level [69]. Appropriate selection of food packaging can reduce food losses both directly and indirectly [71].

2.4. FOOD PACKAGING

2.4.1. Role of packaging

Food packaging is essential to protect the foods. Four primary functions of packaging are defined as containment, protection, convenience and communication [72]. Containment is a one of the basic functions of the packaging because products are need to be packaged before being transported from one place to another place. Secondly, packaging materials should protect the inside food from contamination and spoilage. Packaging materials selection plays an important role in preventing the foods from environmental effects such as odor, oxygen, carbon dioxide, water vapor, microorganisms' etc. For example, moisture sensitive foods such as bread, biscuits, etc. should be packaged with a material showing high barrier properties to water vapor. The desired shelf life can be achieved by selecting the appropriate materials to each type food. Therefore, effective packaging material choice is a critical parameter to preserve the food and reduce the food waste.

Another role of food packaging is convenience. Changes in attitudes towards modern lifestyle have brought changes in consumer demands. Increase in single person living alone

and women involvement in work life resulted in a huge demand for convenient products, such as re-closable opening of drink bottles or apportioned mini-packs of cheese etc.

Communication is another essential function of food packaging. Packages should give information about size, quantity, ingredients, nutritional information etc. related to the product inside. There is a growing need for communication when international trade is comprised. Use of definitive symbols is critical and essential in order to prevent chaotic manner caused by different language uses.

2.4.2. Types of food packaging materials and technologies

2.4.2.1. Conventional food packaging materials

Food can be packaged with different type of materials made of paper and board, rigid plastic, flexible plastic, glass, beverage cans, metals or others. Food packaging material should fulfill the requirements of food preservation such as moisture barrier protection, protection to microorganisms etc. Commonly used polymers as food packaging materials are polyethylene, polypropylene, polystyrene, polyamide, polyvinyl alcohol, polyvinyl acetate etc. [73]. In the last few decades, sustainable packaging materials based on edible, biodegradable materials has gained emphasis by researchers because of the growing concerns in environmental impacts such as shortage of landfill space, incineration emissions, and high cost of disposable methods. Moreover, active or intelligent packaging systems play an important role in reduction of food spoilage and waste.

Primary food packaging materials are described as materials that are in contact with food. A wide range of materials are used to pack the food for protection, safe shipment, storage and extension of shelf life. None of the materials dominate the food industry. Materials that are used for primary packaging are plastics, ceramics, glass, metals, paper and composites.

Plastic materials are used as flexible packaging material in food packaging. Plastics are generally preferred due to their advantages compared to other materials such as low cost, good barrier, optical and thermal properties [74]. Plastic materials used in flexible packaging are polyolefins, polyester, poly styrene, poly vinyl chloride, polyamide and copolymers of

all of them [75]. Apart from flexible packaging, plastics are also used for producing rigid packaging with advantage of being light weight and low-cost materials.

Glass is generally used as a rigid material to preserve perishable foods such as cereals. Some features of glass such as inertness, transparency, impermeability and heat resistance make glass a very attractive primary packaging material. However, its usage is rather limited due to its high brittleness, heavy-weight and lack of flexibility [76].

Metals are also used as food container materials from ancient times. Steel is one of the mostly used metals in food industry. Steel is generally preferred due to its strength, ductility and recyclability. Another mostly used metal in food packaging, mainly in beverage industry, is alumina which is generally preferred due to its light weight compared to steel [76].

Additionally, **paper** is also used to pack foods. Paper is composed of synthetic or natural fibers. Paper has limited applications as a food packaging material due to its poor barrier properties. Other drawbacks of paper are that it cannot be used for high moisture foods and it is not suitable for heat sealing. In order to overcome these poor features, paper is generally coated, laminated or impregnated with materials [74]. Thus, a combination of two or more of these materials can be used for food packaging as well.

2.4.2.2. Hydrogels as a food packaging material

Petroleum-based polymers have been used for most food packaging applications because of their desired properties like good mechanical performance, their large availability at relatively low cost etc. Petroleum-based polymers generally used as food packing materials are polyethylene, polypropylene, polystyrene, polyamide, polyvinyl alcohol, polyvinyl acetate etc. [73]. In last decades, biopolymer based packaging materials are also used instead of petroleum-based polymers. However, the use of biopolymers in food packaging is restricted due to their poor barrier properties, weak mechanical performance, processability difficulties and high cost. Thus, studies on development of biopolymer based hydrogel films is gaining importance in order to have new materials with desired properties (durability, biodegradability, mechanical properties etc.) and new opportunities in food packaging applications [73, 77].

Biopolymers are generally used as binary pairs together while constructing hydrogel systems because hydrogel films prepared by using single biopolymer exhibit weak properties. Polyionic complexes prepared by interaction of oppositely charged molecules display strong intermolecular chains. The pair of polyscharracide and protein based hydrogels for example, are extensively investigated for potential applications in food packaging area. Müller et al. have prepared starch based films by addition of cellulose fibers by solution casting method to investigate its affects on mechanical and moisture barrier properties within films. The developed films showed poor optical properties though having good tensile strength [78]. Liu et al. have studied gelatin and sodium alginate blend composite films manufactured by extrusion for coating sausages in order to increase the shelf life by stabilizing the product quality [79]. Lee et al. have reported the preparation of composite films based on gelatin and gellan gum and investigated their mechanical properties and potential applications as packaging and coating materials [80].

Ryu et al. have shown the preparation of zein-coated starch film to be used as inner packaging material for sliced cheese by both dipping and solution casting methods and have characterized their physical and barrier properties. The developed films have exhibited poor flexibility though good water vapor transmission rate [81]. Gregorova et al. have studied the preparation of hydrogel films based on CMC and polyvinyl pyrrolidone (PVP) which can be used as a food packaging material and have demonstrated the mechanical and viscoelastic properties of newly developed hydrogels [77].

Rhim et al. have developed agar/-carrageenan/konjac glucomannan hydrogel blend film with desired features for food packaging applications. Mechanical and water vapor barrier properties of films were evaluated and preliminary tests were studied for packaging of fresh spinach which is selected as highly respiring fresh agricultural product. The developed hydrogel films have played an important role in preventing the formation of water condensation on the surface of the packaging film. Therefore the developed hydrogel films have a great potential for use as an antifogging packaging film for fresh fruits and vegetables having high respiration rate. They have also reported that the films are good candidates for use in biomedical fiels as wound dressings or skin care products [82].

Saha et al. have prepared a hydrogel film based on PVP and CMC to extent the shelf life of fresh fruits and vegetables which protect them from early spoilage by absorbing the excess water vapor during dehydration. Grape was selected as the example fruit due to its problems

associated with its postharvest handling. They have concluded that the developed hydrogel film was successful in extending the shelf-life of grapes compared to conventional packaging material although their mechanical properties are still needed to be improved [73]. Wang et al. have carried out a study on the incorporation of silver nanoparticles (AgNPs) and grapefruit seed extract (GSE) into a ternary blend biohydrogel film based on agar, alginate and collagen. The developed hydrogel films have been tested for shelf life extension of fresh potatoes. They have reported that the newly developed hydrogel films were successful not only in extending the shelf-life of fresh potatoes but also they prevented the greening of potatoes. Moreover, hydrogel films have displayed strong antimicrobial activity against both *Gram-positive* and *Gram-negative* food-borne pathogenic bacteria due to antimicrobial fillers [83].

2.4.2.3. Modified Atmosphere Packaging (MAP)

Air is composed of nitrogen (N₂) 78.08%, oxygen (O₂) 20.96%, carbon dioxide (CO₂) 0.03%, water vapor and traces of some other gases. Changes in the composition of gases in the packaging atmosphere might enhance the growth of microorganism, thus cause food spoilage. The required composition of modified gaseous atmosphere totally depends on the food type. Modified atmosphere packaging is a very useful technology to extend the shelf life by maintaining the gas composition inside the packaging atmosphere. For example, fresh vegetables consume O₂ and produce CO₂ and ethylene (C₂H₄) which is a gaseous hormone produced by the plant itself and accelerates the senescence. In order to extend the shelf life of fresh vegetables, respiration rate is generally slowed down by reducing O₂ and increasing CO₂ concentrations within the packaging atmosphere compared to air. Modified atmosphere packaging applications have great potential to maintain the quality, assure the microbial safety of fresh prepared produces and extend their shelf-life [84].

2.4.2.4. Intelligent Packaging

Intelligent packaging is the system which monitors the quality and safety circumstances of a food product, sense the internal and external conditions of the packaging atmosphere and

provides instantaneous information about the food product to consumers. Thus the intelligent packaging enhances food safety, quality and convenience.

Temperature is the most important external factor which affects the food quality. Temperature fluctuations during transportation of food products from farm to fork is a serious problem encountered in food industry. Time-temperature indicators (TTI) are designed to follow the cold chain breakage by monitoring the temperature throughout the packaging atmosphere. TTI is a very critical system used to report temperature history of chilled/frozen food products. Moreover, freshness indicators are used to monitor the remaining shelf life of the perishable products.

Another vital factor affecting food quality is gas composition inside the package. Gas composition may change due to the respiration rate of packaged product, generation of spoilage microorganisms etc. Gas indicators such as oxygen, water vapor, carbon dioxide, ethanol are used to sense and monitor the gas composition to prevent the rancidity, color change, and microbial spoilage caused by gases [85].

2.4.2.5. Active packaging

Active packaging is a system which aimed to extend the shelf-life of foods by incorporation of some additives capable of different properties into packaging materials to ensure food safety. There are some intrinsic or extrinsic factors affecting the shelf life of foods. Acidity (pH), water activity, nutrient content, respiration rate are intrinsic factors and temperature, relative humidity, gaseous composition within the packaging atmosphere, light are extrinsic factors. Active packaging system controls these mentioned parameters to preserve the foods. Antimicrobial packaging materials, oxygen scavengers, moisture absorbers, ethanol emitters/releasers, carbon dioxide absorbers/emitters, ethylene absorbers are some significant and widely used examples of active packaging system [2].

Moisture absorbers are one of widely used active packaging systems in food industry. Fresh products such as vegetables, fruits, poultry, meat products have high respiration rates and water loss occurs as a result of evaporation. When the packaging material shows high barrier properties to water vapor, water vapor cannot permeate throughout the materials and condenses as liquid droplets on the surface. Especially for packed high humidity food

products, moisture loss may increase upon exposure to high temperatures and increased humidity in the package headspace may condensate on the surface of the product itself and the packaging film. Further in the supply chain these condensed water droplets may provide a favorable environment for microbial growth resulting in product loss. Moreover, condensation inside the package is also considered as an esthetic problem which often decreases the consumer appeal. In order to avoid this unpleasant condensation or sweating problem, some desiccants are used to absorb the excess humidity within packaging headspace. Silica gels, different salts, molecular sieves, clays, pads based on cellulose fibers etc. are used in sachet for controlling the moisture. In addition, some of these dessicants can be integrated within the packaging materials to maintain the dry conditions within the package.

3. AIM OF THESIS

Some moisture absorption systems such as permeable plastic bags containing silica, calcium oxide and active clay are developed and used in the food industry. The main risk to the use of these food packaging bags is that these may be accidentally consumed by children and may come into contact with food when the bags are perforated. Furthermore, integration of these bags inside the packaging is not practical because of their size and volume. Because of these risks, their use in the food industry is rather limited. Therefore, hydrogel films can be a good alternative for moisture sensitive foods. Besides the packets of moisture absorbers, there are food packaging films made from gelatin and pectin having the anti-humidity property. However, these films have some disadvantages such as their low mechanical strength. Therefore, a new packaging system having capability to absorb/regulate moisture, high chemical stability and appropriate mechanical properties might be a good alternative.

In this study, the hydrogel film structure will be strengthened by existence of covalently cross-linked structure which should result in better mechanical performance.

Chitosan and carboxymethyl cellulose are two of the most commonly used biopolymers in preparation of hydrogels. In literature, chitosan was generally crosslinked by using glutaraldehyde as a crosslinking agent. In present study, genipin was used as a crosslinking agent instead of glutaraldehyde. It is a natural compound derived from geniposide of gardenia fruit extract and it is widely used in Asia as a medicinal herb. Genipin constitutes an excellent crosslinker for chitosan, proteins and collagen and it has the advantage of being much less toxic and less pollutant than glutaraldehyde or other synthetic agents [86, 87].

The main aim of this study is to develop biopolymer based chemical permanent hydrogel films which can be used as a moisture absorber/regulator in food packaging systems with an ultimate goal to prolong the shelf-life of products. For this purpose, semi-interpenetrating polymer network (Semi-IPN) hydrogel films based on genipin crosslinked-chitosan (Ch) and sodium carboxymethyl cellulose (NaCMC) were prepared and characterized. In this system, a portion of the the amino groups of Ch were cross-linked with GNP and the remaining un-crosslinked positively charged amino groups interacted with the negatively charged carboxyl groups of CMC to produce the final permanent semi-interpenetrating polymeric network (Semi-IPN) structure. In this study, the hydrogel film structure were strengthened

by existence of covalently cross-linked structure which should result in better mechanical performance and introducing of carboxymethyl cellulose into the crosslinked network as a guest polymer enabled high moisture absorbing capacity. Figure 3.1 depicts the structural representation of Semi-IPN of genipin crosslinked chitosan and carboxymethyl cellulose.

Up to our knowledge, semi-interpenetrating polymeric networks of genipin crosslinked-chitosan and CMC prepared and characterized for food packaging applications have not been reported. In the present study, the developed hydrogel films will be applied in food packaging systems for Turkish coffee, mushrooms and broccoli for absorbing/regulating excess moisture in packaging atmosphere and their suitability in these applications will be investigated.

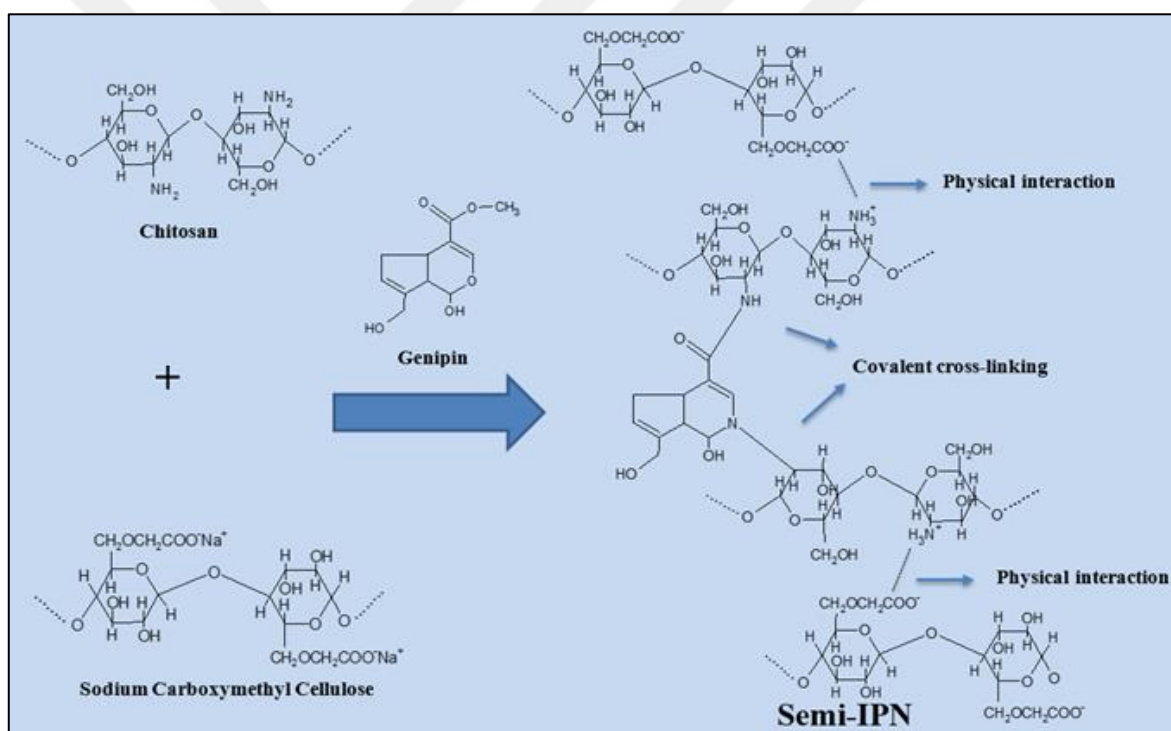


Figure 3. 1. Representation of the Semi-IPN hydrogel structure

4. MATERIALS AND METHODS

4.1. CHEMICALS

4.1.1. Chemicals Used in Titration Experiments

Chitosan (Mw 50-190 kDa) with a degree of deacetylation greater than 0.75, sodium carboxymethyl cellulose (Mw 90 kDa) with a degree of substitution of 0.7, acetic acid (≥ 99.7) and hydrochloric acid (37%) were purchased from Sigma-Aldrich. All chemicals were used without further purification.

4.1.2. Chemicals Used in Preparation of Hydrogel Films

Chitosan (Mw 50-190 kDa) with a degree of deacetylation greater than 0.75, sodium carboxymethyl cellulose (Mw 90 kDa) with a degree of substitution of 0.7, genipin with a purity of greater than 98% and ethanol were all purchased from Sigma-Aldrich. Glycerol was purchased from Carlo-Erba. Hydrochloric acid (37%) was purchased from Sigma Aldrich. All chemicals were used without further purification.

4.1.3. Chemicals Used in Biodegradation Tests

Soda lime (sodium hydroxide on support, granulated about 2-5 mm), soda talc (sodium hydroxide on support, granulated about 1.6-3 mm), calcium chlorite (2-6 mm), silica gel (1-4 mm), cellulose powder (cellulose microcrystalline for thin layer chromatography) and sulfuric acid (purity with 95%) were purchased from Merck. Sea sand (0.425-800mm) and controlled compost were gifted and used as received. All other reagents were analytical grade and purchased from Sigma-Aldrich. All chemicals were used without further purification.

4.1.4. Chemicals Used in Packaging for High Moisture Foods

The humidity within desiccators was independently controlled by using saturated solutions of cobalt (II) chloride, potassium chloride and water giving 65, 85 and 100% RH, respectively.

4.1.5. Chemicals Used in Microbiological Tests

Plate Count Agar (PCA), Dichloran Rose Bengal Chloramphenicol (DRBC) Agar and Maximum recovery Diluent (MRD) were purchased from MERCK (Darmstadt, Germany).

4.1.6. Foods used in shelf-life studies

Turkish coffee, fresh mushrooms and broccoli florets were purchased from a local supermarket. Mushrooms and broccoli florets were purchased on the day of experiment and used within 12 hours upon arrival to the laboratory.

4.2. METHODS

In this study, charge distribution of physical hydrogel complexes were evaluated by potentiometric and conductometric titration methods in solution. Physical and chemical bonds formed between the functional groups of CMC and Ch were followed via FT-IR spectroscopic technique. The thermal transitions of the hydrogel films were analyzed via Differential Scanning Calorimetry (DSC). Thermal stability of the hydrogel films were characterized by Thermal Gravimetric Analysis (TGA). Viscoelastic properties of hydrogel films were characterized by Dynamic Mechanical Analysis (DMA) technique. The tensile properties of the prepared films and firmness of fresh produces were determined using a Texture Analyzer. Swelling degree of developed hydrogel films were evaluated by gravimetric method. Biodegradation tests were performed by Microbial Degradation Oxidative Analyzer (MODA) test equipment. Color of the produces were measured by using a Computer Vision System (CVS). Relative humidity and temperature within the test container were recorded continuously via data logger. Moisture loss of fresh prodeces and

water absorbing capacity were determined by gravimetric method. Microbial load were determined by spread plate technique.

4.2.1. Fourier Transform Infrared Spectroscopy (FT-IR)

Infrared (IR) spectroscopy measures the infrared intensity versus wavelength (wavenumber) of light. Infrared light can be categorized in three distinct regions as far infrared ($4 \sim 400\text{cm}^{-1}$), mid infrared ($400 \sim 4,000\text{cm}^{-1}$) and near infrared ($4,000 \sim 14,000\text{cm}^{-1}$) in terms of the wavenumber.

Fourier Transform Infrared Spectrometry (FT-IR) is one of the most important spectroscopic techniques to obtain some basic information about the chemical structure of a material. In the FT-IR spectrometer, a beam is transferred from source to interferometer where encoding process occurs. This infrared beam enters into interferometer and split into two optical beams. One of them is reflected on a flat mirror, the other one is reflected on a moving mirror which is very close to the beamsplitter. These two optical beams are interfered with each other and exits from the interferometer. This beam is transferred to the detector after reaching the sample. This data, which is called as thermogram is converted and transferred to the computer. The output gives a plot of transmittance or absorbance as a measure of band intensity (ordinate) versus wavenumber (cm^{-1}) (abscissa). The schematic illustration of an FTIR spectrometer is shown in Figure 4.1.

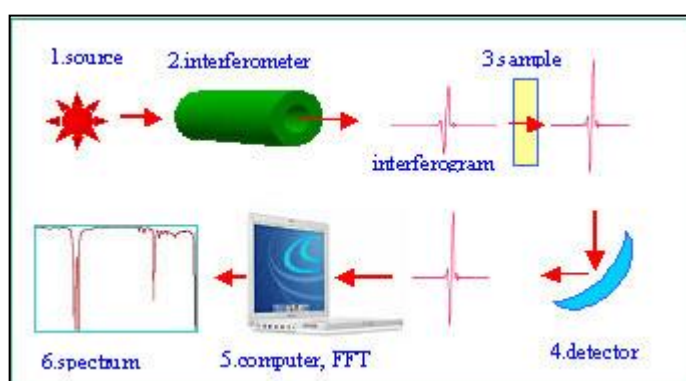


Figure 4.1. Schematic illustration of the FT-IR system [88]

4.2.2. Differential Scanning Calorimetry (DSC)

Differential Scanning Calorimetry (DSC) is one of the most important tools to determine the thermal properties of a variety of materials. DSC is known as a very useful technique to detect the phase transitions in materials such as glass transition, phase changes, curing, melting etc. Besides, it is a fundamental instrument in thermal analysis. Hence, it can be used in many industrial areas such as pharmaceutical, polymer, food, electronic etc. [89].

DSC characterizes the physical changes of a sample with respect to temperature against time. An inert reference pan and a pan enclosed with sample are placed in a controlled temperature environment in nitrogen atmosphere. Heat is passed from a furnace to the sample and inert reference pan, temperature difference between sample and reference causes difference in heat flow rate resulting from the thermal transition of the sample [89]. Heat flow is determined by Ohm' Law equation (3.1);

$$\Delta Q = \frac{\Delta T}{R} \quad (3.1)$$

A schematic illustration of the DSC system is presented in Figure 4.2.

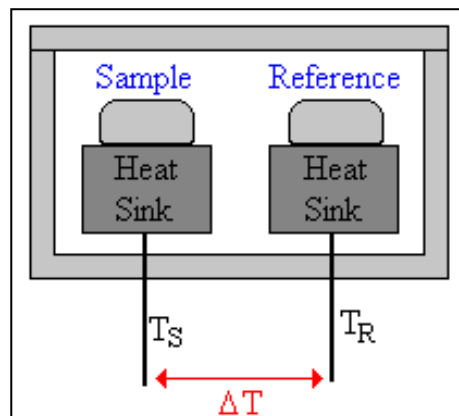


Figure 4.2. Schematic illustration of DSC system [85]

4.2.3. Dynamic Mechanical Analysis (DMA)

Dynamic Mechanical Analysis (DMA) is a very useful thermal analysis technique to characterize the viscoelastic properties of polymers as a function of time, temperature and frequency. A force is applied to the sample which results in the deformation of the sample. Applied force is called as stress and expressed with the symbol δ and deformation is called as strain and expressed with the symbol γ . DMA measures the elastic or viscous response of the sample as a function of stored or lost energy to the applied force. The relation between the applied force, stress and deformation, strain gives Young Modulus which is the measure of the stiffness of the material. Storage modulus is defined as ability of a material to store energy elastically during a loading cycle, loss modulus is defined as ability of a material to dissipate energy such as lost as heat. Tan delta which is also known as damping, is the ratio of storage modulus (E') to loss modulus (E'') is a measure of energy dissipation of a material under a cyclic load. DMA can be used to determine the glass transition temperature of materials. An oscillatory stress is applied to the material and responses of the material is measured as a function of temperature during the test. Storage modulus, loss modulus or tan delta signals are followed. A sharp decrease in storage modulus or a peak observed in both loss modulus and tan delta shows the glass transition temperature [90].

4.2.4. Thermal Gravimetric Analysis (TGA)

Thermogravimetric analysis or Thermal Gravimetric Analysis (TGA) is one of the most widely used tools in thermal analysis of a sample. A thermal gravimetric analyzer consists of a sample pan, a balance and a furnace as a heating device. TGA measures the mass change in the sample with temperature against time in a controlled atmosphere. This mass change can be caused from decomposition of the material, loss of some volatiles such as moisture, solvents, monomer etc. The mass loss is weighed and recorded by a highly precise electronic balance. TGA gives a plot of mass (ordinate) versus temperature (abscissa) [91]. A schematic illustration of a TGA device is shown in Figure 4.3.

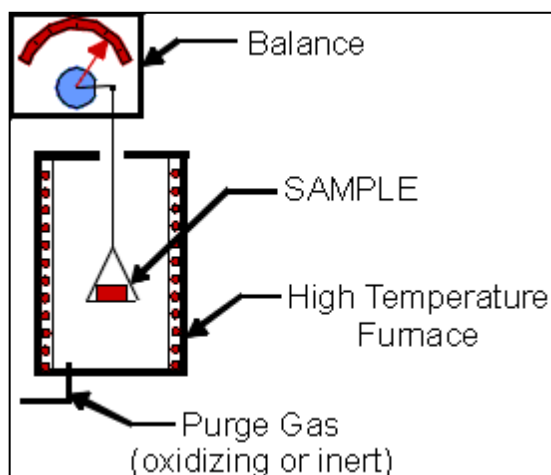


Figure 4.3. Schematic illustration of a TGA system [88]

4.2.5. Biodegradability Tests

Microbial Degradation Oxidative Analyzer (MODA) apparatus is a newly developed apparatus to test the biodegradation degree of plastic materials in certain environmental conditions. MODA apparatus is used in accordance with ISO 14855-2 standard for testing the biodegradation of plastics by gravimetric method. This method is based on the gravimetric measurement of evolved carbon dioxide during the process to determine the ultimate aerobic biodegradability of plastic materials under controlled compost environment. In this system, tests are performed in controlled compost at 58 °C for at least 45 days and extended to a maximum of 6 months according to ISO 14855-2.

Six reaction columns are available in the system which are placed in an environmental chamber keeping the temperature conditions constant. 2 of them are for test materials, 2 for reference materials and 2 for blank. The test material is mixed with the controlled compost and performed under air eliminated from CO₂. Ammonia and water produced from the reaction during degradation are removed and CO₂ is absorbed on soda lime/soda talc mixture. The weight differences of soda lime/soda talc absorption column are recorded daily and evolved CO₂ is determined by gravimetric method. Percentage biodegradation is calculated using the evolved and theoretical CO₂ measurements.



The schematic illustration of a MODA apparatus is shown in Figure 4.4.

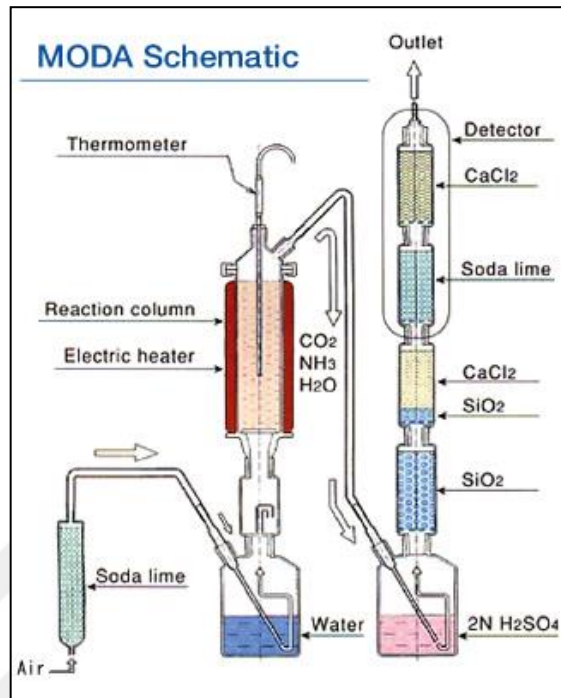


Figure 4.4. Schematic of a MODA apparatus [92]

4.2.6. Statistical Analysis

Differences between means were determined by analysis of variance (ANOVA) followed by TUKEY's HSD post-hoc test where significant differences were found ($p < 0.05$). All statistical analyses were carried out using XLStat (version 2013, Addinsoft, France) software.

5. EXPERIMENTAL STUDY

5.1. TITRATION EXPERIMENTS FOR DETERMINATION OF THE OPTIMUM CMC / CH RATIO

To determine the optimum ratio between the chitosan (Ch) and carboxymethyl cellulose (CMC) for physical interaction, the isoelectric points were monitored by potentiometric titration between chitosan-HCl solution and solution of CMC. For this purpose the chitosan-HCl solution should be prepared in stoichiometric ratio to prevent the excess acid during titration with CMC solution. Thus first, 1g of chitosan was dissolved in 0.1 M acetic acid solution and titrated with 0.1 M HCl solution. The required volume of HCl solution was calculated using the turning point to dissolve chitosan at a stoichiometric ratio. The potentiometric titration was carried out between this chitosan-HCl solution and carboxymethyl cellulose (CMC) solution to determine the optimum ratio between the two for physical interaction. At the same time, conductiometric titration was performed in the same solution parallel with potentiometric titration. For this purpose, 1 g of chitosan (Ch) was dissolved in 40.2 mL of deionized water by adding the stoichiometric amount of 0.1M HCl solution (2.5% w/v) and 1 g of the sodium carboxymethyl cellulose (CMC) was dissolved in 100 ml of deionized water (1% w/v). 5 ml of the chitosan-HCl solution was diluted to 20 ml with deionized water and titrated with 1% w/v CMC solution.

5.2. FILM PREPARATION

5.2.1. Preparation of physical hydrogel films

1 g of chitosan (Ch) was dissolved 40.2 mL of water by adding the stoichiometric amount of 0.1 M HCl solution (2.5% w/v). The mixture was kept at 50 °C for 8 hours and then it was placed in an ultrasonic bath for 30 min at room temperature for dissolution of chitosan. The viscous solution was then centrifuged at 4500 rpm for 10 min to eliminate any undissolved matter. 1 g of the sodiumcarboxymethyl cellulose (CMC) was dissolved in water to obtain a 1 % (w/v) solution. All hydrogel films were prepared by solution casting method. 5 ml of

the chitosan-HCl solution was diluted to 20 ml with deionized water and 12 ml of 1 % (w/v) CMC solution was added into this chitosan-HCl solution under constant stirring drop by drop. Glycerol was also added as a plasticizer to obtain 15 % of the total dry matter amount in the Ch-CMC solution. This solution was homogenized at 20,000 rpm for 5 min by using a homogenizator (Yellow Line DI25 basic). The final film-forming solution was immediately cast into petri dishes with 90 mm diameter and left at room temperature for drying.

5.2.2. Preparation of chemically cross-linked hydrogel films

Genipin was used as the cross-linker for chitosan and the amount of genipin used was fixed as 0.5, 1, 2 and 3 wt % based on the weight of chitosan with a constant Ch:CMC ratio of 1:0.96 (w/w) for the preparation of the chemically cross-linked hydrogel films. Thus first, genipin was dissolved in ethanol to obtain 0.1 % (w/v) solution. Chitosan and CMC solutions were prepared with the procedure described above. 5 ml chitosan solution was diluted to 20ml with deionized water. 12 ml of 1% (w/v) CMC solution was added into chitosan solution under constant stirring drop by drop. Glycerol was added as a plasticizer to obtain 15% of the total dry matter amount in the Ch-CMC solution. This solution was homogenized at 20,000 rpm for 5 min by using a homogenizator. Required amount of genipin solution was then added into this solution. The solution was kept at 50 °C under constant stirring until it became viscous and turned to blue. The final film-forming solution was immediately cast into petri dishes with 90 mm diameter and left at room temperature for drying. The designations of all the hydrogel films prepared are listed Table 5.1.

Table 5.1. Designations of prepared hydrogel films

Ch/CMC (w/w) ratio	Gnp wt% (based on Ch)	Designations
1:0.96	-	Uncross-linked
1:0.96	0.5	Gnp05
1:0.96	1	Gnp1
1:0.96	2	Gnp2
1:0.96	3	Gnp3

5.2.3. Crosslinking evidences of hydrogel films

It is known that chitosan dissolves in acidic solutions and CMC dissolves in water. Thus, it is expected that hydrogel film that is not crosslinked successfully by genipin loses its integrity when it gets contact with the hydrochloric acid solution. So in order to examine whether chitosan was crosslinked or not by genipin with the applied procedure, the hydrogel films were cut into 1*1 cm² dimensions and immersed in 0.1N HCl solution. It was followed if the hydrogel film keeps its integrity in 0.1N HCl solution or it disintegrates.

5.2.4. Determination of swelling degree of the hydrogel films in water

The water sorption capacity of the hydrogel films with a known amount was determined by swelling the films in deionized water at room temperature. Swelling degree and dissolution degree of hydrogel films were calculated by gravimetric method.

The water sorption capacity of the cross-linked hydrogel films was determined by swelling the films in distilled water at room temperature. For this purpose, all samples were placed in a desiccator with silica gel at least 1 week prior to the swelling degree analysis. Film samples were cut into 1*1 cm² dimensions and then were weighed and placed in metal spheres. These spheres with the samples were immersed in beakers filled with 100 ml Milli-Q water (pH=7). The swollen films were collected at different time intervals and after having been superficially dried with a tissue paper, they were weighed immediately on an analytical balance. The swelling degrees of the films were calculated according to the Equation 4.1.

$$\text{Swelling degree (\%)} = [(W_s - W_i) / W_i] * 100 \quad (4.1)$$

W_s: Weight of the sample after swelling (g)

W_i: Weight of the sample before swelling (g)

5.3. FT-IR SPECTROSCOPY

The ionic interactions between the carboxylate groups of CMC and ammonium groups of the acidified chitosan as well as the cross-linking of chitosan with genipin were followed with FT-IR spectroscopic analysis. All the FT-IR spectra were taken with 4 cm^{-1} resolution in the $4000\text{-}650\text{cm}^{-1}$ wavelength region on a Perkin Elmer (Spectrum 400) FT-IR spectrophotometer.

5.4. DIFFERENTIAL SCANNING CALORIMETRY (DSC)

Differential Scanning Calorimetric (DSC) analysis of the Ch/CMC films were performed to determine their thermal transitions. All DSC measurements were carried out on a Perkin Elmer Differential Scanning Calorimeter. For each measurement, about a 6 mg of sample was scanned from $30\text{ }^{\circ}\text{C}$ to $350\text{ }^{\circ}\text{C}$ at a heating rate of $10\text{ }^{\circ}\text{C}/\text{min}$ in nitrogen atmosphere.

5.5. DYNAMIC MECHANICAL ANALYSIS (DMA)

The thermomechanical properties of the hydrogel films were determined via dynamic mechanical analysis (DMA). The measurements were performed on a TA Instruments Q800 model DMA instrument. Films were cut into dimensions of $\sim 22\times 5\times 0.1\text{mm}$ and scanned from $-100\text{ }^{\circ}\text{C}$ to $250\text{ }^{\circ}\text{C}$ at a heating rate of $5\text{ }^{\circ}\text{C}/\text{min}$ under nitrogen atmosphere in the dynamic temperature ramp default mode, using a tension clamp. Each DMA measurement was performed in duplicate.

5.6. THERMAL GRAVIMETRIC ANALYSIS (TGA)

The thermal degradation profiles of the prepared films were determined via thermal gravimetric analysis (TGA). The measurements were performed on a Perkin Elmer Pyris1 model TGA instrument. For each analysis, about a 10 mg of sample was heated from $30\text{ }^{\circ}\text{C}$ to $800\text{ }^{\circ}\text{C}$ at a heating rate of $10\text{ }^{\circ}\text{C}/\text{min}$ under nitrogen atmosphere. The corresponding weight % vs temperature plots were constructed and analyzed. Each thermal analysis was performed in duplicate.

5.7. TENSILE TESTS

The tensile properties of the prepared films were determined using a Texture Analyzer (Stable Micro System, TA.HD.Plus, UK) according to the ASTM D-882-02 standard. A 50N load cell was used. Samples were cut into 11 mm wide and 71 mm length strips. The thickness of each film was measured at 5 different points randomly with a digital micrometer. The initial grip separation and cross-head speed were adjusted to 25 mm and 50 mm/min, respectively. Each mechanical testing was performed 3 times. A stress strain plot was constructed for each sample. Tensile strength (TS) was calculated by dividing the ultimate strength by the cross-sectional area. Elongation at break (EB) (%) was calculated by dividing the elongation at the moment of rupture by the initial length of specimen and multiplying by 100. Tensile modulus (TM) was determined from the initial slope of stress-strain curve.

5.8. BIODEGRADABILITY TESTS

Biodegradability under aerobic conditions feature of hydrogel films were tested for 45 days by using "Microbial Degradation Oxidative Analyzer (MODA)" test equipment according to ISO 14855-2. Biodegradation tests of each hydrogel films were performed in controlled compost at 58°C.

5.8.1. Total organic carbon analysis

Before biodegradation test, total organic carbon (TOC) content of the samples was measured according to the high temperature combustion standard method (2005) by a total organic carbon analyzer (TOC-V- Solid sample module ssm5000A, Shimadzu). TOC values were used to calculate the rate of biodegradation of test materials.

5.8.2. Preparation of controlled compost and sea sand

Controlled compost was given from a composting facility (ISTAC, Istanbul). The properties of the controlled compost are shown in Table 5.2. The received compost was sieved using

a 3.55 mm sieve and kept at room temperature. Sea sand was sieved to obtain particle size between 1.6-0.8 mm. Sea sand was washed 5 times by using tap water to remove impurities, drained and dried in an oven at 105 °C overnight.

Water holding capacity and moisture of the controlled compost should be known in order to control the water content over 80 %. These were determined according to TS EN ISO 1721-1). Known amount of dry controlled compost was saturated with water overnight. Excess water was filtrated under vacuum and weighed. Samples were dried to constant mass at 105°C and weighed again. Water holding capacity and moisture of the controlled compost was calculated by using Eqn. 4.2 and 4.3, respectively. Then, the required amount of water was calculated in order to adjust the compost water content to 90 % of its water holding capacity.

$$WHC (\%) = \frac{(m3 - m4)}{(m4 - m1)} * 100 \quad (4.2)$$

$$\text{Moisture content } (\%) = \frac{(m2 - m4)}{(m4 - m1)} \quad (4.3)$$

m1: mass of empty holders

m2: initial mass of holders with dry compost

m3: mass of holders with saturated compost after vacuum filtration

m4: mass of holders with dried compost at 105°C

The required amount of water was added to 80 g of controlled compost. Adequate water was added to 320 g of sea sand to obtain 15 % water content. The sea sand and controlled compost were mixed well and kept at room temperature overnight. This amount was prepared for each test vessel.

Table 5. 2. Properties of controlled compost

C/N ratio	15
C/P ratio	30
Moisture content	65%
Total dry solids	47%
Volatile solids	42%
pH	7.3
Compost mature	2-3 months

5.8.3. Biodegradation Test by Microbial Oxidative Degradation Analyzer based on ISO 14885-2

Biodegradation tests were carried out using Microbial Oxidative Degradation Analyzer apparatus in controlled compost at 58 °C during 45 days (MODA-6, SAIDA FDS Inc.). The tests were performed by using ISO 14855-2 method. This method is based on the gravimetric measurement of evolved carbon dioxide during the process to determine the ultimate aerobic biodegradability of plastic materials under controlled compost environment.

Test materials which were cut into pieces smaller than 100 mm can be seen in Figure 5.1. 10 g of test material was added to the sea sand and controlled compost mixture and well mixed. The whole mixture was transferred to the reaction vessels. 10 g of microcrystalline cellulose powder was added to the sea sand and controlled compost mixture as a reference material to control the inoculum activity. Sea sand and controlled compost mixture was transferred to reaction vessels as blank to determine the respiration activity of the compost. The sample mixtures prepared can be seen in Figure 5.2. The reaction vessels were placed into the Microbial Oxidative Degradation Analyzer MODA6 equipment at 58 °C as shown in Figure 5.3. Tests were performed under 45 ml/min air flow rate. Air was eliminated from CO₂ by using soda lime pellets before entering to test environment. All measurements were performed in duplicate.

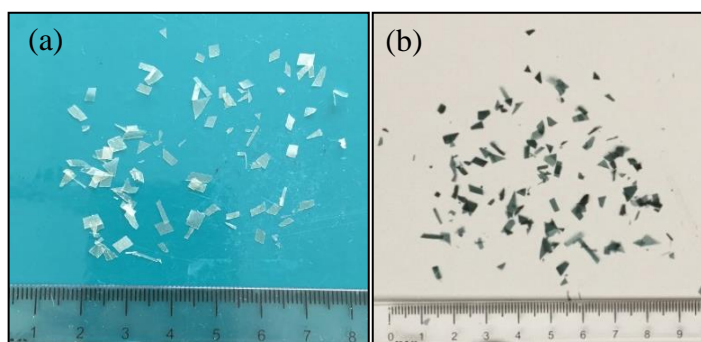


Figure 5.1. Initial sizes of (a) uncross-linked and (b) genipin cross-linked hydrogel films

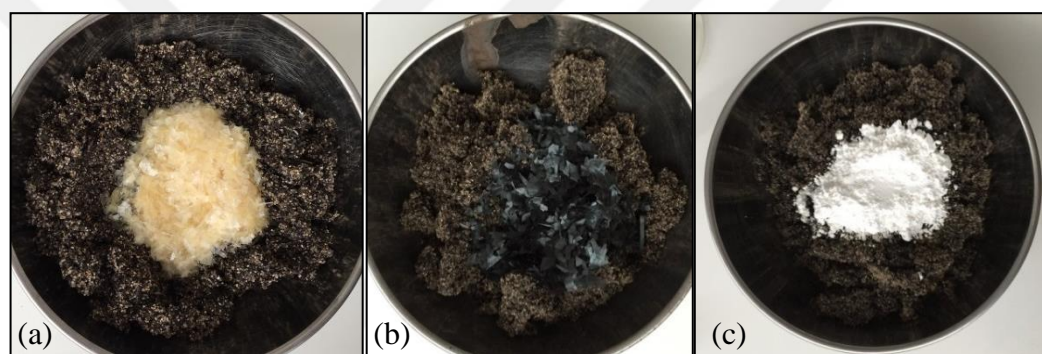


Figure 5.2. (a) Uncross-linked, (b) cross-linked hydrogel samples and (c) cellulose powder in compost initially



Figure 5.3. Microbial oxidative degradation analyzer apparatus with samples

The produced carbon dioxide was measured once a day by weighing the absorption column for carbon dioxide and absorption column for water and recorded once a day. Compost were transferred outside and stirred weekly to homogenize the compost and to enable the micro-organisms uniform attack on the test material. Absorption columns were filled with fresh soda lime-soda talc if needed. Test was terminated after 45 days.

Percentage biodegradation was calculated using equation 4.4.

$$\text{Biodegradation (\%)} = \left(\frac{\sum CO_{2T} - \sum CO_{2B}}{ThCO_2} \right) \quad (4.4)$$

$\sum CO_{2T}$ = is the cumulative amount of carbon dioxide, in grams, evolved in the test vessel between the start of the test and time t

$\sum CO_{2B}$ = is the mean cumulative amount of carbon dioxide, in grams, evolved in the blank vessels between the start of the test and time t

$ThCO_2$ = is the theoretical amount of carbon dioxide, in grams, evolved by the test material

$$ThCO_2 = M_{TOT} \times C_{TOT} \times \frac{44}{12} \quad (4.5)$$

M_{TOT} = is initial weight of test material, in grams

C_{TOT} = is the proportion of total organic carbon in the initial test material, in gram per gram

44 is the molecular mass of carbon dioxide and 12 is the atomic mass of carbon.

5.9. APPLICATIONS OF HYDROGELS IN FOOD PACKAGING

5.9.1. Packaging for moisture sensitive dry foods: The case of Turkish coffee

The duration of secondary shelf life of coffee were determined by simulating the conditions of household consumption. As coffee can be stored either in the refrigerator or at room temperature, the study was carried out at 5 °C and 20 °C, respectively. Three samples of 250 g cans with hydrogel film were prepared in order to evaluate how films affect the quality parameters of coffee during secondary shelf life. The hydrogel films were placed under the lid of each metal box (Figure 4.4a and 4.4c). Initial weight of each film sample was weighed. Three samples of 250 g cans without hydrogel film were prepared as control sample (Figure 4.4b). These metal boxes containing Turkish coffee were placed in the climate chamber set to above mentioned temperatures for 35 days.

It was assumed that coffee is consumed twice a day for a family of two people. Therefore, the boxes were removed from the climatic chamber and opened twice a day and remained open for 30 seconds to simulate household consumption. Appropriate amount of samples was taken on 0, 2, 4, 7, 9, 16, 25 and 35th days. On each sampling day, 5.5 grams of sample was taken from each metal box with hydrogel and control boxes and Turkish coffee was prepared by Turkish coffee machine (Arçelik, Telve) after mixing with 1 cube of sugar (2.2 gram). A coffee machine Turkish coffee machine (Arçelik, Telve) was used to standardize the preparation. Once the coffee was prepared its sensory properties were analyzed by the sensory panel. The sensory panel was consisting of 5 selected trained judges from sensory judge pool of the MRC Food Institute whose members have passed the test of identification

of taste and odor according to ISO 3972 (2011) and ISO 5496 (2006) standards [93, 94]. Five one-hour training sessions were conducted prior to formal evaluation of coffee samples by providing samples. The sensory characteristics and the definitions used during the training sessions were given in Table 5.3. The formal sensory evaluations were conducted by a group of 5 panelists according to ISO 4121 (2003) standard [95]. Sensory parameters were determined as odor (coffee odor, parched odor, stale odor) and taste (sour taste, bitter taste, burnt taste, coffee taste), foam formation and overall liking.

Table 5. 3. Descriptors and definitions used by the trained sensory panel to describe the sensory properties of the Turkish coffee samples

Descriptors	Definitions
Coffee odour	Intensity of the freshly roasted coffee odour
Parched	Used to indicate the degree of roasting perceived ranging from lightly roasted to burnt food or burning wood smoke
Rancid odour	Absent of fresh coffee dour
Sour taste	A basic taste characterized by the solution of an organic acid.
Bitter taste	A primary taste characterized by the solution of caffeine, quinine and certain alkaloids
Burnt taste	Degree of burnt food or burning wood smoke
Coffee taste	Desirable, savory coffee taste
Foam formation	Keeping whole body of foam on the surface

The coffee samples were served immediately to the judges to minimize aroma loss in traditional coffee pots. The judges identified and rated the intensity of each character on a 9 point scale .

Besides, from each metal box samples were taken for relative humidity measurement. The relative humidity of the coffee samples was measured at a constant temperature of 25 ° C by the water activity analyzer (Novas, Labmaster analyzer, Switzerland). All measurements were carried out in triplicate.

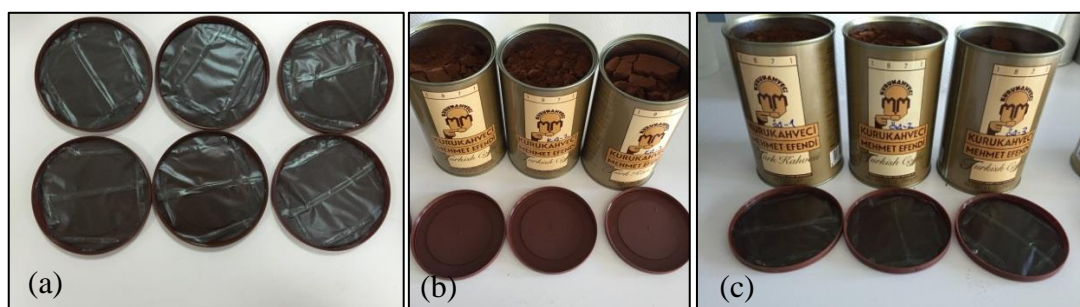


Figure 5.4. Lid of the metal cans with (a) integrated hydrogel films, (b) control coffee sample and (c) coffee package with hydrogel film

5.9.2. Packaging for high moisture foods: The case of mushroom and broccoli

In order to develop effective humidity regulating packaging system based on hydrogels for fresh mushrooms and broccoli, first of all, the moisture loss behavior of these produces were determined under varying relative humidity and temperature conditions. By this way it was possible to have an idea of the amount of water vapor which is expected to accumulate in the headspace package volume. From these findings it will be possible to estimate the amount of water vapor that need to be trapped in order to avoid condensation inside the package. Then the water absorption capacity of the hydrogel was determined under same temperature and relative humidity conditions. In order to have a better idea about the water absorption capacity of the hydrogels the results were compared with that of silica gel which was used as a reference material. The results of these experiments allowed us to calculate the amount of hydrogel required for effectively regulating the relative humidity at an optimum level inside the package headspace. Once the amount of hydrogel was calculated the effectiveness of the hydrogel packaging in relating the humidity inside package headspace was tested with mushrooms and broccoli by continuously monitoring the headspace humidity under constant temperature regimes. Finally, the whole packaging system was tested under fluctuating temperatures between 5 to 25 °C in order to simulate the real life supply chain scenario.

5.9.2.1. *Moisture loss behavior of mushrooms and broccoli florets*

Mushroom and broccoli heads were bought from local market. Broccoli florets were detached from the main stem with a sharp knife. Then mushrooms or broccoli florets were sorted for uniform size and bruised ones were discarded. Before the experiment, the samples were placed in climate cabinet for thermal equilibrium. Moisture loss behavior of each food group was evaluated by performing mass loss technique at three different RH (65, 85 and 100%) and two different temperatures (5 °C and 25 °C). For doing so, three samples of each food group were weighed and placed in desiccator with desired RH and temperature. The humidity within desiccators were independently controlled by using saturated solutions of cobalt (II) chloride, potassium chloride and water giving 65, 85 and 100% RH, respectively (Figure 5.5). Each sample was taken out of the desiccator at determined time intervals (0, 2, 4, 6, 24, 28, 30 and 48 hours) and weighed. The moisture loss behaviors were determined gravimetrically by measuring decrease in weight of each food sample at each time interval. Electronic balance was used to weigh the samples during experiments.

Moisture loss of mushroom and broccoli florets at each RH and T were calculated according to Eqn.4.5.

$$\text{Moisture loss} = (M_i - M) / (t * M_i) \quad (4.5)$$

Moisture loss was expressed in $\text{mg kg}^{-1}\text{s}^{-1}$

M_i is the initial weight of each sample in kg

M is the weight of sample at each time interval, in mg

t is the time at which samples were weighed, in seconds

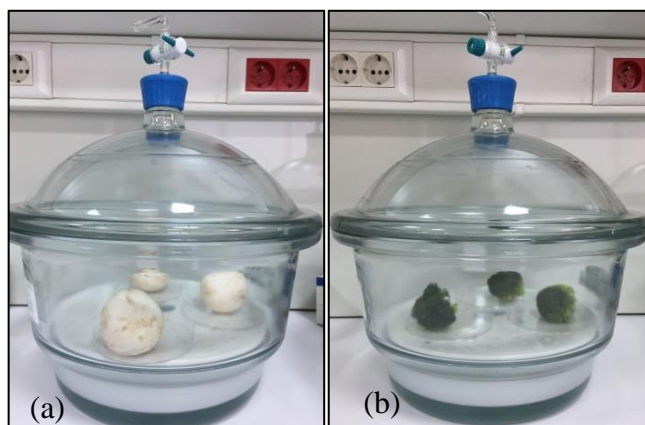


Figure 5.5. (a) Mushroom and (b) broccoli placed in desiccator with desired RH and T

5.9.2.2. *Water absorption capacity of hydrogel*

Water absorption capacity of hydrogel film designated with label Gnp1 and silica were determined. Silica is known for its high water absorption capacity and used as a reference material to compare the water absorption capacity of the hydrogel films. Each experiment was carried out at three different RH (65, 85 and 100%) and two different temperatures (5 °C and 25 °C). Hydrogel films which have been prepared in petri dishes were cut into 4 pieces. Each hydrogel film and silica gels were weighed. Three samples of hydrogel films or silica were weighed and placed in desiccator with desired RH and T (Figure 5.6). Humidity within the desiccators were independently controlled by using saturated solutions of cobalt (II) chloride, potassium chloride and water giving 65, 85 and 100% RH, respectively. Desiccators were placed in the controlled climate cabinet maintained at to desired temperature. Each sample was taken out of desiccator at each determined time intervals during 48 hours and weighed. The water absorption capacities were determined mass gain technique by measuring increase in weight of hydrogel and silica samples at each time intervals. Electronic balance was used to weight the mass off samples during experiments.

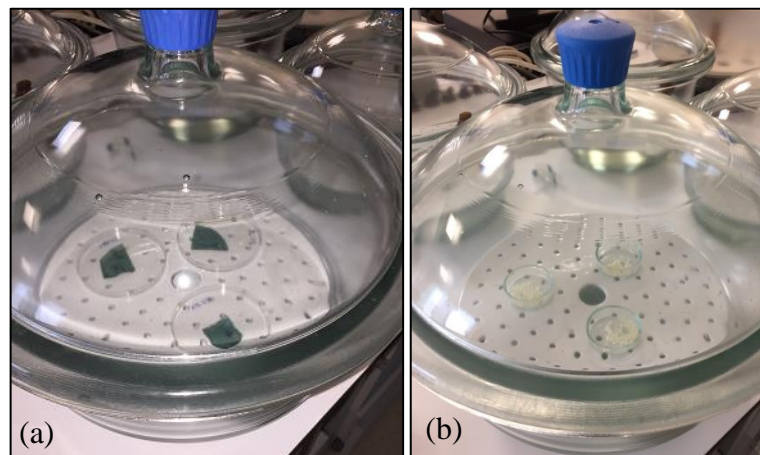


Figure 5.6. (a) Hydrogel film and (b) silica gels placed in desiccator with desired RH and T

5.9.2.3. Humidity regulation by hydrogel in package headspace at constant temperature

In order to determine whether the presence of hydrogel and silica inside the package affect the moisture build up in the mushroom and broccoli package headspace, a separate study was performed. As it can be seen from Figure 5.7 mushroom or broccoli florets were placed into small polystyrene bowls. A small hollow was pierced on the surface of the bowl to integrate the data logger sensor for temperature and relative humidity. Then, mushroom/broccoli and a data logger with humidity/temperature sensor were placed in the bowl. Hydrogel films which have been prepared in petri dishes were cut into 4 pieces and each hydrogel film was weighed and placed in the bowl with mushroom/broccoli. A stretch film was used to pack the bowl. This set up was placed in controlled chamber maintained with 5 °C and 25 °C. Initial weight of mushroom, empty bowl and stretch film were weighed on an electronic balance and recorded. The % RH and temperature within the bowl were recorded each 10 seconds continuously. At the end of the experiments; mushroom/broccoli, bowl and stretch film were weighed again. The presence and severity of water condensation on the packaging film was visually observed and noted. The same experimental set up was done by replacing hydrogel with silica gel which was used as reference. As a control treatment, same experimental set up was used to follow the mushroom behavior without hydrogel. The % RH measurement was continued until getting constant measure. All experiments were done triplicate.

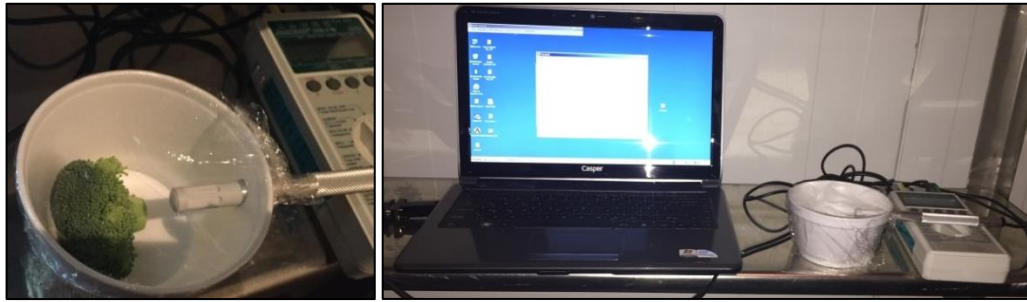


Figure 5.7. Experimental set-up for humidity regulation experiments

5.9.2.4. Humidity regulation with hydrogel in package headspace at fluctuating temperatures

In the final stage of the study, the effect of using hydrogel packaging system on maintaining the quality of fresh mushrooms and broccoli florets in real life supply chain conditions was investigated. For doing so, the mushrooms/broccoli florets were packed in a polystyrene tray with hydrogel film and covered with polyethylene stretch film. Then the packaged produces were subjected to temperature fluctuations for varying durations according to a supply chain scenario as given in Table 5.4. This scenario was constructed based on the prior literature [96]. However, for the estimation of the durations in Turkey the help of experienced food auditors from the TUBITAK MRC Food Institute was sought. As it can be seen from this table, the supply chain assumed to start at packaging house and involves several interruption of the cold chain resulting in sudden increase of the temperature. The last step of the supply chain was 17 hours of storage at home refrigerator. As it was described in previous sections the temperature and the relative humidity inside the packages were monitored continuously all through the simulation study. At each supply chain step, pictures of samples were taken in order to inspect visually the water condensation on the package surface. Besides, at the beginning and at the end of the cycle, weight of each sample, stretch film, box and hydrogel film were recorded. Then microbial load, color and texture of the mushrooms and broccoli florets were analyzed. The results were compared with the experiment carried out with packages which do not contain hydrogels.

Table 5.4. Transportation stages simulation cycle

Duration	Temperature	Supply Chain Step
1 hour	5 °C	Transportation from packaging house to supermarket
2.5 hours	20 °C	Cold chain interruption before storage
1 hour	5 °C	Supermarket warehouse
0.5 hour	20 °C	Cold chain interruption before display in the supermarket
1 hour	5 °C	Retail display
1 hour	20 °C	Transportation from market to home
17 hours	5 °C	Home refrigerator

25 g of mushroom or broccoli florets were mixed with Maximum Recovery Diluent (MRD) and placed in a sterile stomacher bag before being homogenized for 5 min at a normal speed with a stomacher machine (Bag mixer, Interscience, Saint Nom, France). Then serial dilutions were made from homogenized samples and enumerated on Plate Count Agar (PCA) for total aerobic bacteria and Dichloran Rose Bengal Chloramphenicol (DRBC) Agar for mold and yeast determination. For total bacteria analysis, the petries in duplicate were incubated at 30 °C for 24-48 h. At the end of the incubation time colonies were counted and results were expressed as log CFU/g. For mold and yeast analysis, the petries in duplicate were incubated at 22 °C for 48-120 h. At the end of the incubation time colonies were counted and results were expressed as log CFU/g.

Colors of the produces were measured by using a computer vision system (CVS) (VeriVide, UK). The system consists of a closed cabinet which was illuminated with two D65 lamps through reflective plates in diffuse mode. The photo of the fruit was taken from the top of the cabinet using a Nikon D90 digital camera equipped with 35 mm Nikon Nikkor lens. Before taking the image, white balance of the camera was made and calibrated by using colour chart provided by the manufacturer of the CVS. The images were taken at a shutter speed of 1/10 with 6.3 aperture and 200 sensitivity. Captured raw image was transmitted to the computer for colour measurement using colour clustering feature of the DigiEye Software. The software calculated the colour of the selected fruit surface by taking the average CIE L*, a* and b* values of each pixel of the fruit image. The L* value, represents brightness and darkness, a* value indicates greenish and redness as the value increases from negative to positive, and b* represents bluish and yellowish.

C^* is saturation and represents the brightness or dullness, calculated according to following equation ($C^* = \sqrt{(a^*)^2 + (b^*)^2}$). The hue angle represent the difference in hue and was calculated according to following equation ($h^\circ = \arctan(b^* / a^*)$). Hue angle is shown in degrees and 0° , 90° , 180° and 360° represents coordinate of $+a^*$, $+b^*$, $-a^*$ and $-b^*$, respectively. Figure 5.8 depicts the illustration of CIE L a b color space.

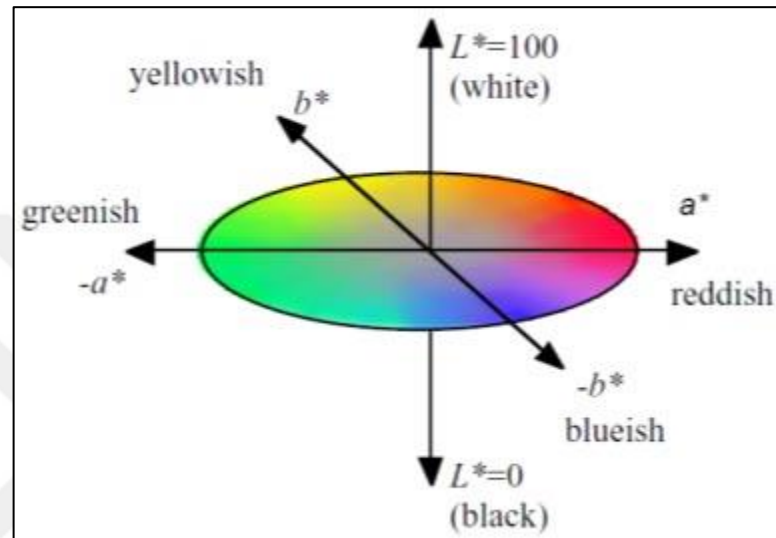


Figure 5.8. Illustration of CIE L a b color space [97]

The firmness of mushrooms and broccoli florets were determined by using a TA-XT plus Texture Analyser (Stable MicroSystems, UK) with a 2 mm diameter needle probe attached to 50 kg load cell and peel was punctured at a speed of 1 mm s^{-1} to a depth of 4 mm. Measurements were made on the center of the cap of mushrooms and broccoli florets.

6. CHARACTERIZATION OF CHITOSAN-CARBOXYMETHYL CELLULOSE HYDROGEL FILMS AND THEIR PROPERTIES

6.1. DETERMINATION OF THE OPTIMUM CMC / CH RATIO

The chitosan-HCl solution prepared in stoichiometric ratio was titrated with 1% (w/v) CMC solution to determine the turning point. pH and dpH (change in pH) values were plotted as a function of mass ratio between titrating partners as shown in Figure 6.1 (a). The pH of the chitosan solution was increased from 4.73 to 6.30 by addition of CMC solution. Approximately, 24 mL of CMC solution was consumed for 10 mL of chitosan solution for the turning point to be observed. This corresponds to a Ch:CMC mole ratio of 694.4:1 and an approximate mass ratio of 1:0.96, for maximum interaction between the two.

For the conductometric titration experiment, the conductivity was plotted against the mass ratio of CMC/Ch as shown in Figure 6.1(b). As can be seen in the figure, at the beginning, the conductivity of the Ch(HCl) solution showed small fluctuations, refers to neutralization of ammonium groups of chitosan then, it began to increase with the CMC addition. After the equivalence point of the solution, the conductivity continued to increase due to excess negatively charged COO^- ions of CMC. At the equivalence point, positive ions of Ch and negative ions of CMC were in equal proportions. Conductometric titration results agreed with the potentiometric titration results, showing that electrostatic interaction between Ch and CMC occurred in an approximate mass ratio of 1:0.96.

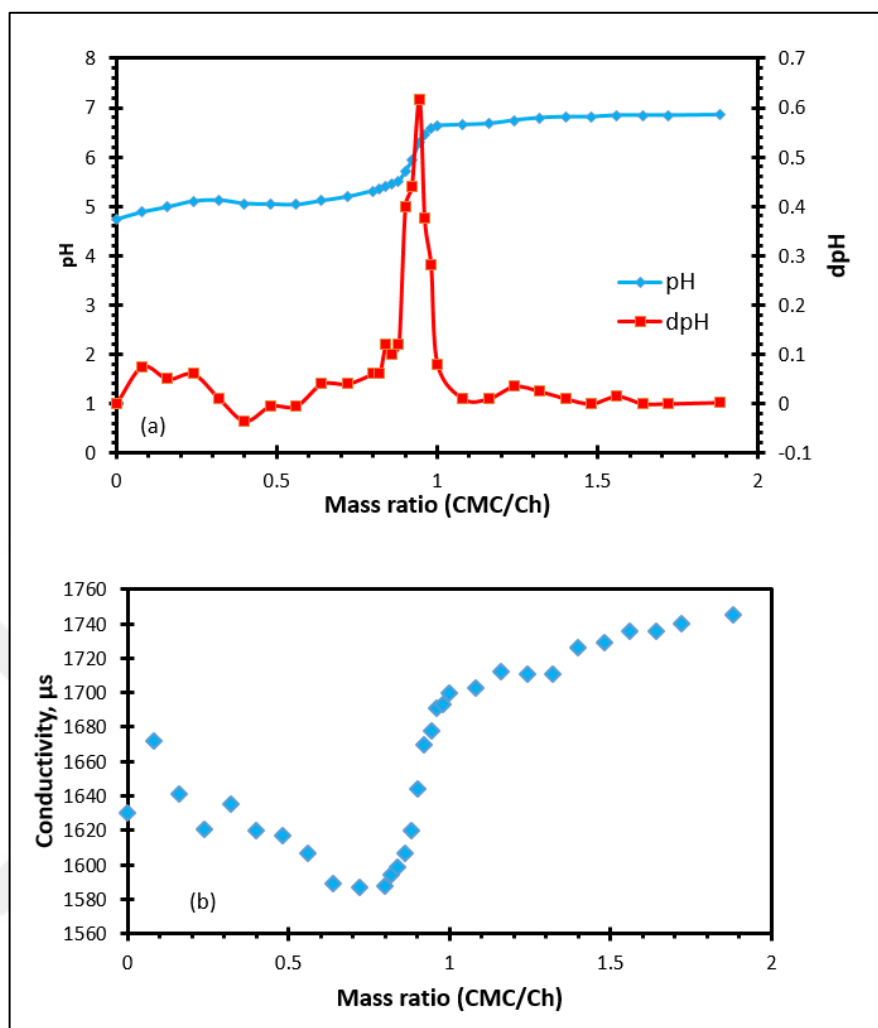


Figure 6.1. (a) Potentiometric and (b) conductimetric titration curves for the titration of Ch (HCl) solution with CMC solution

6.2. STRUCTURAL CHARACTERIZATION OF THE HYDROGEL FILMS BY FT-IR SPECTROSCOPY

Figure 6.2 (a) shows the FT-IR spectra of the chitosan (Ch(HCl)), CMC and physical hydrogel films prepared between Ch(HCl) and CMC. The FT-IR spectrum of chitosan (Ch(HCl)) showed a broad absorption band at 3278 cm^{-1} which corresponds to hydroxyl stretching. The sharp peaks at 1161 , 1072 and 1056 cm^{-1} belong to polysaccharide skeleton. The absorption band at 2913 cm^{-1} is attributed to C-H stretching. The characteristic absorption band at 1526 cm^{-1} corresponds to ammonium groups on the chitosan backbone [98].

For the FT-IR spectrum of CMC, the two main characteristics bands of CMC can be seen at 1599 cm^{-1} and 1420 cm^{-1} , which correspond to asymmetrical and symmetrical stretching vibrations of carboxylate (COO^-) groups, respectively. The FT-IR spectrum of physical hydrogel film formed between $\text{Ch}(\text{HCl})$ and CMC differs from its polymer partners. Characteristic peak of COO^- groups in CMC at 1599 cm^{-1} shifted to a slightly lower wavenumber and formed a broad peak at 1586 cm^{-1} [99]. The 1526 cm^{-1} peak of the ammonium group ($-\text{NH}_3^+$) of $\text{Ch}(\text{HCl})$ seems to shift to a higher wavenumber and appeared as a shoulder on the right side of the 1586 cm^{-1} band for the $\text{Ch}(\text{HCl})$ -CMC film, which might be the result of the electrostatic interaction between ammonium group of $\text{Ch}(\text{HCl})$ and carboxylate group of NaCMC [53, 100]. Thus the FT-IR data showed that an inter polymer complex has formed between $\text{Ch}(\text{HCl})$ and CMC as a result of the electrostatic interaction of the ammonium groups ($-\text{NH}_3^+$) of $\text{Ch}(\text{HCl})$ with the carboxylate groups ($-\text{COO}^-$) of CMC.

Figure 6.2 (b) shows the FT-IR spectra of hydrogel films cross-linked with changing amounts of genipin as well as the un-cross-linked film. Liu et al. [101] and Aldana et al. [102] in their studies of genipin cross-linked chitosan and its IPNs with polyethylene glycol, suggest that a new band appeared at 1640 cm^{-1} that resulted by the formation of the secondary amide bond formed with the interaction between the carboxymethyl group of genipin and amino group of chitosan. In Figure 3(b), all the cross-linked films showed the broad peak at around 1586 cm^{-1} that stands for the stretching vibrations of carboxylate (COO^-) group of CMC interacting with the ammonium groups of chitosan similar to that of un-crosslinked film. The spectrum of the Gnp2 cross-linked hydrogel film exhibited a shoulder on the left side of absorption band at 1586 cm^{-1} which may correspond to the absorption band of 1640 cm^{-1} suggesting that the secondary amide band was formed due to crosslinking reaction between genipin and chitosan for the Gnp2 hydrogel film. For the other cross-linked hydrogel film samples, Gnp05 and Gnp1, this secondary amide band was not detectable in the FT-IR spectra. In addition this area also interferes with chitosan absorption band in the same region. Thus, FT-IR spectroscopy was not an effective method to follow the crosslinking of chitosan with genipin.

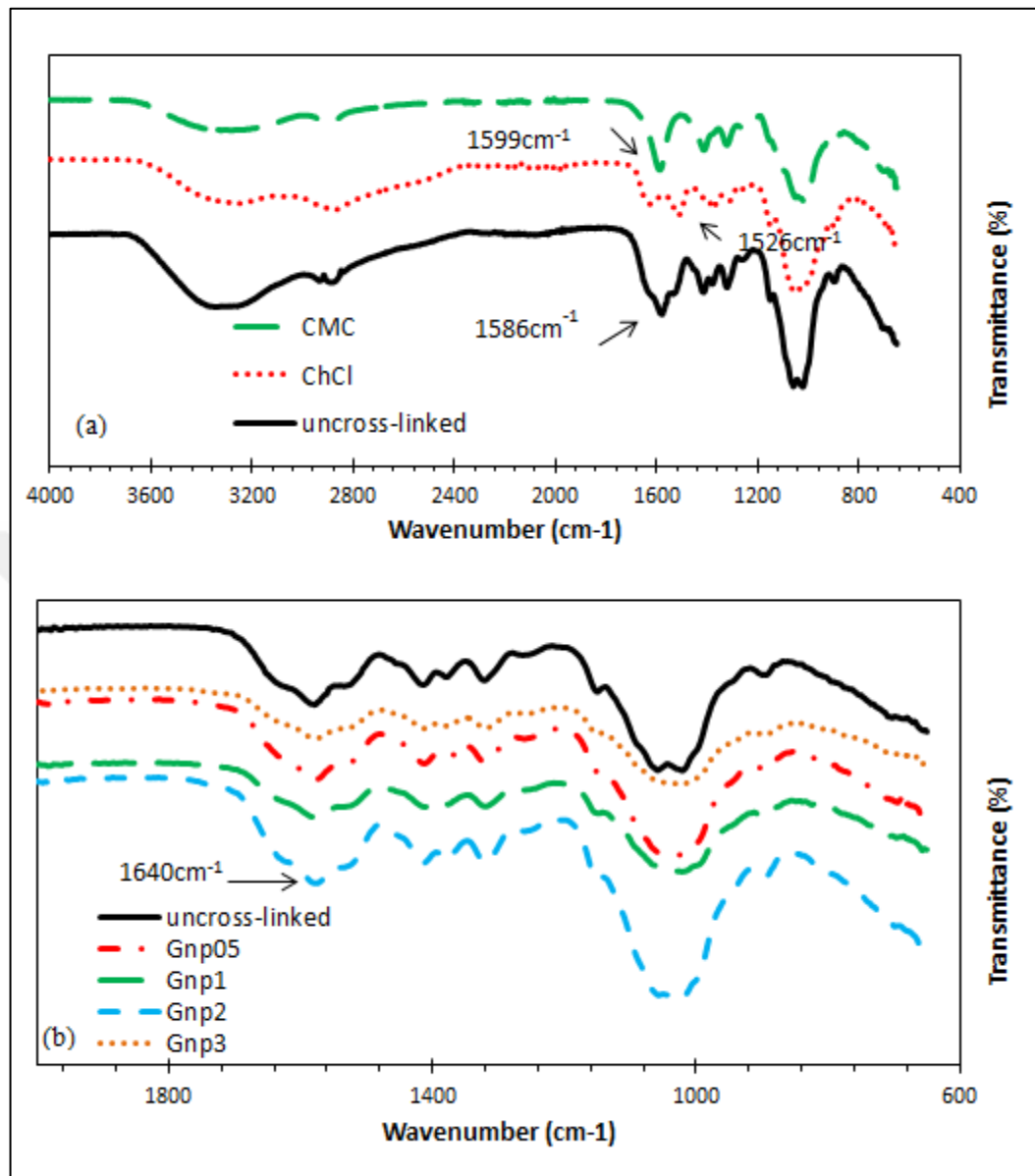


Figure 6.2. FT-IR spectra of (a) chitosan (Ch(HCl)), Na-CMC and physical hydrogel films prepared between Ch(HCl) and (b) Na-CMC and hydrogel films of Na-CMC and Ch(HCl), cross-linked with genipin

6.3. CROSSLINKING EVIDENCES OF HYDROGEL FILMS

The uncross-linked film and Gnp05 film disintegrated immediately with the contact of 0.1N HCl solution. Gnp1, Gnp2 and Gnp3 films kept their uniformity during 168 hours without any disintegration. These results show that genipin crosslinked hydrogel films were obtained

with all formulations except Gnp05 sample. The experimental results show that permanent interpenetrating polyion complex hydrogel films were prepared for higher genipin content.

There are some studies in the literature that describe the presumed mechanism of the crosslinking of genipin with primary amine groups and formation of the blue pigments [103-105]. These studies suggest that blue pigment formation is an evidence that the crosslinking reaction occurred. Touyama et al. studied on the formation of blue pigments caused by mechanism between genipin and methylamine, which is the simplest primary amine group. Genipin reacts with primary amine group to form secondary amino group. Oxygen radical-induced polymerization reaction forms between genipin and air. Dehydrogenation of the intermediate compound appeared by ring opening reaction of genipin. Butler et al. also reported that no blue pigment was appeared with the addition of genipin to acetylglucosamine unit [103]. It can be seen in Figure 6.3 that the Gnp1, Gnp2 and Gnp3 film exhibit a blue color. The Gnp05 film shows a transparent color without any blue pigment. The blue color gets darker with increase in the crosslinking agent content. This information also confirms that crosslinking has occurred in the Gnp1, Gnp2 and Gnp3 hydrogel films. The result for sample Gnp05 is also consistent with the crosslinking test above.



Figure 6.3. Hydrogel film samples with ratios of genipin/chitosan of Gnp05, Gnp1, Gnp2 and Gnp3, w/w from left to right

6.4. SWELLING DEGREE OF HYDROGEL FILMS IN WATER

Swelling ratio of chitosan networks is pH and temperature dependent. It swells more and faster in acidic medium and higher temperatures rather than at basic medium and lower temperatures. In acidic medium, protonation of amino groups of chitosan causes electrostatic repulsion along the polymer chains throughout the chitosan network and leads to expansion

in the network. In basic medium, electrostatic repulsion is decreased due to the deprotonation of amino groups, leads shrinking within the chitosan network [106, 107].

Figure 6.4 shows the swelling degree as a function of time for uncross-linked and cross-linked hydrogel films. Maximum swelling was reached for uncross-linked hydrogel film. For the uncross-linked film, swelling degree increased within first 18 min, stayed constant till 60 min and then decreased and finally reached a plateau. The uncross-linked sample reached a higher swelling degree because of a lower and less efficient cross-link density as compared to Ch -CMC films with covalent cross-links. Because only physical interactions exist between Ch and CMC within network for the physical hydrogel film, weak ionic bonds might be broken first resulting in the first plateau with a higher swelling degree observed and the decrease in the swelling degree to a second plateau may suggest that some of these ionic bonds were re-established within the network. The hydrogel film sample Gnp05 exhibited a similar behavior as the uncross-linked sample, but with a lower swelling degree. This may indicate that physical interaction predominates and chitosan was covalently cross-linked only to a limited extent for samples cross-linked with 0.5% genipin. The crosslinking evidence experiment results explained these observations for uncross-linked and hydrogel with designation Gnp05 and why they possessed lower swelling degree compared to Gnp1, Gnp2 and Gnp3. For the other hydrogel films cross-linked with higher contents of genipin, swelling degree increased sharply within the first few minutes then reached a plateau within 30 min. The observance of such a plateau in the swelling degree vs time plots confirms the existence of stable chemical crosslinks within the network. In addition, the fact that the swelling degree decreased with increasing genipin content from 1 to 3 wt% (based on chitosan weight) indicates that cross-linking density increased with increasing genipin content. The hydrogel films cross-linked by higher amount of crosslinking agent possess higher crosslinking density, allowing less water into the hydrogel network. On the other hand, more water diffuses within lower polymeric network density, leading to an increase in swelling ratio [108]. The swelling degree (%) values of the hydrogel films at equilibrium after 210 minutes can be seen in Table 6.1.

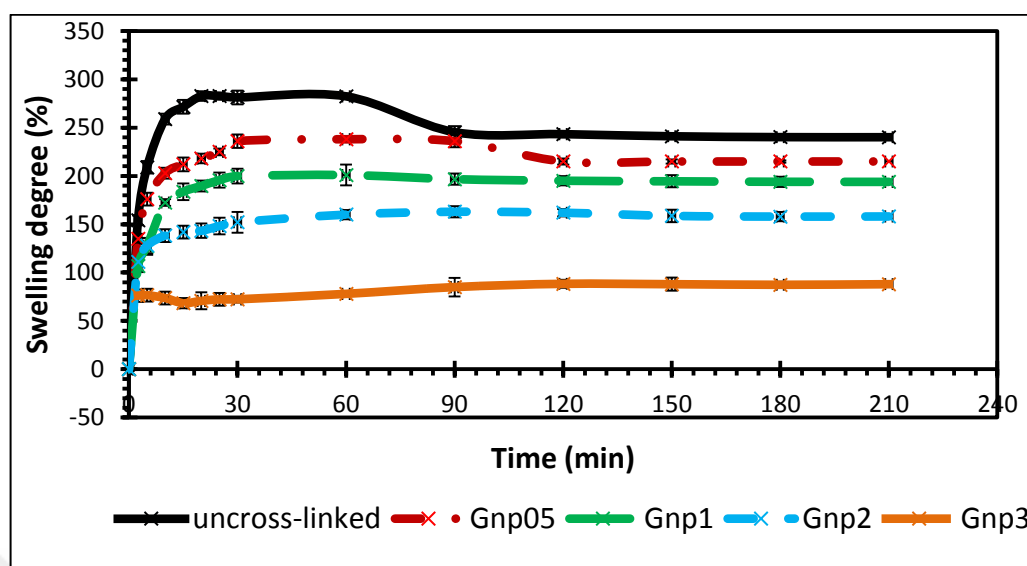


Figure 6.4. Swelling degrees (%) of uncross-linked and cross-linked hydrogel films as a function of time

Table 6.1. The swelling degree (%) of the hydrogel films in water at equilibrium after 210 minutes

	Swelling degree (%)
Uncross-linked	240
Gnp05	215
Gnp1	194
Gnp2	158
Gnp3	91

6.5. DIFFERENTIAL SCANNING CALORIMETRIC (DSC) ANALYSIS

Figure 6.5 shows the DSC curves of the hydrogel films. The broad endothermic peaks at around 120 °C, 120 °C, 125 °C, 105 °C and 132 °C for uncross-linked, Gnp05, Gnp1, Gnp2 and Gnp3 film samples respectively, may be attributed to the evaporation of residual water and/or acetic acid from the films. The temperature at which the residual water evaporates in the system seems to increase with cross-linking with the exception of sample Gnp2. Increase in the cross-link density with the increase in cross-linker ratio (from 0 wt % to 1 wt % and then to 3 wt % genipin respectively) may enhance the capability of caging the water within

the network. Therefore, residual water in hydrogel film with higher crosslinking density evaporates at higher temperature. The exo-thermic peaks observed at around 240-250 °C for all the films, can be attributed to degradation of chitosan and carboxymethyl cellulose units within the network [109, 110].

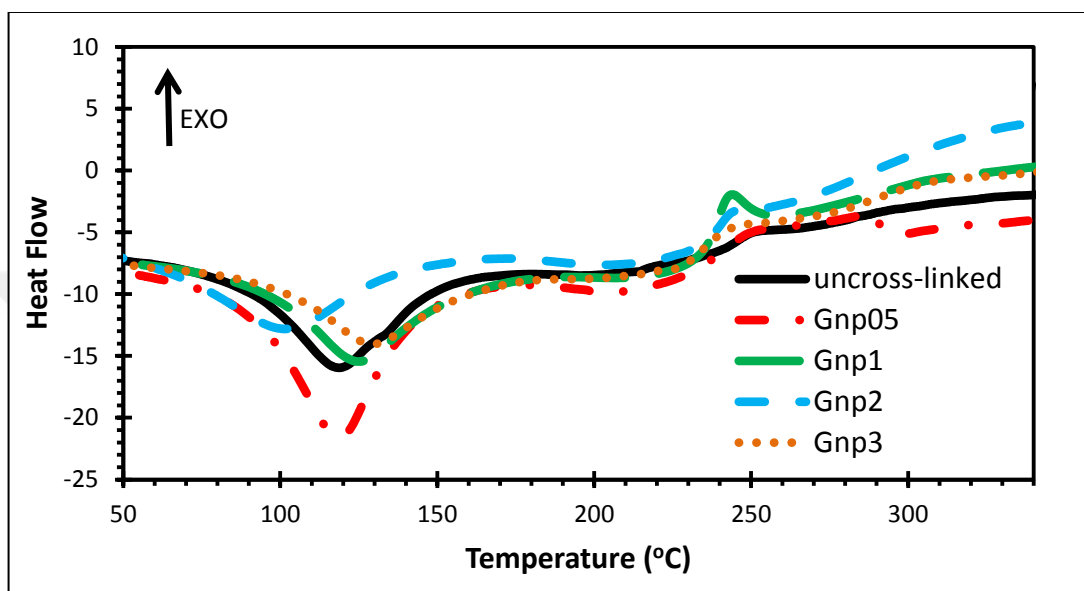


Figure 6.5. DSC thermograms for uncross-linked and cross-linked hydrogel films

6.6. DYNAMIC MECHANICAL ANALYSIS (DMA)

The thermomechanical properties of the hydrogel films prepared were determined by DMA. Figure 6.6 (a), and (b) show the storage modulus, and tan delta versus temperature plots of the hydrogel films. Figure 6.6 (a) shows that between -5 °C and 50 °C which includes a temperature region where these materials can be used as packaging films, the storage modulus values are generally higher for the cross-linked films as compared to un-cross-linked film with the exception of the Gnp3 film. The room temperature (25 °C) storage modulus values of the hydrogel films are also listed in Table 6.2. As can be seen the Gnp 3 film exhibits a storage modulus value lower than that of both the uncross-linked film and the other cross-linked films (Gnp 0.5, Gnp 1, Gnp 2). One explanation for this result can be given as the following. This system involves only physical cross-links for the covalently un-crosslinked film and both physical and covalent cross-links for the films cross-linked with genipin, thus the further use of NH₂ groups of chitosan for cross-linking with genipin

at the higher contents of genipin (3wt% based on Ch weight) instead of ionic crosslinks with CMC might have resulted in a too loose interaction with the CMC component within the network resulting in the lowering of the storage modulus values. T_g for cross-linked hydrogel films was determined using the peak temperatures of the tan δ curves shown in Figure 6.6 (c). J. Bonilla et al. reported that there are many parameters effecting T_g of chitosan such as extraction methods, source or deacetylation degree [111]. Some studies report that there is no evidence for the T_g of chitosan and discuss that T_g for chitosan is higher than its degradation temperature making it difficult to determine its T_g [112]. However some previous studies reported that T_g of pure chitosan and CMC as 203 °C [113] and 75 °C [114], respectively. In our study, the tan delta curve (Figure 6(b)) for the uncross-linked hydrogel film exhibits two major peaks at 41 and 206 °C which were attributed to the T_g of CMC and Ch components respectively. The tan delta curves of the cross-linked films on the other hand exhibited only one peak in the 205 to 222 °C region, close to Ch's T_g, indicating that the phase separation of CMC and Ch disappeared for the chemically cross-linked films with interpenetration of CMC within chitosan polymer network. The T_g values as determined from the temperature of the maxima in the tan delta curves of the hydrogel films are also listed in Table 6.2. As can be seen, the T_g of the uncross-linked film that occurs in the glass transition region of pure Ch is 206 °C, and this T_g value increases to 209 °C and 221 °C for the cross-linked films Gnp0.5 and Gnp1 respectively and then decreases back to around 206-205 °C for the Gnp2 and Gnp3 films.

Swelling studies in water as well as TGA data indicate that the cross-link density of the chemically cross-linked hydrogel films increases with increasing genipin content of the films, and for each of the analysis this cross-link density should refer to the permanent covalent cross-links. Thus an increase in the T_g with increasing cross-link density for the Gnp2 and Gnp 3 films is expected. However, as mentioned earlier, since the cross-linked hydrogel films possess both physical and covalent cross-links, at higher Gnp contents, the further use of NH₂ groups of chitosan for cross-linking with genipin instead of ionic crosslinks with CMC might have resulted in a looser interaction with the CMC component of the system where CMC acts to lower the T_g. Finally, the third peak starting to appear at around 300 °C on the Tan delta curves of the hydrogel films, may correspond to the beginning of degradation of polymers, in accordance with DSC and TGA results.

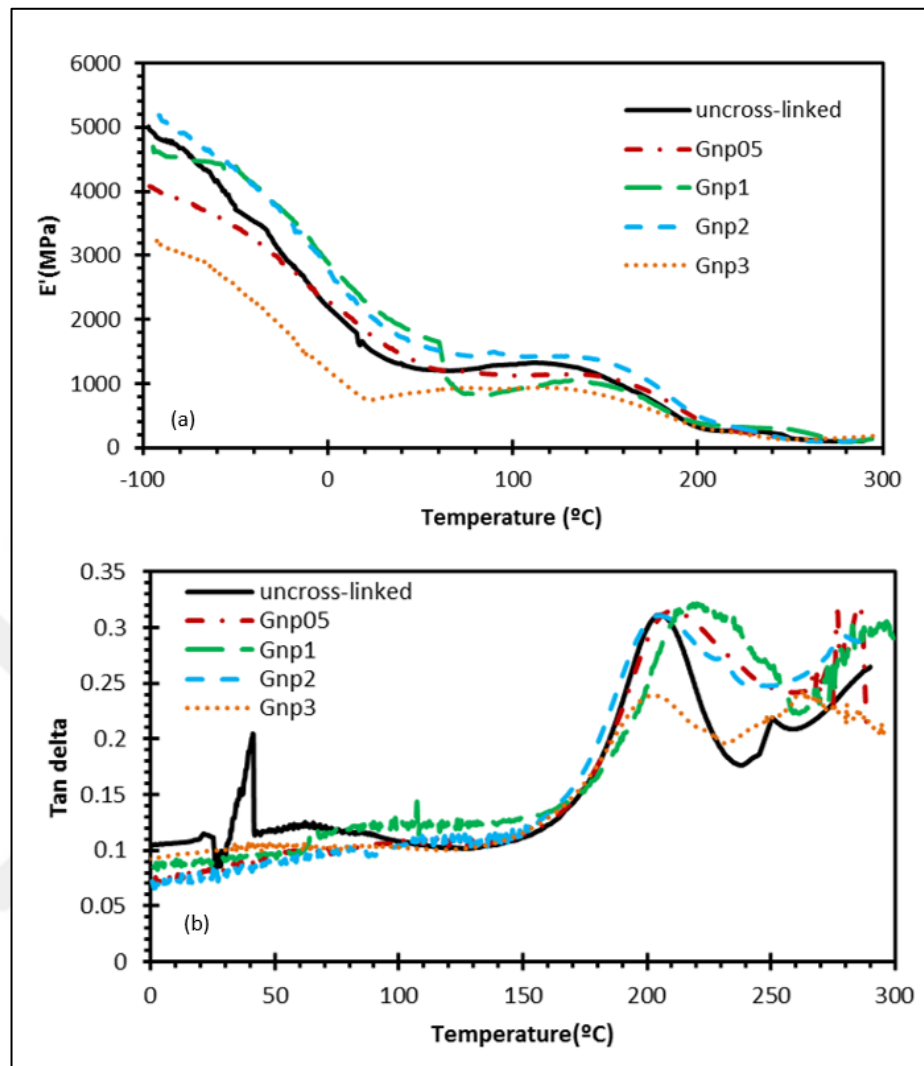


Figure 6.6. (a) Storage modulus (E') and (b) tan delta variation with temperature for uncross-linked and cross-linked hydrogel films

Table 6.2. Storage modulus values at 25 °C and T_g values of hydrogel films as determined from DMA

	$E'(25\text{ °C})$ (MPa)	T_g (°C) (Tan delta max.)
Uncross-linked	1480	41(CMC), 206(Ch)
Gnp05	1704	209
Gnp1	2176	221
Gnp2	2000	206
Gnp3	750	205

6.7. THERMAL GRAVIMETRIC ANALYSIS (TGA)

There are two significant weight loss stages observed in the TGA curves of newly developed hydrogel film samples, shown in Figure 6.7. The first weight loss observed at 25–120 °C may be attributed to the evaporation of residual water and/or acetic acid from film samples [114, 115]. This weight loss for uncross-linked sample is around 25%. It is accompanied by the weight loss of around 17-20% for the cross-linked hydrogel films. The second weight loss step occurs in range of 250–500 °C. This second weight loss can be attributed to the thermal degradation of chitosan and carboxymethyl cellulose and volatilization of glycerol having boiling point around 298 °C [110, 116, 117]. Char residue at 800 °C is 4% for uncross-linked hydrogel film, 14% for Gnp05, 29% for Gnp1, 33% for Gnp2 and 32% for Gnp3. Looking at the thermal degradation profiles of all the films, one can say that, thermal stability decreases in order Gnp3>Gnp2> Gnp1> Gnp05> uncross-linked hydrogel films. In addition the char residue contents of the films, indicate that films prepared with higher amount of cross-linker possess higher crosslink density as the char residue for network polymers should increase with increasing crosslink density.

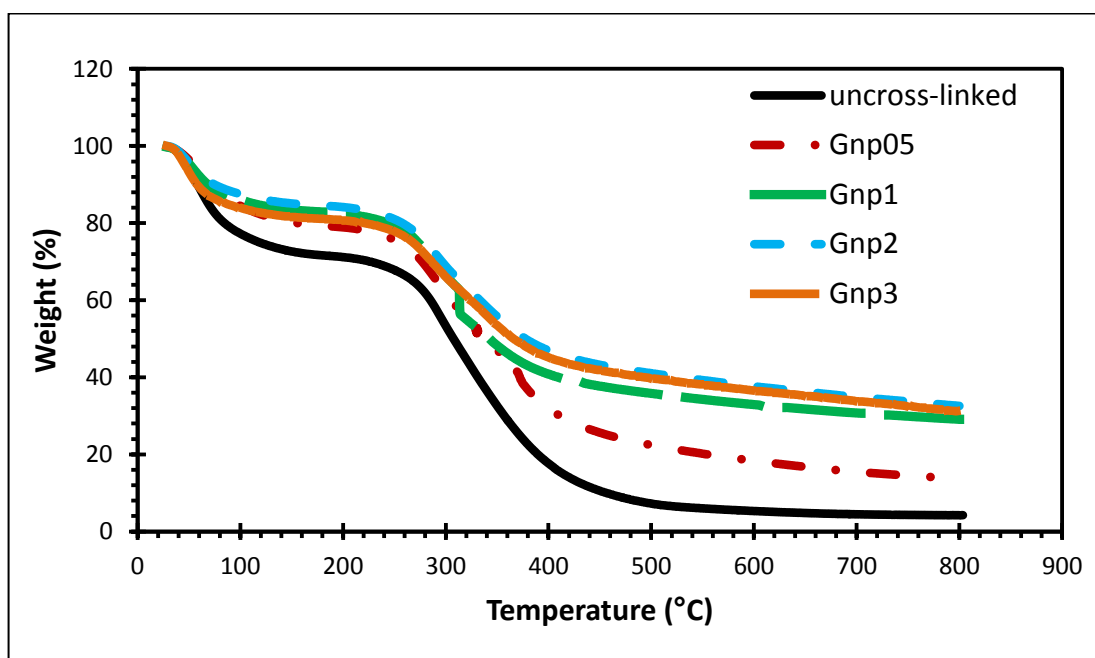


Figure 6.7. TGA curves for uncross-linked and cross-linked hydrogel films

6.8. TENSILE TESTS

The tensile modulus, tensile strength and elongation at break values for the hydrogel films, calculated as described in Section 5.7 are shown in column graphs in Figure 6.8 (a), (b) and (c) respectively. As can be seen in Figure 5.8 (a), the lowest tensile modulus was observed for uncross-linked film as 281 MPa and it increased for hydrogel films with increasing genipin content to 663 MPa for the Gnp3 film. The tensile strength of the hydrogel films in a similar manner, increased with crosslinking, the tensile strength of the uncross-linked film was 11.9 MPa, this value increased to 15.3 MPa and 15.4 MPa for the cross-linked films Gnp3 and Gnp2 respectively. Thus the increase in cross-link density of the chitosan component of the Ch: CMC system with increasing genipin content acted to increase both the tensile modulus and strength of the hydrogel films. In addition, as can be seen from Figure 5.8 (c), the elongation at break values decreased gradually with the increase in genipin content of the films, due to increase in cross-link density as expected.

Tensile test results were similar with the results of thermo-mechanical tests. Regarding to DMA results, the storage modulus values were generally higher for the cross-linked films as compared to uncross-linked film as also seen for the tensile modulus data.

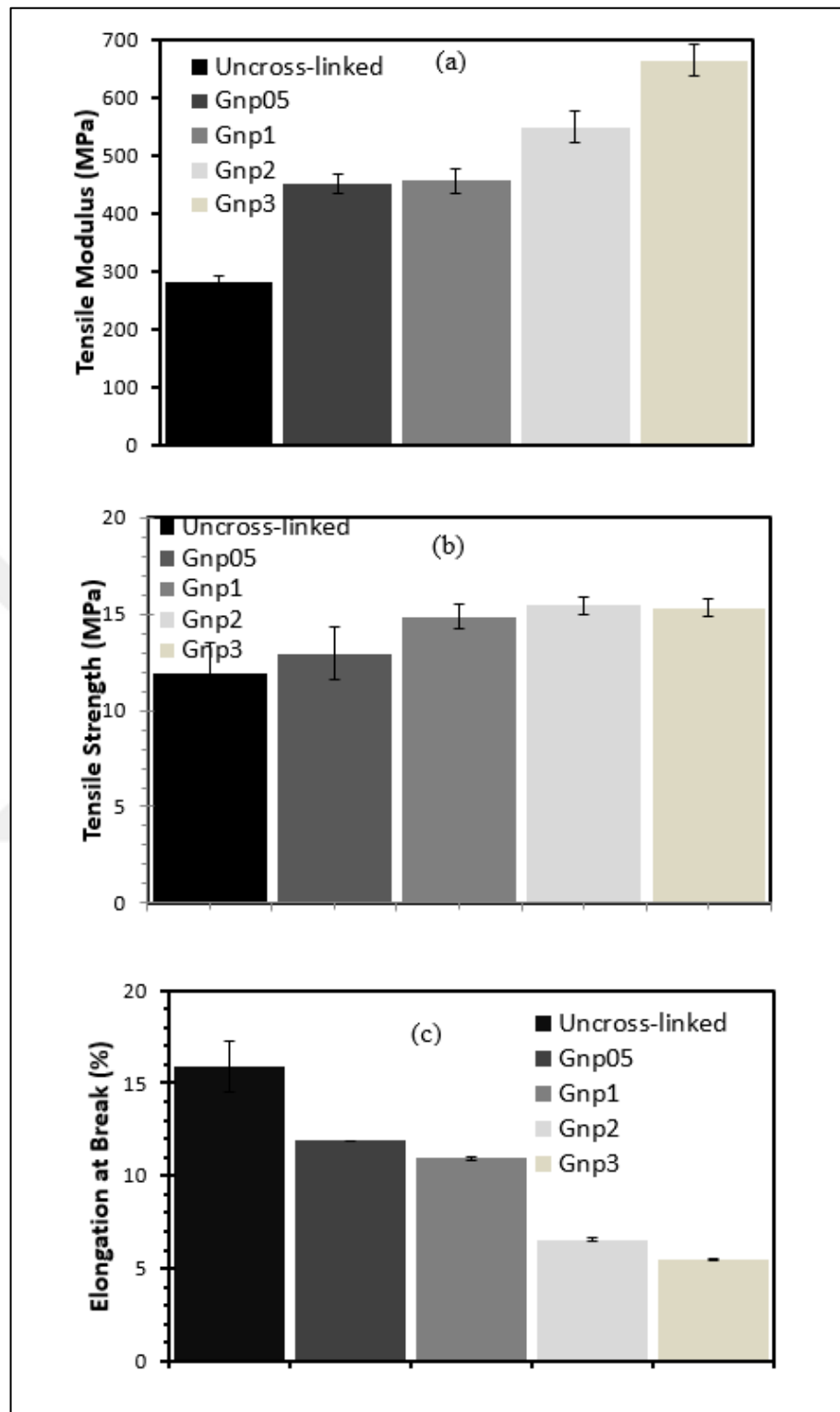


Figure 6.8. (a) Tensile modulus, (b) tensile strength and (c) elongation at break (%) values of uncross-linked and cross-linked hydrogel films presented in column graphs

6.9. BIODEGRADABILITY

As these biobased hydrogel films are designed to be used as food packaging materials, their biodegradability characteristics are important. Aerobic biodegradation of uncross-linked and genipin cross-linked (Gnp1) hydrogel films based on chitosan and Na-CMC in controlled compost at 58°C were measured by using MODA apparatus during 45 days according to ISO 14855-2 test method as described in the experimental section. The biodegradation degree of microcrystalline cellulose used as a reference material was over 70% in the controlled compost after 45 days. This showed that our experiments were valid according to ISO 14855-2.

All test materials in the controlled compost were disintegrated and disappeared At the end of the biodegradation tests,, as can be seen in Figure 6.9.

Cumulative evolved carbon dioxide during the tests can be seen in Figure 6.10 (a). Amount of carbon dioxide produced in test material containing compost vessel is greater compared to the blank compost for both samples. The difference between uncross-linked and genipin cross-linked hydrogel films is clearly observed. Biodegradation degrees (%) of test materials and microcrystalline cellulose as a reference material can be seen in Figure 6.10 (b). No lag phase was observed for uncross-linked and cross-linked hydrogel films and the microcrystalline cellulose powder. All started to degrade within the first day. A plateau phase was reached after 35 days, 35 days and 13 days for microcrystalline cellulose, uncross-linked film and cross-linked film, respectively. After 45 days, biodegradation degrees according to ISO 14855-2 method were 87 %, 72 % and 47 % for microcrystalline cellulose, uncross-linked and cross-linked hydrogel films, respectively. As can be clearly seen in Figure 6.10 (b), the degradation of genipin cross-linked hydrogel film is considerably slower as compared to that of the uncross-linked hydrogel film. As a result , the biodegradation degree of cross-linked hydrogel film after 45 days is significantly lower as compared to that of the uncross-linked film. In the uncross-linked system, all the amino groups of chitosan get only electrostatic interaction with carboxyl groups of Na-CMC. These physical hydrogels are reversible which means that these hydrogel structures can be easily disrupted by changes in physical conditions or application of a stress. In cross-linked network system, a portion of the amino groups of chitosan was cross-linked with genipin and CMC was introduced to this system by physical interaction. The chemically cross-linked hydrogel

system is more permanent and stable and has strong chemical bonds within network structure. Because only physical interactions exist between polymer chains of Ch and CMC and between the two, within uncross-linked hydrogel film network, these weak Van der Waals forces and ionic bonds might be easily broken within time resulting in much more swelling in high moisturized compost. The genipin cross-linked hydrogel film in which Ch chains are cross-linked via covalent bonds and CMC chains are interpenetrated in it via physical interactions, allows less water into the hydrogel network. As less water diffuses within this high polymeric network density, a decrease in swelling ratio is observed. This situation may enable that the uncross-linked hydrogel film structure gets subjected to attacks of microorganisms much more easily compared to the genipin cross-linked film resulting in a higher consumption rate by microorganisms. Thus, the difference between the swelling behaviors of the uncross-linked and cross-linked hydrogel films must be responsible for the differences in their biodegradation rates and biodegradation degrees. The crosslinking of the Ch component of the system with genipin and the formation of a semi interpenetrating polymer network (SIPN) significantly decreases the biodegradation rate of the Ch-CMC hydrogel films as compared to the un-crosslinked physical Ch-CMC hydrogel film.

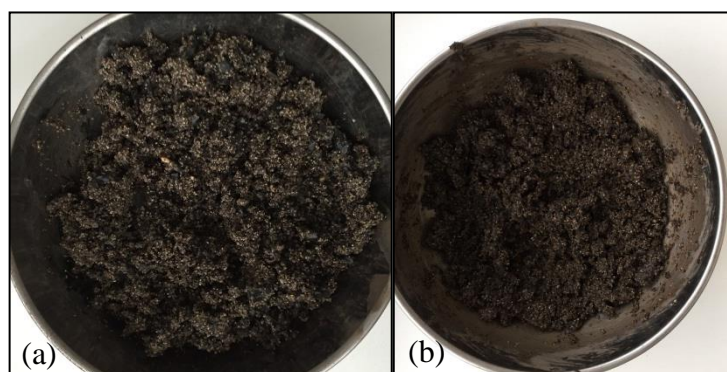


Figure 6.9. Test materials in compost after 45 days (a) uncross-linked film and (b) genipin-crosslinked film (Gnp1)

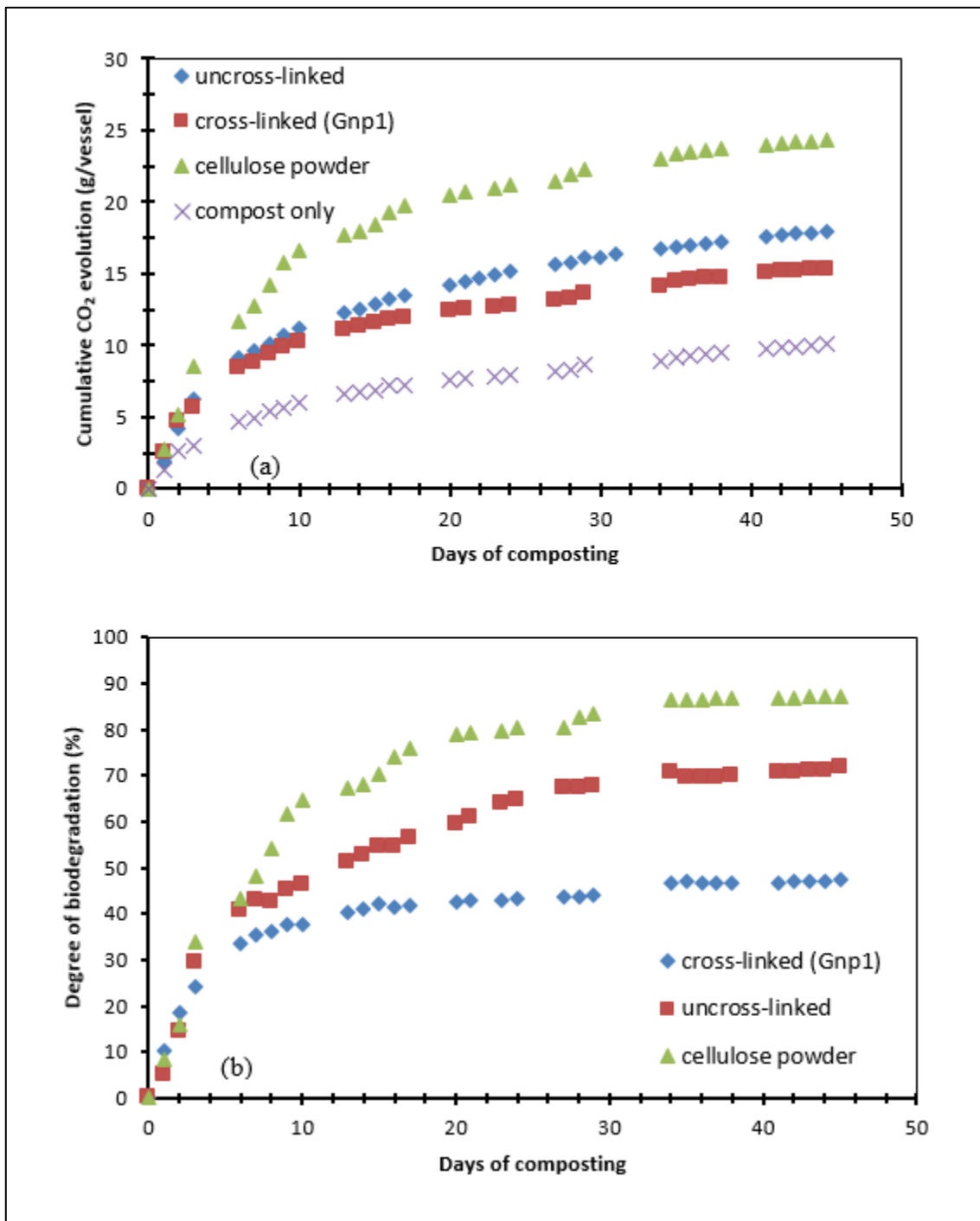


Figure 6.10. (a) Cumulative CO₂ evolution and (b) percentage biodegradation during 45 days

7. APPLICATIONS OF CHITOSAN-CARBOXYMETHYL CELLULOSE HYDROGEL FILMS IN FOOD PACKAGING

7.1. PACKAGING FOR MOISTURE SENSITIVE DRY FOODS: THE CASE OF TURKISH COFFEE

7.1.1. Relative Humidity

In Figure 7.1, relative humidity vs time curve can be seen for Turkish coffee stored at 5 °C and 20 °C. Initial value of the water activity of coffee was 0.162. The relative humidity increased within first 16 days and reached to equilibrium gradually until the end of the 36 days. The relative humidity at 5 °C reached to 0.189 and 0.171 for coffee stored in metal box control and metal box with hydrogel film after 16 days of storage, respectively. Whereas, the relative humidity at 20 °C reached to 0.199 and 0.249 for coffee stored in metal box control and metal box with hydrogel film after 16 days of storage, respectively. At the end of the storage time, the relative humidity of the samples were 0.195 and 0.182 at 5 °C and 0.210 and 0.285 at 20 °C for coffee stored in the metal box control and the metal box with hydrogel film, respectively.

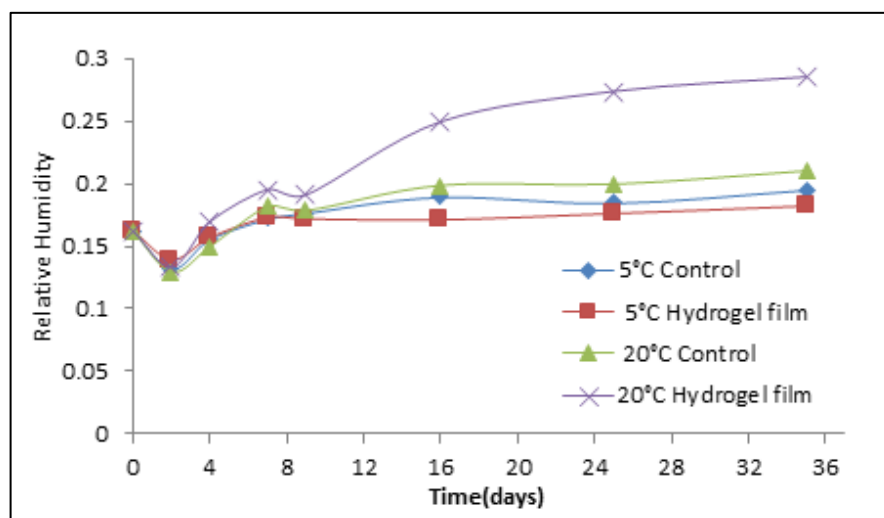


Figure 7.1. Relative humidity vs storage time plots of Turkish coffee at 5 °C and 25 °C

Relative humidity value at the equilibrium of coffee stored in the metal box with hydrogel film was greater than that of control at 20 °C although it was slightly less than that of the control at 5°C. These observations were somewhat in contradiction with our starting hypothesis. Actually, it was expected that hydrogel film would help to circumvent the increase in the relative humidity of coffee by absorbing excess moisture in the headspace of the metal box which ingress after multiple opening of the lid before usage. However, we measured lower relative humidity in coffees stored in the metal boxes without hydrogel film at 20 °C. This might be due to fact that the hydrogel film desorbs the absorbed excess moisture after closing the lid of the metal box which in turn reaches to moisture equilibrium with the coffee. This indicates that the hydrogel does not bind water permanently and it releases water when there is a water vapor deficit in surrounding atmosphere. It is also interesting to note that the moisture absorption capacity of the hydrogel increased with increasing temperature. The relative humidity of coffee stored in the control metal box and the metal box with hydrogel film were very similar within first 9 days for 20 °C and 4 days for 5 °C. After that point, the difference between two metal boxes began to increase and differs from each other. In Figure 6.1, it can be seen that the rise in the relative humidity of the coffee stored in the metal box with hydrogel film at 20 °C is considerably steeper than other samples after 9 days of storage. The amount of moisture absorbed by hydrogel film at 20 °C was higher than that measured at 5 °C. Therefore, more water vapor was desorbed into the headspace of the metal box at 25 °C than 5 °C, thus resulting in higher relative humidity value.

7.1.2. Sensorial Quality

Sensorial quality of the coffee was evaluated on the basis of odor (coffee odor, parched odor, stale odor) and taste (sour taste, bitter, burnt taste, coffee taste), foam formation and overall liking parameters. For coffee odor, parched odor, foam formation and general assessment, score of 1 represents “the worse” and 9 represents “excellent”. For rancid odor, bitter, burnt taste and coffee taste, 9 represents “the worse” and 1 represents “excellent”.

In Figure 6.2 and 6.3, the changes in the sensory evaluation scores versus storage time are given. The coffee samples stored in all conditions began to loose their coffee odor and parched odor from the first day as it can be seen in Figure 6.2 (a) and (b). These results were

in accordance with that of Anese et al. [118] and Makri et al. [119] who carried out a similar study on the secondary shelf life of ground roasted coffee. In these quoted studies, home storage conditions were also simulated by opening the package periodically for a while for a duration of 1 month. Authors concluded that the volatile compounds in the package headspace are representative indexes of the quality depletion of roasted ground coffee during home usage. Stale odor, sourish odor, bitterness, burnt odor and coffee flavor steadily increased during the course of storage regardless of the packaging type and storage temperature (Figure 7.2 c, Figure 7.3 a-d). The increase in the negative sensorial attributes during storage period can be attributed to the increase in the moisture content of coffee which further triggers oxidative reactions leading to the development of off-flavors and stale taste. In addition, the intensity of foam formation on the surface of coffee samples reduced day by day throughout the shelf life period.

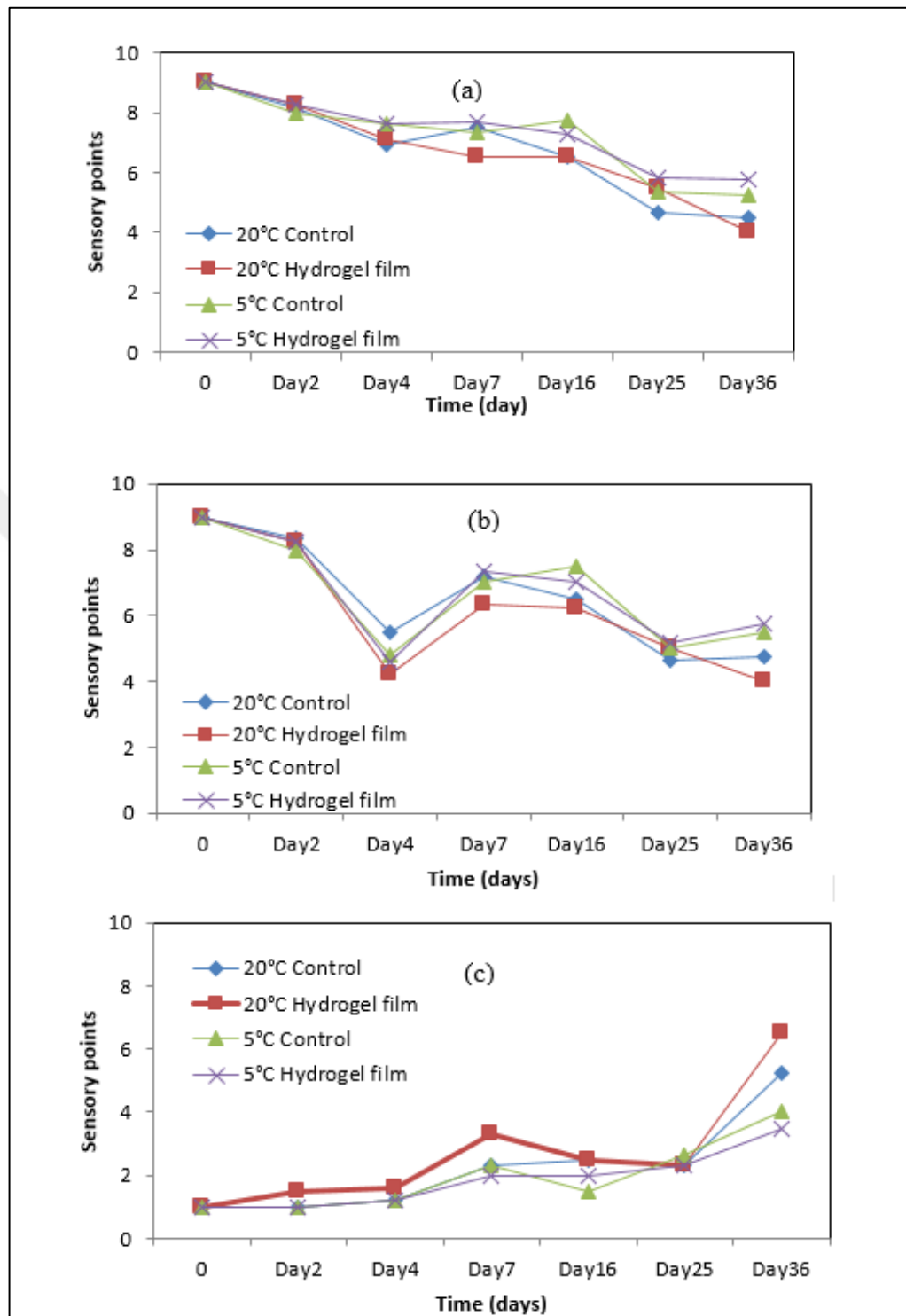
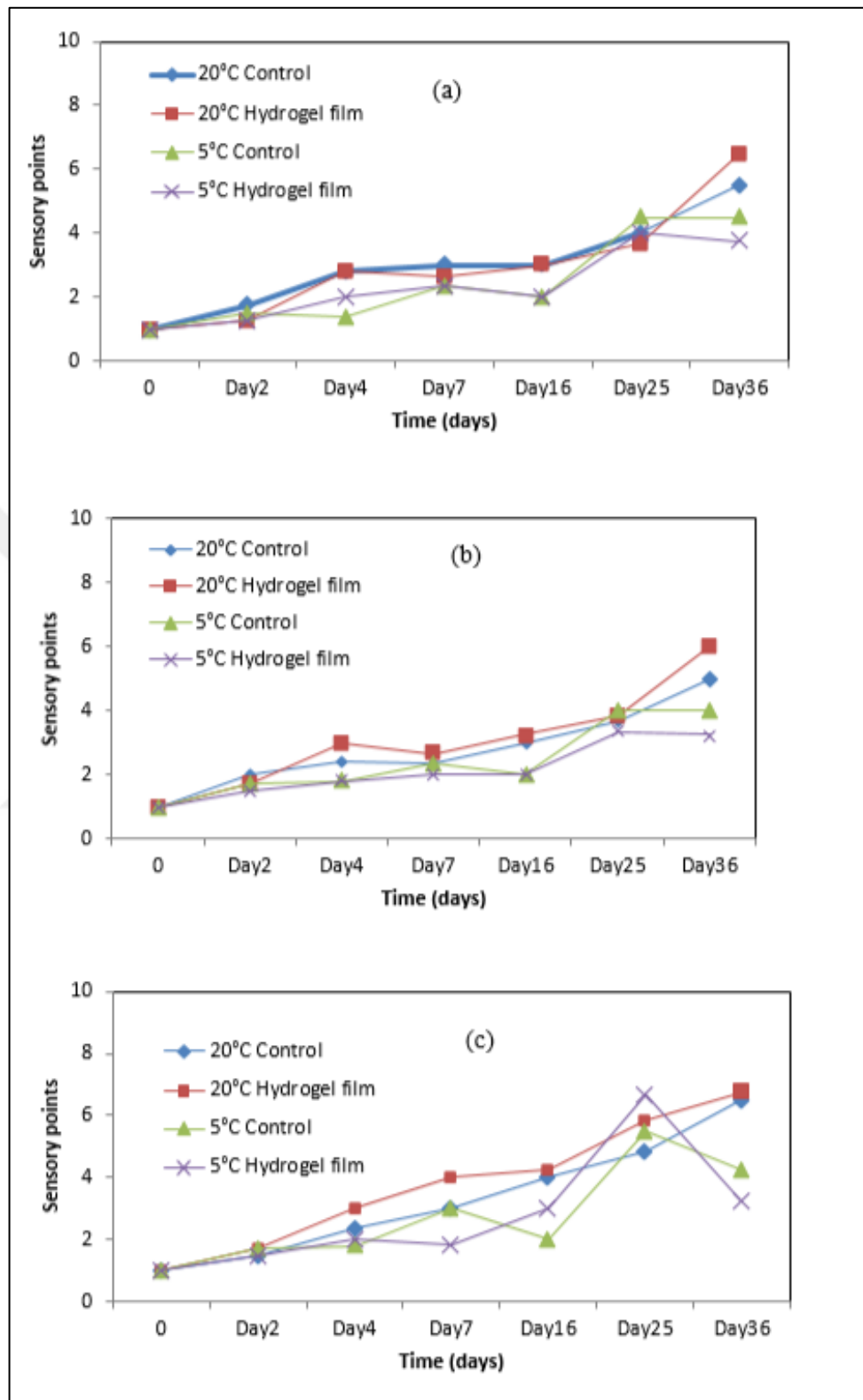


Figure 7. 2. Odor parameters used in sensory evaluation; (a) coffee odor, (b) parched odor and (c) stale odor



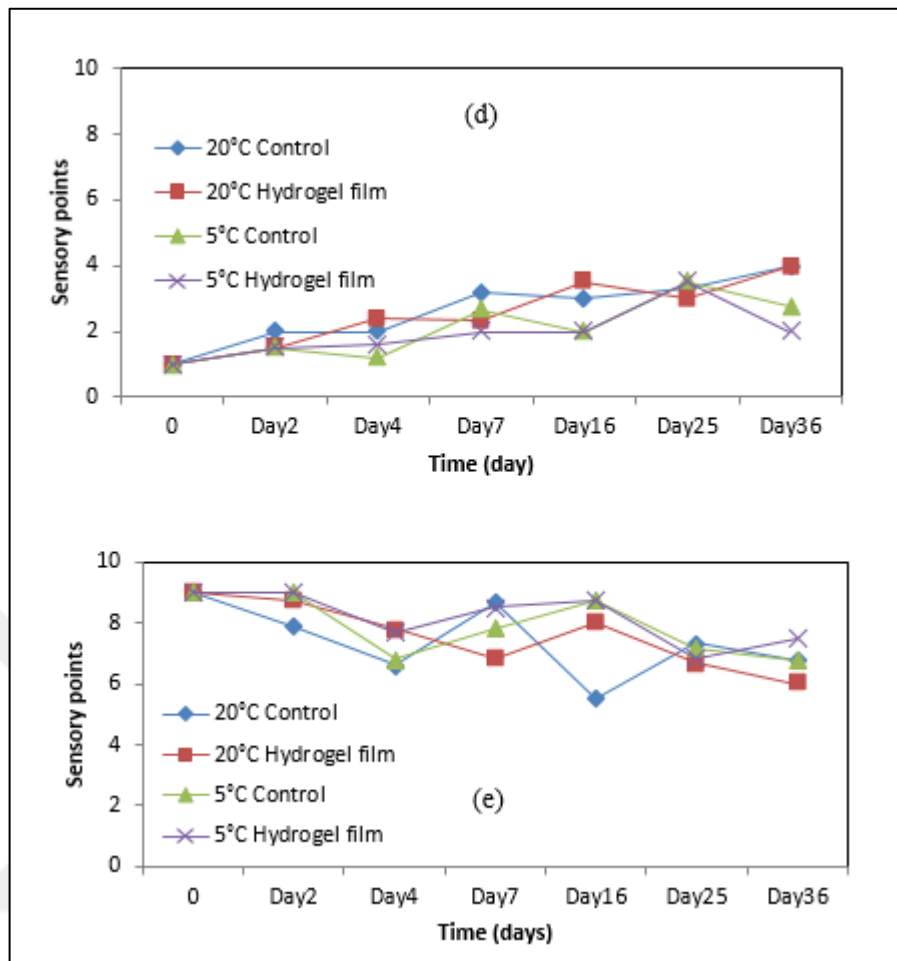


Figure 7.3. Aroma flavor parameters used in sensory evaluation; (a) coffee bitterness, (b) burnt flavor, (c) coffee flavor, (d) sourish flavor and (e) foam formation

The coffee samples were also evaluated for the overall liking criteria by the sensory panelists through the course of storage period and the results are given in Figure 7.4. At the end of the shelf life study, the coffee samples stored at 5 °C were evaluated to be more acceptable than coffee stored at 25 °C. However, there was no significant difference between coffee stored in metal can with and without hydrogel film.

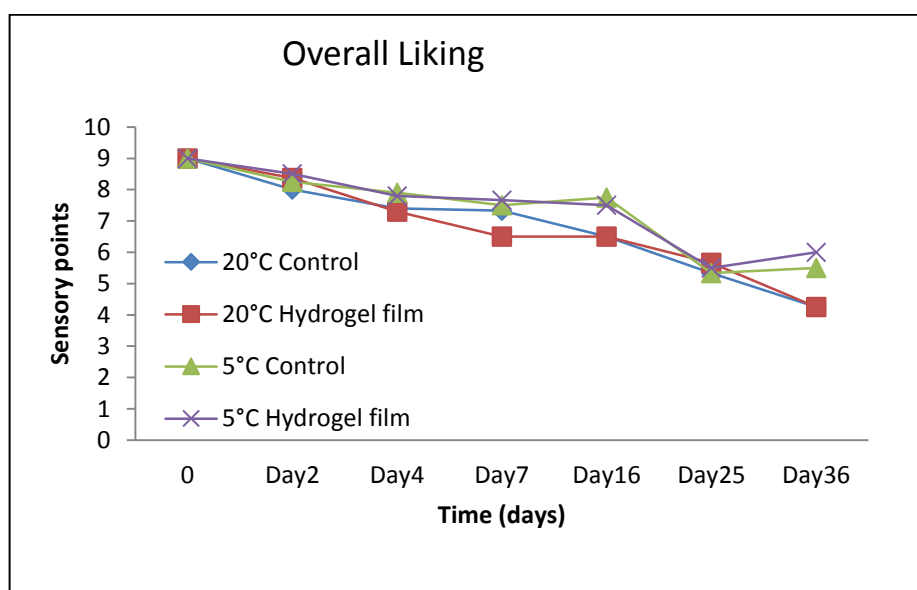


Figure 7.4. The change in the sensory scores for overall liking parameters for the coffees as a function of storage time

7.2. PACKAGING FOR HIGH MOISTURE FOODS: THE CASE OF MUSHROOM AND BROCCOLI

7.2.1. Moisture loss behavior of mushrooms and broccoli florets

Considering all the temperature and RH combinations tested in this study, the moisture loss of mushrooms and broccoli florets ranged from 0.14 to 0.57 $\text{mg kg}^{-1} \text{s}^{-1}$ and from 0.12 to 0.62 $\text{mg kg}^{-1} \text{s}^{-1}$, respectively (Figure 7.5 and 6.6). The transpiration rate of mushrooms was found to be higher than that of broccoli florets. We observed that the transpiration rate of the mushrooms and broccoli florets were substantially affected by both storage temperature and the % RH of the surrounding atmosphere. However, compared to the effect of the % RH the effect of temperature was more significant on the transpiration rate of the both produces. Those were in accordance with the results of study performed by Mahajan et. al. [120] and Rux et al. (2015) [121]. Mahajan et al. studied the mass loss or transpiration of mushroom at different relative humidity (76 %, 86 % and 96 %) and temperature (4, 10 and 16 °C) environments. They reported that both temperature and RH had significant effect on moisture loss behaviour of mushroom stored at various combinations of different relative humidity (76 %, 86 % and 96 %) and temperature (4, 10 and 16 °C) environments

nonetheless % RH had the greatest effect. They resulted that increase in % RH and/or decrease in temperature within the storage container reduced moisture loss [120]. Additionally, Rux et al. (2015) performed a similar study in which they evaluated the effect of using NaCl embedded PP tray on formation of condensation on mushrooms stored at similar temperature (4, 12 and 20 °C) and relative humidity (76, 86, 96 and 100%) conditions. They also evaluated the moisture loss of mushrooms stored in desiccators under different temperature and % RH combinations. They resulted that % RH has more significant effect on moisture loss of mushroom than temperature [121].

An increase in % RH of the surrounding atmosphere from 65 to 100 % decreased the transpiration rate by 28.1 % for mushrooms and 50.0 % for broccoli florets at 25 °C, whereas decreasing the temperature from 25 to 5 °C for mushrooms decreased the transpiration rate by 67 % and 61 % for broccoli florets. The results of this study showed that a mushroom (30 g) and a broccoli floret (10 g) stored at 5 °C and 100 % RH will produce almost 0.38 and 0.11 g of water per day, respectively. Furthermore, under a storage temperature of 25 °C and 100 % RH, the mushrooms and broccoli florets will produce about 0.98 and 0.26 g of water per day, respectively. Therefore, in order to prevent condensation on the surface of the packaging and product and maintain RH below 100 %, for the hydrogels for mushrooms and broccoli florets, the moisture absorption rate of the hydrogels must be at least 0.98 g per day at 25 °C.

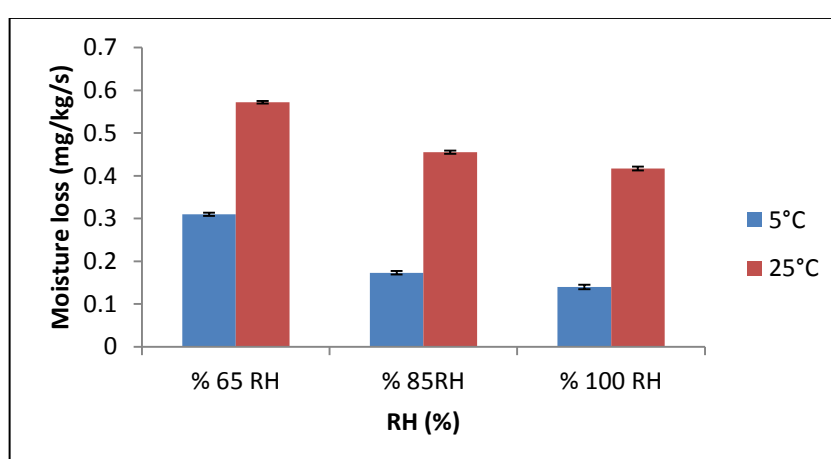


Figure 7.5. Moisture loss of mushrooms within all the combinations of temperature and RH

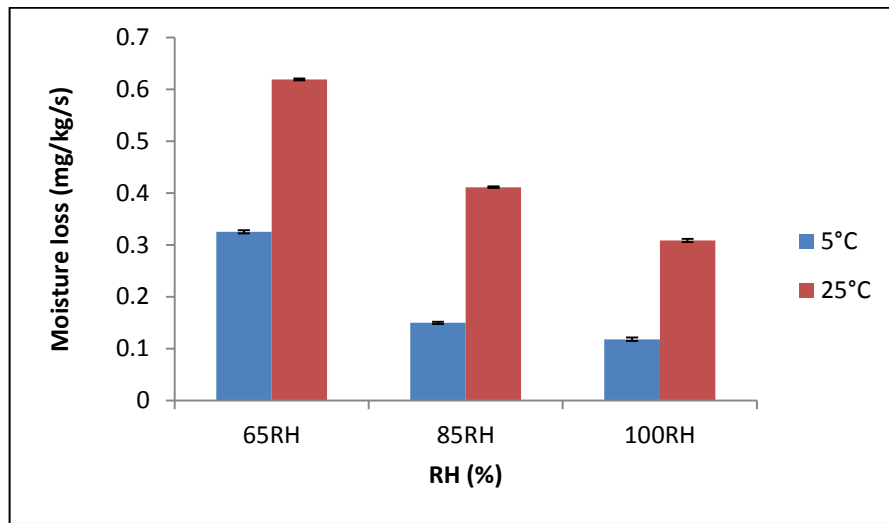


Figure 7.6. Moisture loss of broccoli florets within all the combinations of temperature and % RH

Also, changes in mass of mushroom and broccoli florets over time were normalized and moisture loss behavior within all combinations of T and RH can be seen in Figure 7.7 and 6.8, respectively. The detailed images of mushroom and broccoli florets can be seen in Appendix A and Appendix B, respectively.

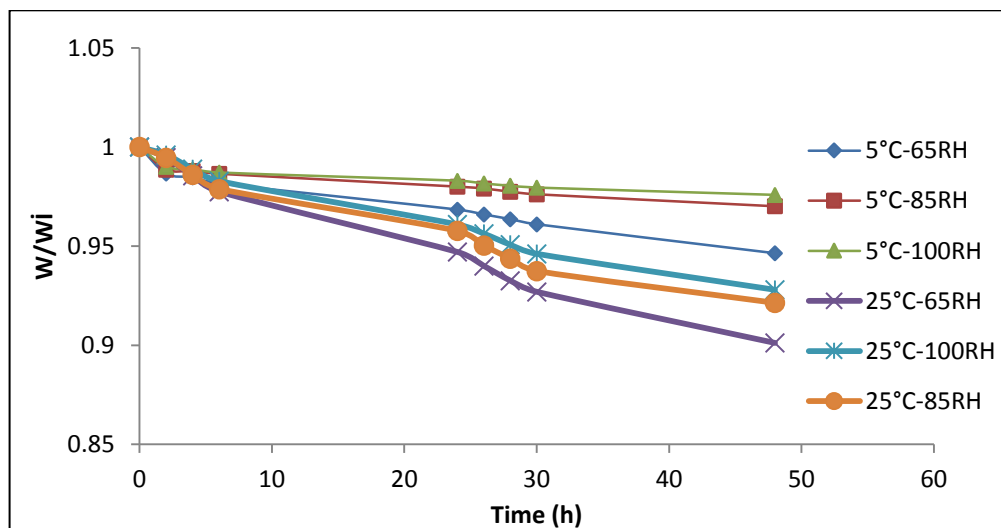


Figure 7.7. Changes in mass of mushrooms (W , mg) over time. The values were normalized with respect to the initial mass of mushrooms (W_i , mg)

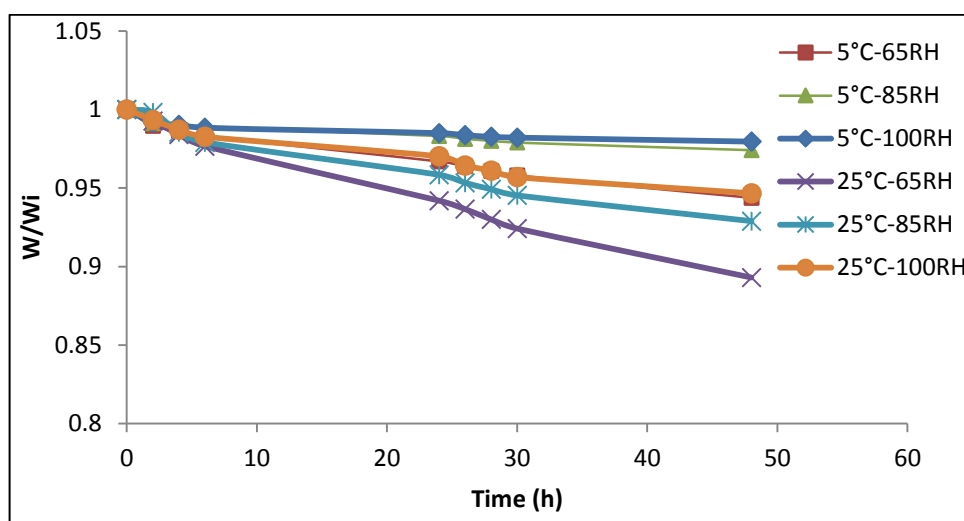


Figure 7.8. Changes in mass of broccoli (W , mg) over time. The values were normalized with respect to the initial mass of broccoli (W_i , mg)

7.2.2. Moisture gain behavior of the cross-linked Ch-CMC hydrogel (Gnp-1)

Water absorption capacity for the cross-linked Ch-CMC hydrogel film (Gnp1) was performed within all combinations of temperature and RH. In order to have a better idea of the water absorption capacity of the Gnp1 hydrogel, experiments with silica gel were also performed in parallel. As it can be seen from Figure 7.9 (a) and 7.9 (b) the amount of moisture absorbed by the Gnp1 hydrogel and silica gel during storage increased and showed similar general profiles. It is also clearly seen from the figures that the hydrogel film sample Gnp1 exhibited much higher moisture absorption capacity compared to the silica gel.

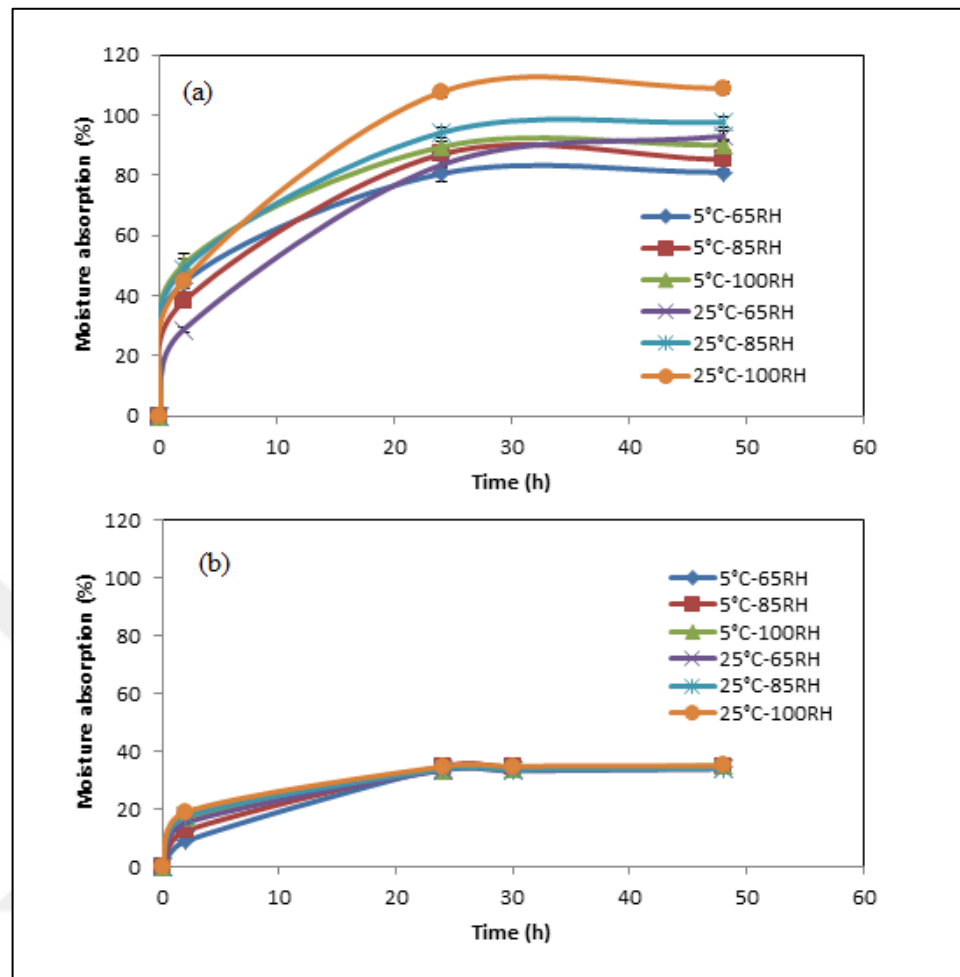


Figure 7.9. Moisture absorption behaviors of (a) the Ch-CMC hydrogel film (Gnp1) and (b) silica gel at different RH and temperatures

The moisture absorption of the Gnp1 hydrogel film was rapid within first 2 hours and began getting slower than after. This indicated that moisture absorption capacity reduced as the film reached equilibrium. The moisture absorption capacity was found as 81, 85 and 90 % for hydrogel films under 65, 85 and 100 % RH at 5 °C. The same hydrogel film exhibited 93, 98 and 109 % moisture absorption capacity for 65, 85 and 100 % RH at 25 °C. It was also observed that the moisture absorption capacity of the hydrogel film increased with increasing storage temperature regardless of the RH of the surrounding atmosphere. The moisture absorption capacity of the hydrogel film increased from 90 % to 109 % when temperature increased from 5 °C to 25 °C. This result showed that the water absorption capacity of the hydrogel film was dependent both on the temperature and the relative humidity of the environment. The highest and the lowest moisture absorption capacity was

observed as 109% and 81% at 100 % RH-25 °C and 65 % RH-5 °C, conditions, respectively. Moisture absorption is temperature and RH dependent, resulting in an increase by fast diffusion and high moisture content at high temperature and relative humidity [122].

Gao et al. studied moisture absorption capacity of superabsorbent polymer clay composite (SAPC) hydrogels under varying relative humidity environment at room temperature. They reported that a nearly linear relationship existed between relative humidity and the maximum moisture absorption capacity which increase by increasing relative humidity [123].

Regarding the moisture absorption of silica gel, the moisture uptake was rapid within first hours and began getting slower throughout the storage time similar to the trend observed for the hydrogel. However, contrary to the results of the experiments with the hydrogel, the moisture absorption capacity at equilibrium was almost identical for all RH and temperature conditions for the silica gel.

The highest and the lowest moisture absorption capacity at equilibrium for the Gnp1 hydrogel and silica gel were 109 % and 90 % for hydrogel film and 35 % for the silica gel for both 100 % RH-25 °C and 65 % RH-5 °C, respectively.

It has been reported that silica gel probably is the best known moisture absorber that can be integrated within the packaging materials with its absorption capacity up to 35% of its own dry weight [124]. However, the results of our study indicate that the Ch-CMC hydrogel film (Gnp1) exhibited 3 times greater moisture absorption capacity than the silica gel.

7.2.3. Humidity regulation by the hydrogel (Gnp1) in package headspace at constant temperature

7.2.3.1. Mushrooms

This part of experiment was performed to understand whether the hydrogel film is capable of regulating the headspace humidity within a storage box. The experimental set-up showing the mushrooms with silica gel and hydrogel at the beginning and at the end of the storage at 5 °C, is presented in Figure 7.10. Headspace RH and temperature vs. storage time curves for 5 °C for mushroom are shown in Figure 6.11 .

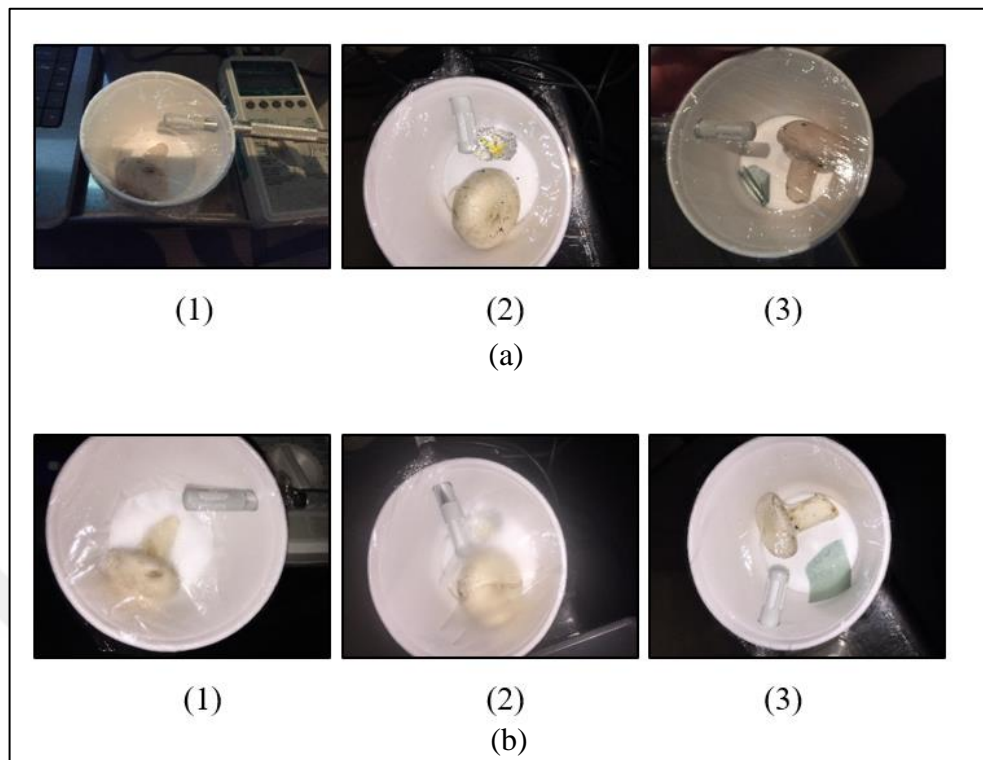


Figure 7.10. The experimental set-up showing the mushrooms in (1) control box, (2) with silica gel and (3) hydrogel at the beginning (a) and at the end (b) of the storage at 5 °C

In Figure 7.11, the RH in control box was rapidly increased within first 300 seconds to 77% and continued rising slowly until equilibrium. The headspace RH in storage box with silica gel and hydrogel film were still 67 % and 66 % for the first 300 seconds. Increase in the headspace RH in storage box with silica gel and hydrogel film reached equilibrium later compared to the control sample. Headspace RH within the storage box with hydrogel film began to reduce after 1000 seconds and reached equilibrium at the end of the storage time. Hydrogel film absorbed rapidly evaporated moisture loss from mushroom. Moisture loss of mushroom was faster at the beginning and began to reduce within time thus resulting decrease in moisture content within the headspace [125].

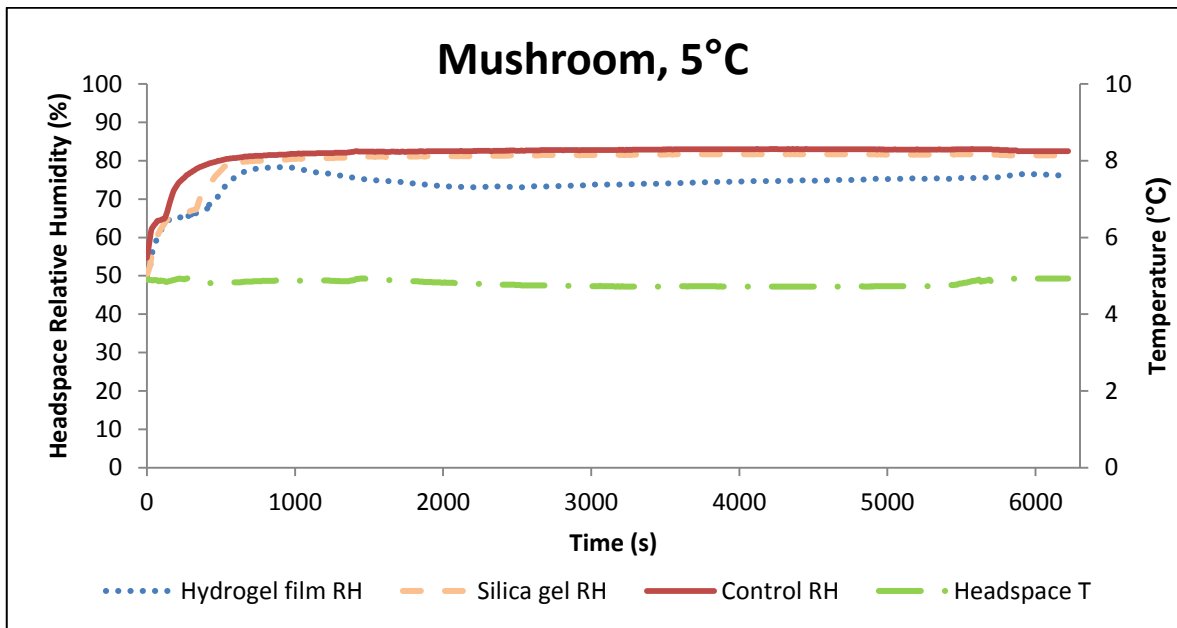


Figure 7.11. Headspace % RH and temperature versus storage time curves, measured in packages of mushrooms stored at 5 °C

Moisture absorption capacity of hydrogel film did not reach equilibrium and the hydrogel still continued absorption. Moisture absorption rate of the hydrogel film was faster than moisture loss rate of mushroom, thus resulting in decrease in RH within the package headspace. The control storage box reached 82.5 % RH at the end of the storage time whereas 81.4% RH in the storage box with silica gel and 75.6 % RH in the storage box with hydrogel film. In Figure 7.10, no water condensation was observed on the stretch film surface for the box with hydrogel film. There was a water vapor condensation on the stretch film surface for control box with the silica gel. Small water droplets condensed on the stretch film surface of the control box.

Rux et al. (2015) have performed a similar study and evaluated the effects of NaCl embedded PP tray as moisture absorber for mushrooms. They have reported that RH within the control trays rapidly increased and reached 100 % RH throughout 6 days of storage at 7 °C while it was 93 % RH within trays with NaCl as moisture absorbers. These results are in accordance with observations in our study [121].

The experimental set-up showing the mushrooms with silica gel and hydrogel at the beginning and at the end of the storage at 25 °C are presented in Figure 7.12. Headspace

RH and temperature vs. storage time curves for 25 °C for mushroom are shown in Figure 7.13.

In Figure 7.13 for 25 °C, the RHs in control box, box with silica gel and box with the hydrogel film were similar. Headspace RH within all boxes increased slowly until equilibrium. The control storage box reached 67.3 % RH at the end of the storage time, whereas 69.6 % RH in the storage box with silica gel and 66.5 % RH in the storage box with hydrogel film were observed. Thus the hydrogel film (Gnp1) did not effectively decrease the RH of the storage box at 25°C. Thus a significant difference in water condensation on the stretch film surface was not observed for the box with the hydrogel film, can be seen in Figure 7.12.

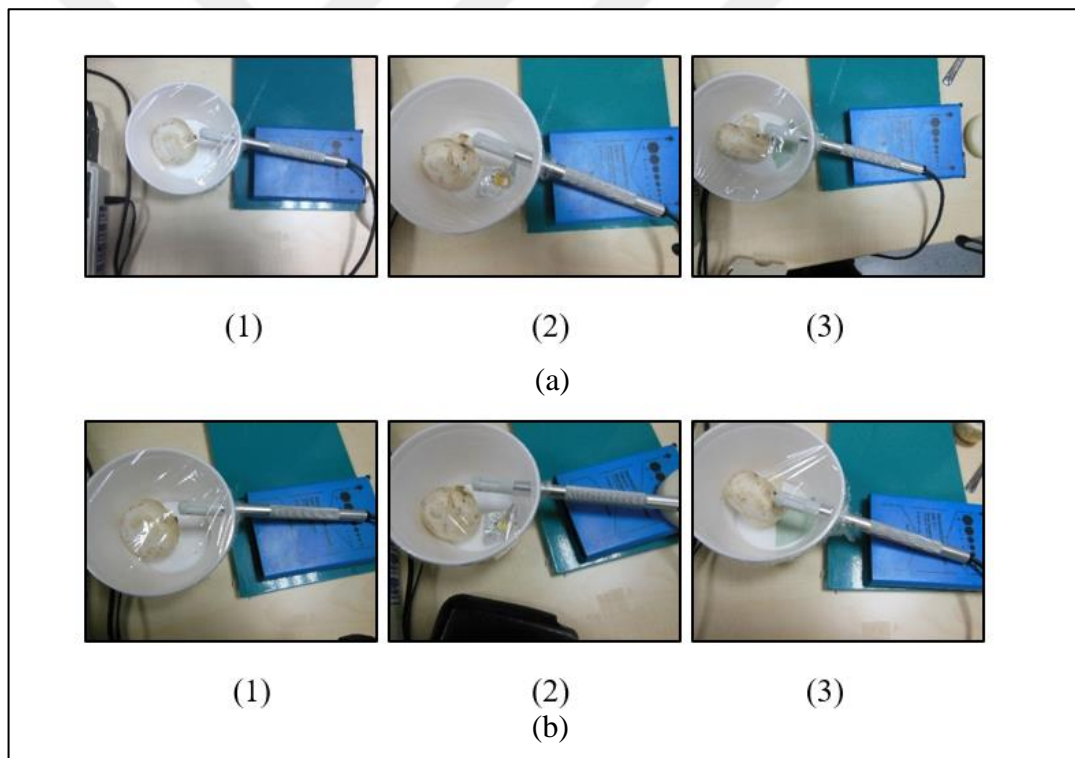


Figure 7.12. The experimental set-up showing the mushrooms in control box (1) with silica gel (2) and hydrogel (3) at the beginning (a) and at the end (b) of the storage at 25 °C

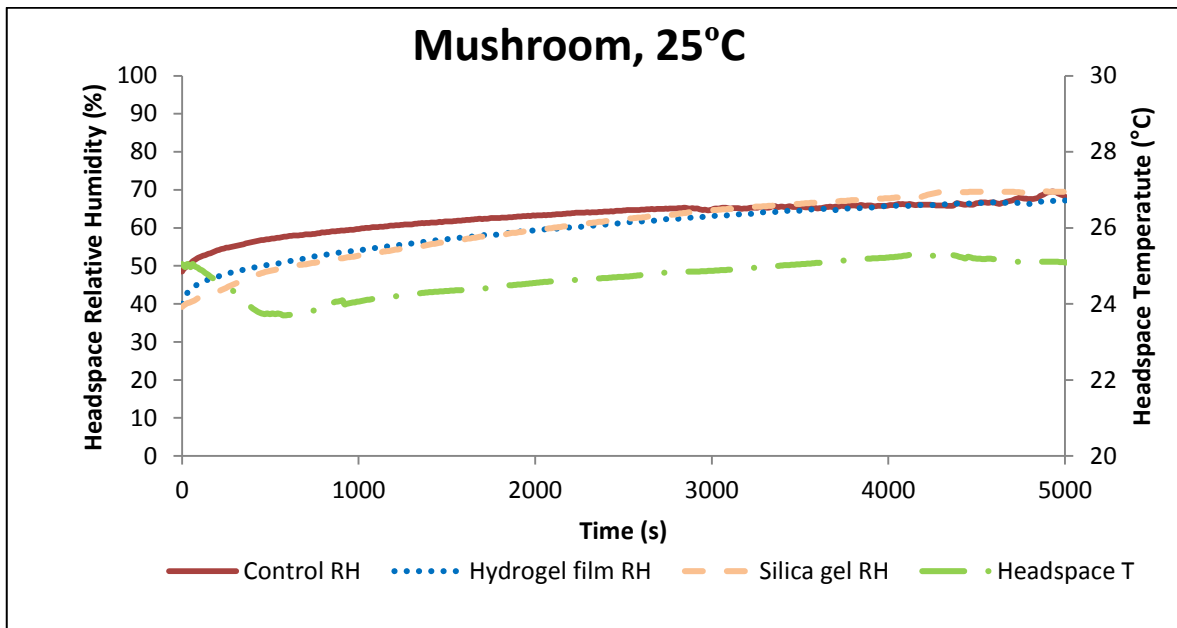


Figure 7.13. Headspace % RH and temperature versus storage time curves measured in packages of mushrooms stored at 25 °C

7.2.3.2. Broccoli florets

The experimental set-up showing the broccoli florets with silica gel and hydrogel at the beginning and at the end of the storage at 5 °C is presented in Figure 7.14. The headspace % RH and temperature versus storage time curves measured in packages of broccoli florets stored at 5 °C are shown in Figure 7.15. In Figure 7.15, the RH in the headspace of the storage box with silica gel was increased within first 200 seconds to 84 % and continued rising slowly until equilibrium. The headspace RH in storage box with the hydrogel film was 79.2 % and that of the control box was 79.6 % for the first 200 seconds. Headspace RH within the storage box with the hydrogel film began to reduce after 1200 seconds and reached equilibrium at the end of the storage time. The control storage box reached 86.5 % RH at the end of the storage time whereas the storage box with silica gel and the storage box with hydrogel film stored at 5 °C reached 82.3 % and 71.9 % RH, respectively. In Figure 7.14, no water condensation was observed for the experimental set up with the silica gel and the hydrogel film. However, small water droplets condensed on the stretch film surface for the control box.

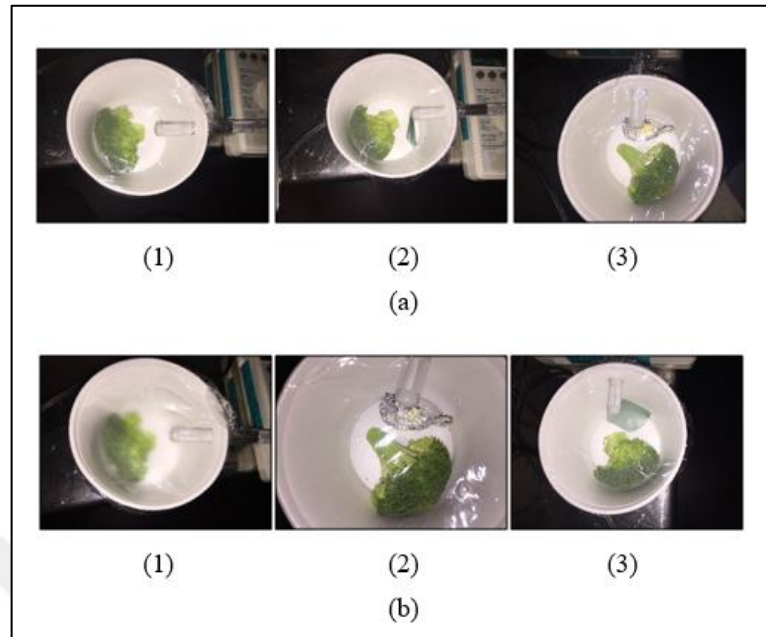


Figure 7.14. The experimental set-up showing the broccoli florets in (1) control box, (2) with silica gel and (3) hydrogel at the beginning (a) and at the end (b) of the storage at 5 °C

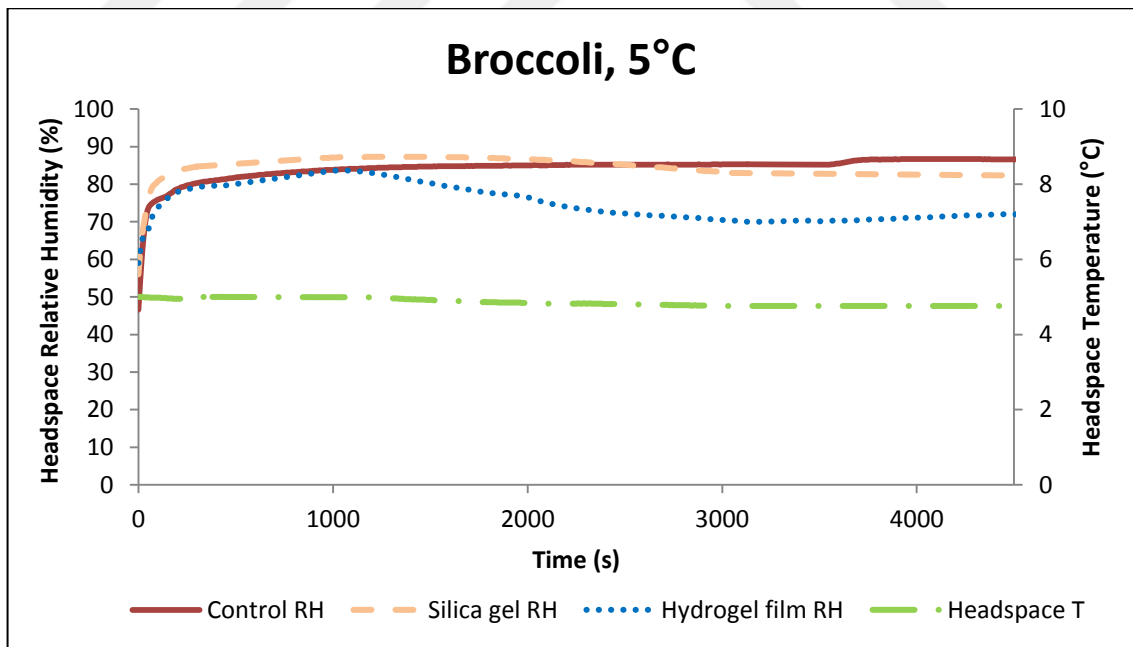


Figure 7.15. Headspace % RH and temperature versus storage time curves measured in packages of broccoli florets stored at 5 °C

The experimental set-up showing the broccoli florets with silica gel and hydrogel at the beginning and at the end of the storage at 25 °C are presented in Figure 7.16. Headspace % RH and temperature versus storage time curves measured in packages of broccoli florets stored at 25 °C are shown in Figure 7.17. In Figure 7.17 for 25 °C, the RH in the control box was rapidly increased within first 100 seconds to 60.4 % and continued rising slowly until equilibrium. The headspace RH in storage box with silica gel and hydrogel film were still around 50.5 and 46.4 % within first 100 seconds, respectively. The control storage box reached 71 % RH at the end of the storage time whereas 68.7 % RH in the storage box with silica gel and 68.5 % RH in the storage box with hydrogel film. As can be seen in Figure 7.16, no water condensation was observed in the stretch film for the boxes with silica gel, hydrogel film or control box.

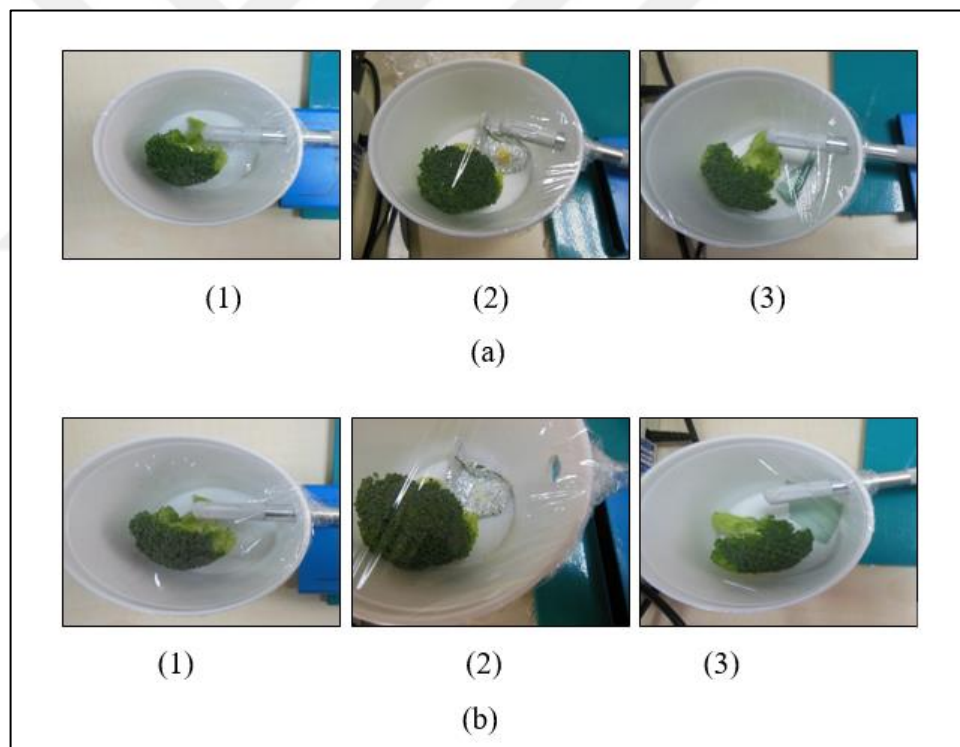


Figure 7.16. The experimental set-up showing the broccoli florets in (1) control box, (2) with silica gel and (3) hydrogel at the beginning (a) and at the end (b) of the storage at 25 °C

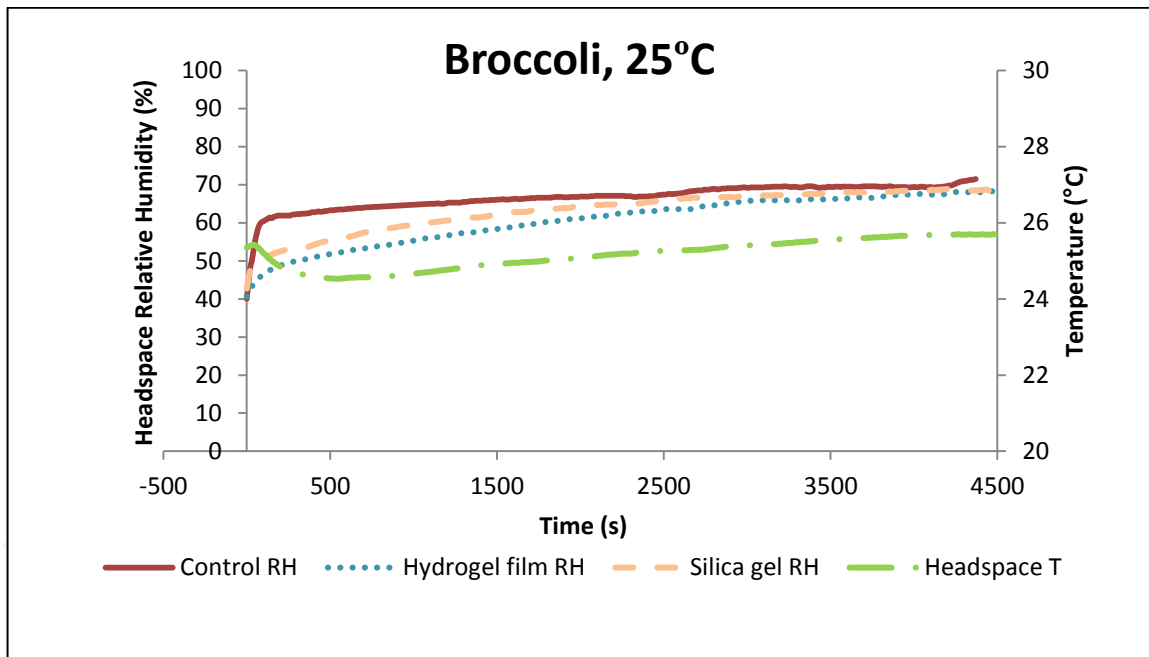


Figure .17. Headspace % RH and temperature versus storage time curves measured in packages of broccoli florets stored at 25 °C

7.2.4. Humidity regulation with the hydrogel film (Gnp1) in package headspace at fluctuating temperatures

7.2.4.1. Mushrooms

The efficacy of hydrogels in regulating the RH in package headspace under fluctuating temperature regime and its effect on the quality of the mushrooms was assessed. For this purpose, mushrooms were placed in polystyrene boxes with or without hydrogel film and covered with a polyethylene stretch film. Then the package was exposed to fluctuating temperatures as described in materials and methods section. The temperature fluctuating scheme was based on a putative real life scenario of a typical fresh produce supply chain comprising storage and transportation stages at/between the packaging house, supermarket retail display and home refrigerator. In this experiment, the temperature and the relative humidity inside the package headspace was continuously recorded. At different stages of the experiment, photos were taken and the water condensation on the surface of the packaging film was visually assessed. At the end of the experiment after 24 hours, mushroom samples

were taken and their microbial load (total aerobic bacteria, yeast, mold), firmness and color were analyzed and the results were compared with their value at the beginning of the experiment.

Headspace % RH and temperature versus storage time curves measured in the packages of mushrooms stored for 24 hours under fluctuating temperature regime are shown in Figure 7.18. As it can be seen from Figure 7.18, the headspace relative humidity within the box with the hydrogel film rapidly reached its maximum value of 87.3 % when exposed to 5 °C for 1 h whereas in the control box, 89.8 % RH, was recorded. At the second stage, when the mushroom packages were exposed to 25 °C, the relative humidity inside the packages decreased sharply at first in both control and hydrogel packages but there after started to increase with a faster pace in control than the hydrogel package. At the third stage the packages were exposed again to 5 °C as a result of which the relative humidity inside the packages increased sharply to a similar level in both packages. After being held at 5 °C for 1 h, the temperature was increased briefly for 0.5 h to 25 °C and again much lower relative values were attained in hydrogel package (39.1 %) than control (74.5 %). At the fifth stage the temperature was decreased to 5 °C and the relative humidity inside the package headspace in both control and hydrogel packages increased sharply but this time lower values were recorded for hydrogel package (86.2 %) than control (94.6 %). At the sixth stage the temperature was increased to 25 °C as a result of which the headspace relative humidity of the both packages decreased to around 77.8 % for control package and 75.6 % for the hydrogel package. At the last and the longest stage, the bowl with the mushroom was placed at 5 °C for 17 h, which corresponds to the home refrigerator conditions, the temperature was decreased to 13 °C, the headspace RH within the control box increased to 84.1 % and to 80.1 % for the package with the hydrogel film. Regarding the overall performance of the hydrogel film, it can be concluded that, apart from the first stage, in all other stages it succeeded in lowering the relative humidity inside the package headspace from what is observed in control packages.

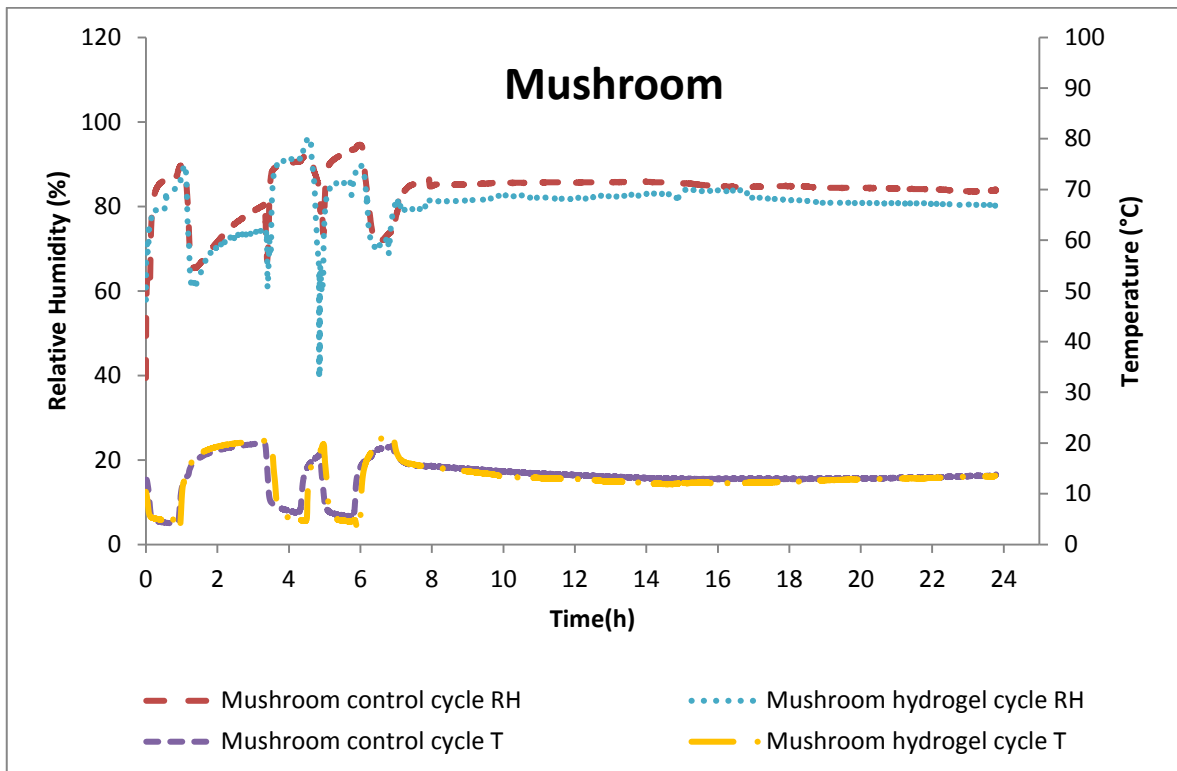


Figure 7.18. Headspace % RH and temperature versus storage time curves measured in the packages of mushrooms stored for 24 hours under fluctuating temperature regime

Apart from the temperature and relative humidity measurements inside the packages, the changes in the physical and microbial quality of the mushrooms were also assessed. Pictures of mushrooms stored both in control and hydrogel packages at the beginning and at the end of 24 hours fluctuating temperature regime, can be seen in Figure 7.19. Quality fresh mushrooms should have light cap color, closed gills with pinkish-brown color, firm texture and microbial load at around $6 \log \text{CFU/g}$ [126]. In the present study, fresh mushrooms were initially appeared in white color, gills were closed completely and had no defect. The gills of mushroom stored in box without hydrogel film (used as control) were opened after 1 day whereas the gills of mushroom stored in box with hydrogel film opened less and had more acceptable appearance when compared to control sample after 1 day.

These findings were in agreement with that of Rux et al. They evaluated that mushrooms stored in control PP trays as unacceptable due to color and gills exposure at the end of storage of 6 days whereas samples stored in humidity-regulating PP-trays were still above the marketable limits [121].

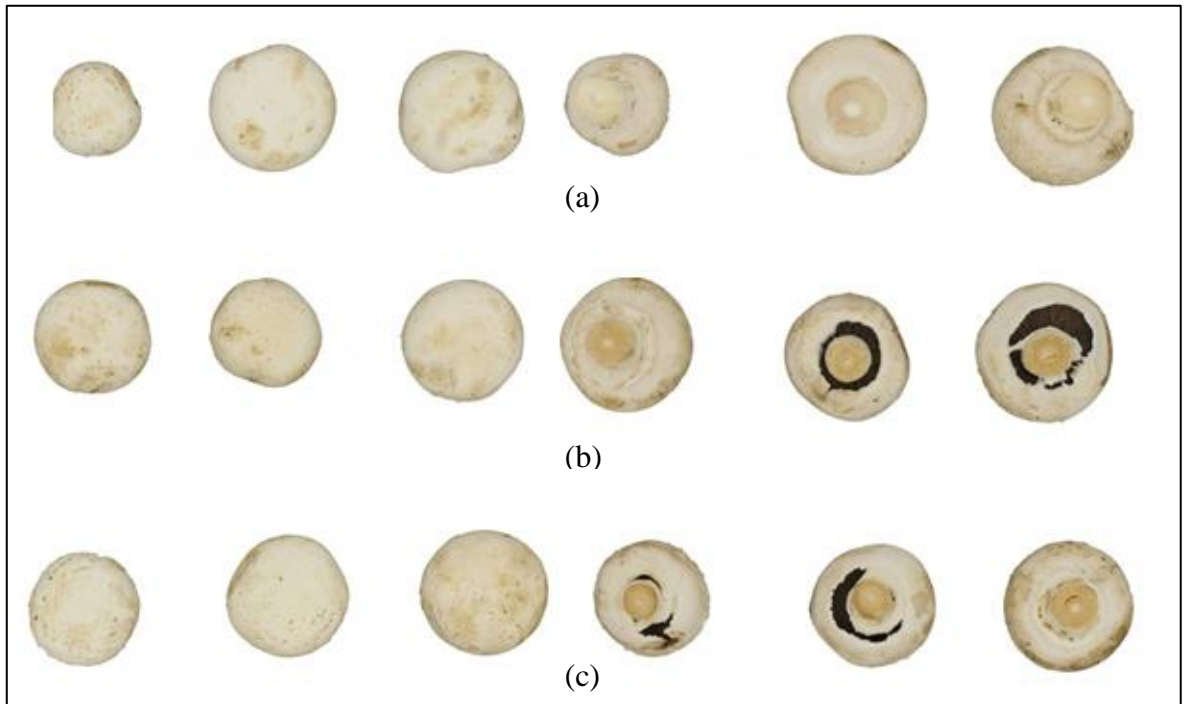


Figure 7.19. Appearance of the gills and the cap of mushrooms exposed to fluctuating temperatures (a) initially, (b) in control package after 1 day and (c) in hydrogel package after 1 day

The detailed pictures of mushroom control cycle set-up and mushroom hydrogel cycle set-up which were recorded at each time intervals can be seen in Appendix-D.

The results of the physical measurements showed that the mushrooms stored in hydrogel packages were firmer than the ones stored in control packages after exposure to fluctuating temperatures for 24 h (Figure 7.20). Compared to the values initially measured the firmness of the mushrooms stored in the hydrogel packages increased whereas that were in the control packages decreased after 24 h exposure to fluctuating temperatures. Since good quality mushrooms are expected to have a firm texture [127], it can be deduced that hydrogel package was more effective in keeping textural quality of the mushrooms than control packages which do not contain hydrogels. This observation can be attributed to lower % RH in hydrogel containing packages which might have led to surface desiccation of the mushroom cap and resulted in tissue stiffening. Differences between conditions were found insignificant ($p > 0.05$). The detailed results can be seen in Appendix E.

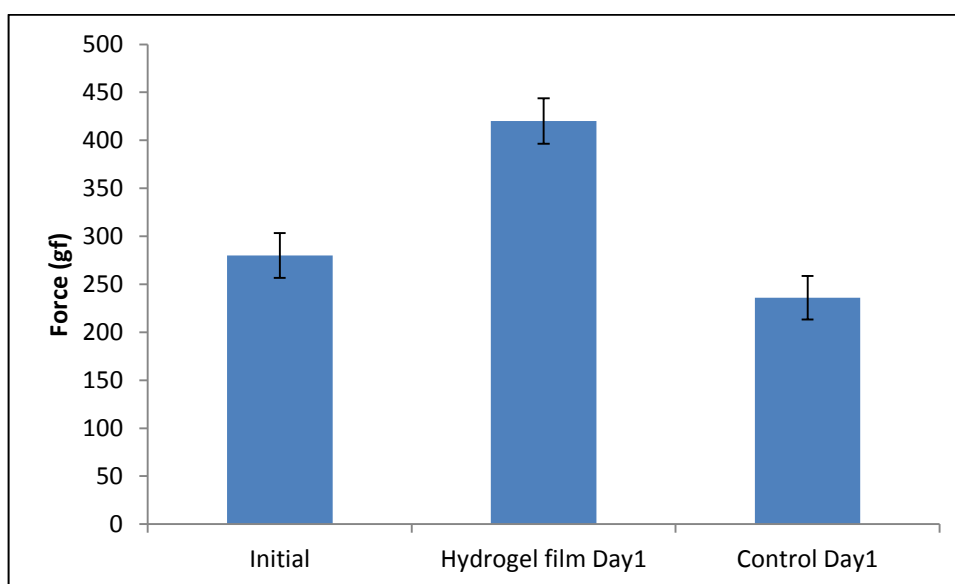


Figure 7.20. Firmness values of the mushrooms exposed to fluctuating temperatures at the end of 24 hours

The CIE $L^*a^*b^*$ color parameters measured at the beginning and at the end of 24h storage under fluctuating temperatures on mushrooms stored in control and hydrogel packages are given in Figure 7.21. As it can be seen from this figure, the L^* which represent the whiteness of the mushrooms stayed closer to initial value for mushrooms stored in hydrogel packages whereas it decreased in control samples. Also the control samples were darker (higher a^* value) and yellower (higher b^*) than mushrooms stored in hydrogel packages. C^* is saturation and represents the brightness or dullness of mushroom. Control sample developed a more saturated color than the other samples. Differences between conditions were found insignificant ($p > 0.05$). The detailed results can be seen in Appendix F.

The change in cap color of fresh mushrooms can be attributed to both enzymatic reactions and microbial action [126]. The enzymatic browning is a result of the reaction of phenolics with polyphenol oxidase (PPO) in the presence of oxygen. The concentration of phenolic compounds, pH, temperature, relative humidity and oxygen availability affect substantially the extent of browning [128]. Improper handling, senescence and bacterial infection, especially with *Pseudomonas tolaasii* can trigger discoloration reactions [129]. Severe infections of fluorescent pseudomonads can also lead to darkened or yellowed lesions on fresh mushroom cap [130].

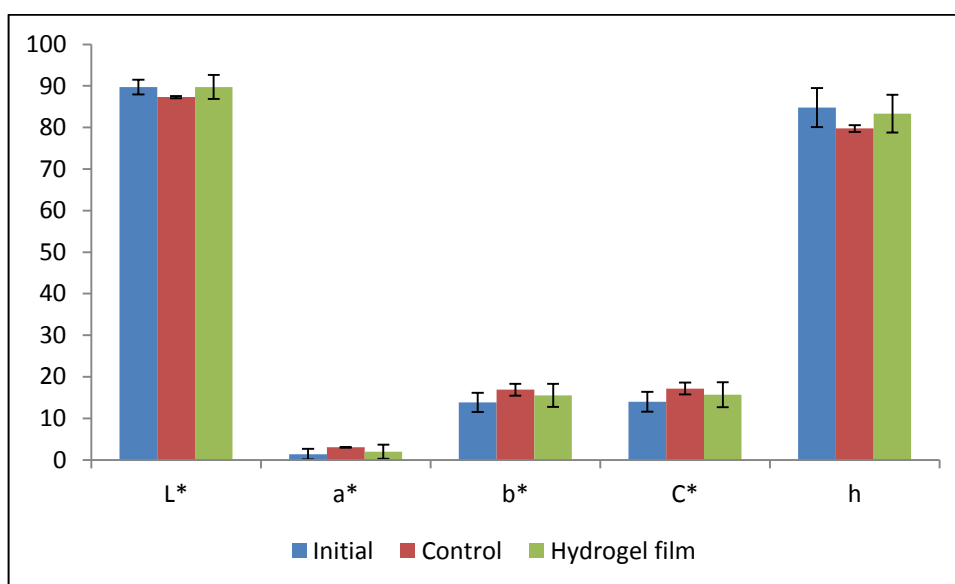


Figure 7.21. CIE L*a*b* color parameter values of the mushrooms exposed to fluctuating temperatures at the end of 24 hours

The total aerobic bacteria (TBC), yeast and mold load at the beginning and at the end of 24 h storage under fluctuating temperatures of mushrooms stored in control and hydrogel packages are given in Figure 7.22. As it can be seen from this figure, fresh mushrooms have $6.13 \log \text{CFU g}^{-1}$ of bacteria which is in accordance with the findings of Doores et al. [131], who reported that total bacterial count of fresh mushrooms ranged from 6.3 to $7.2 \log \text{CFU g}^{-1}$. Compared to initial values, TBC of the mushrooms increased after 24 h storage in both mushrooms stored in control and hydrogel packages. However, the increase in the control mushrooms was more significant than hydrogel package samples as their bacterial load increased almost $1 \log_{10}(\text{CFU/g})$ within 24 h. The amount of increase in the bacterial count of control samples were similar to that reported by Chikthimmahand Beelman [132] who also observed an increase from 7.3 to $8.4 \log \text{cfu g}^{-1}$ during a 1-day storage period at 4°C . It is interesting to note that in this study the yeast load of the samples in hydrogel packages decreased whereas that of control samples increased after 24 h of storage under fluctuating temperatures which is in confirmation with the findings of by Chikthimmah and Beelman [132] who reported that yeast populations of fresh mushrooms increased from 6.9 to $8.0 \log \text{CFU g}^{-1}$ during a 1-day storage period at 4°C . We also observed a decrease in mould population in hydrogel samples whereas the mould population did not show any significant change in control samples during 24 h of storage under fluctuating temperatures which is in

line with findings of Chikthimmah et al. [133] who also did not observe any change in mould populations during a 1-day storage period at 4 °C. However, the amount of mould population observed in their work (3 log CFU g⁻¹) was considerably lower than that observed in this study (4.65 log CFU g⁻¹). Differences between conditions were found insignificant ($p > 0.05$). The detailed results can be seen in Appendix E.

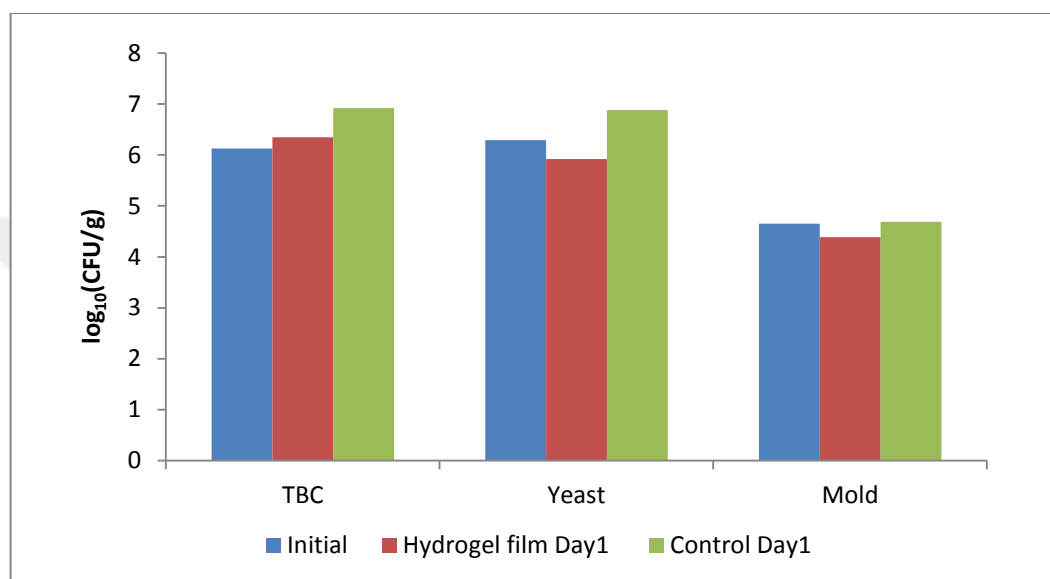


Figure 7.22. The total aerobic bacteria (TBC), yeast and mold load of the mushrooms exposed to fluctuating temperatures at the end of 24 hours

As a result, incorporation of hydrogel films inside mushroom packages resulted in better humidity regulation and avoids water condensation. In consequence, the mushrooms in hydrogel containing packages maintained their organoleptic and microbial quality better than control samples. Differences between conditions were found insignificant ($p > 0.05$). The detailed results can be seen in Appendix G.

7.2.4.2. *Broccoli florets*

Similar to the experiments carried out on mushrooms, the efficacy of hydrogels in regulating the RH in package headspace under fluctuating temperature regime and its effect on the quality of the broccoli florets was also assessed. The same experimental set up used in humidity regulating experiment for mushrooms was used for broccoli.

Headspace relative humidity and temperature values were recorded simultaneously during the experiment. Headspace % RH and temperature versus storage time curves measured in the packages of broccoli florets stored for 24 hours under fluctuating temperature regime is presented in Figure 7.23. At the first stage of the experiment, packages were exposed to 5 °C for 1 h, as a result of which the headspace relative humidity within the package with hydrogel film reached maximum value to 85.8 % and to 89.3 % for the control box. At the second stage, when the broccoli packages were exposed to 25 °C, the relative humidity inside the packages decreased sharply at first in both control and hydrogel packages but there after started to increase with a faster pace in control (to 86.8 %) than hydrogel package (to 73.6 %). At the third stage the packages were exposed again to 5 °C as a result of which the relative humidity inside the packages increased sharply to a similar level in both packages. After being held at 5 °C for 1 h, the temperature was increased briefly for 0.5 h to 25 °C and relative values in both package types slightly increased to a similar level (100 %). At the fifth stage the temperature was decreased to 5 °C and the relative humidity inside the package headspace in both control and hydrogel packages increased sharply without any significant differences in attained relative humidity values. At the sixth stage the temperature was increased to 25 °C as result of which the headspace relative humidity of the both packages decreased to around 76.9 % for control package and 74.8 % for hydrogel package. At the last and the longest stage, the bowl with the broccoli was placed at 5 °C for 17 h, which corresponds to the home refrigerator conditions, the temperature was decreased to 13 °C, the headspace RH within the control box increased to 85.3 % and to 80.7 % for the box with the hydrogel film. Regarding the overall performance of the hydrogel film, it can be concluded that, apart from the first stage, in all other stages hydrogel film succeeded in lowering the relative humidity inside the package headspace from what is observed in control packages. Pictures of both broccoli stored in control box and broccoli stored in box with hydrogel at the end of 24 hours cycle period, as well as pictures of broccoli at the beginning of the experiment can be seen in Figure 7.24. The detailed pictures of broccoli florets which were recorded at each time interval can be seen in Appendix-D.

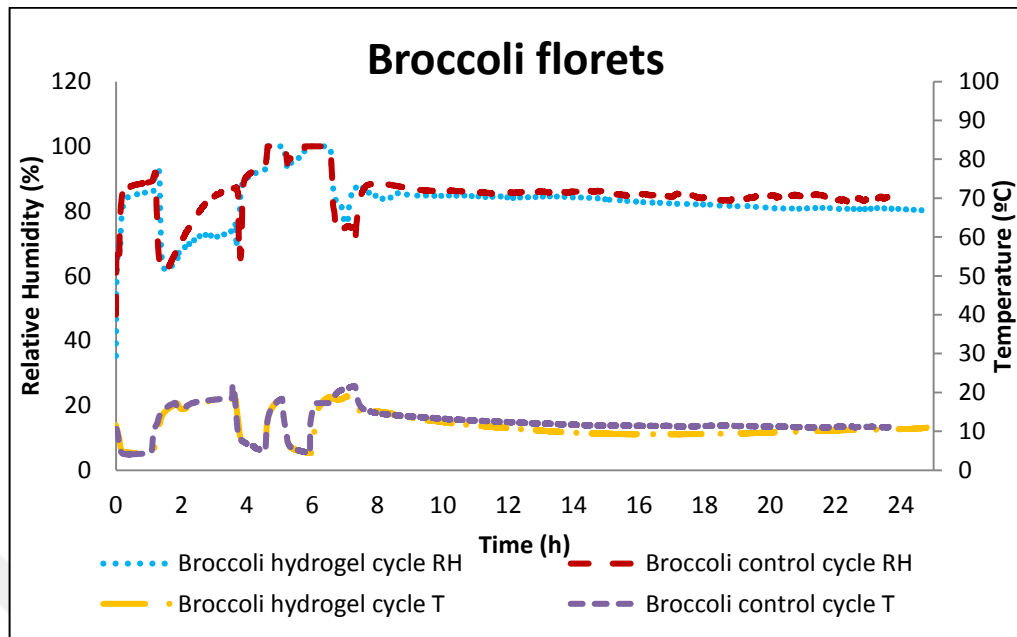


Figure 7.23. Headspace % RH and temperature versus storage time curves measured in the packages of broccoli florets stored for 24 hours under fluctuating temperature regime

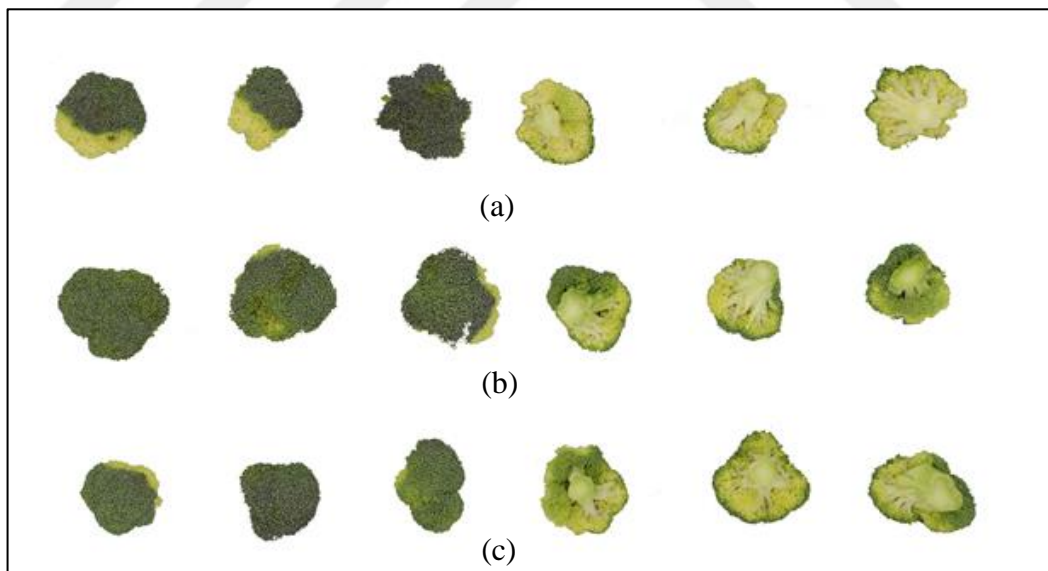


Figure 7.24. Appearance of broccoli florets exposed to fluctuating temperatures (a) initially, (b) in control package after 1 day and (c) in hydrogel package after 1 day

The results of the physical measurements showed that the broccoli florets stored in hydrogel packages were looser than the ones stored in control packages after exposure to fluctuating

temperatures for 24 h (Figure 7.25). Compared to values initially measured, the firmness of the broccoli florets stored in both control and the hydrogel packages decreased after 24 h exposure to fluctuating temperatures. Since good quality broccoli florets are expected to have a firm texture, it can be deduced that hydrogel package could not bring any extra benefit in keeping the textural quality of the broccoli florets than control packages which do not contain hydrogels. Differences between conditions were found insignificant ($p > 0.05$). The detailed results can be seen in Appendix E.

The CIE $L^*a^*b^*$ color parameters measured at the beginning and at the end of 24 h storage under fluctuating temperatures on broccoli florets stored in control and hydrogel packages are given in Figure 7.26. As it can be seen from this figure the L^* which represents the whiteness of the broccoli florets stayed closer to initial value for both package type but was slightly higher for the hydrogel package. Also the control sample was darker (higher a^* value) and yellower (higher b^*) than broccoli florets stored in hydrogel packages. Yellowing of broccoli florets is due to the chlorophyll degradation which occurs during natural senescence of the broccoli florets. During postharvest handling, yellowing is one of the major quality loss factors observed in broccoli florets which affect negatively the consumer preference [134]. Therefore in the present study, broccoli florets packed with hydrogel preserved their visual quality better than the control samples. C^* represents the brightness of broccoli florets. Control sample was more brighter than the others. Differences between conditions for L^* was found significant ($p < 0.05$). However, Differences between conditions for a^* and b^* was found insignificant ($p > 0.05$). The detailed results can be seen in Appendix F.

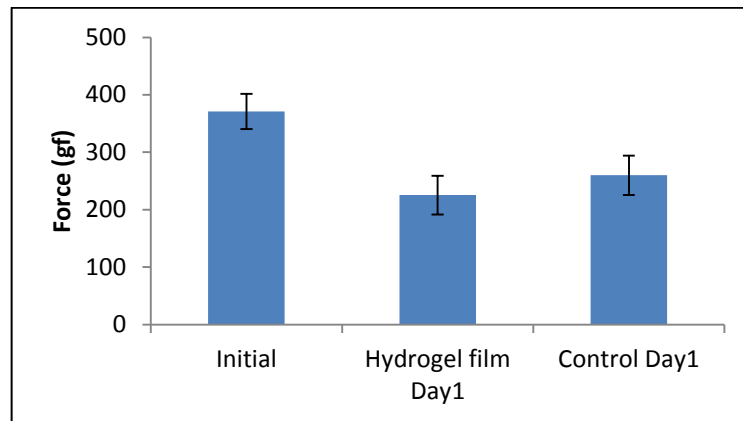


Figure 7.25. Firmness values of the broccoli florets exposed to fluctuating temperatures at the end of 24 hours

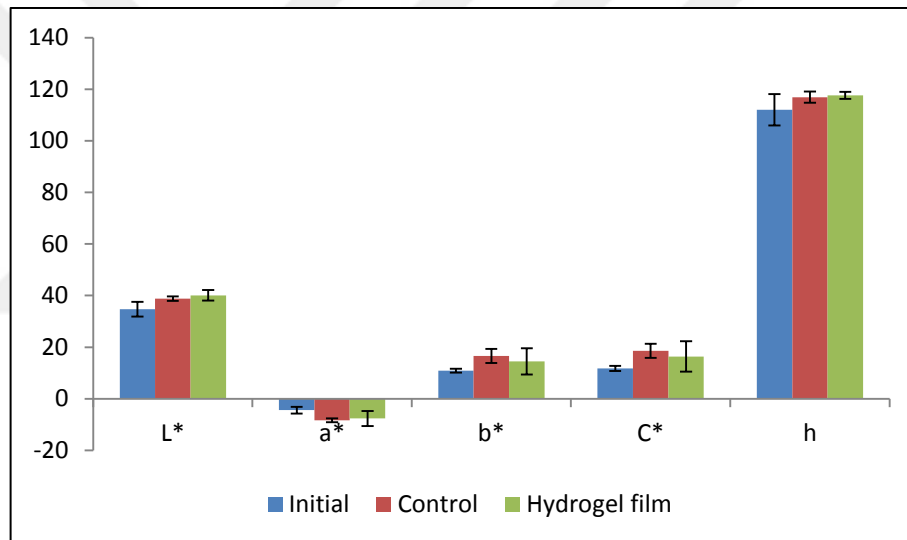


Figure 7.26. CIE L*a*b* color parameter values of the broccoli florets exposed to fluctuating temperatures at the end of 24 hours

The total aerobic bacteria (TBC), yeast and mold load at the beginning and at the end of 24 h storage under fluctuating temperatures of broccoli florets stored in control and hydrogel packages are given in Figure 7.27. As it can be seen from this figure, compared to initial values, TBC of the broccoli florets increased after 24 h storage in both broccoli florets stored in control and hydrogel packages. However, the increase in the control broccoli florets was more significant than hydrogel package samples as their bacterial load increased more than $1 \log_{10}(\text{CFU/g})$ within 24 h. This difference can be attributed to the water condensation on the produce surface in control samples which in turn provide a more favorable environment

for bacterial growth. It is worth to mention that broccoli florets had a very high initial bacterial load of $6.59 \log_{10}(\text{CFU/g})$, a value even higher than mushrooms which is known as one of the highly contaminated fresh produces. Therefore, limiting effect of hydrogel packaging on bacterial growth is considered as an important advantage over control samples which reached to a bacterial count of $7.74 \log_{10}(\text{CFU/g})$ after 24 h of storage. Likewise, the yeast load of the samples in hydrogel packages remained unchanged whereas that of control samples increased after 24 h of storage under fluctuating temperatures. The mold load in both type of samples decreased after 24 h of storage under fluctuating temperatures and the extent of the decrease was higher in control sample than hydrogel sample. As a result, incorporation of hydrogel films inside broccoli florets packages resulted in better humidity regulation and avoided water condensation. In consequence, the broccoli florets in hydrogel containing packages maintained their organoleptic and microbial quality better than control samples. Differences between conditions for TBC was found significant ($p < 0.05$). However, Differences between conditions for yeast and mold was found insignificant ($p > 0.05$). The detailed results can be seen in Appendix G.

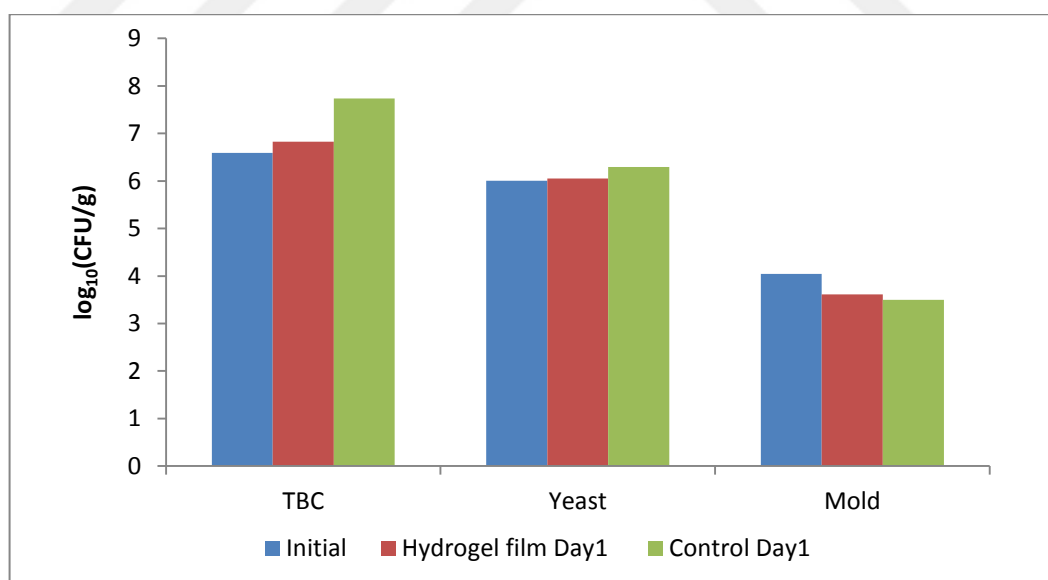


Figure 7.27. The total aerobic bacteria (TBC), yeast and mold load of the broccoli florets exposed to fluctuating temperatures at the end of 24 hours.

8. CONCLUSIONS AND RECOMMENDATIONS FOR FUTURE WORK

8.1. CONCLUSIONS

In the first part of the study, semi-interpenetrating polymer network (Semi-IPN) hydrogel films based on genipin-crosslinked chitosan and CMC were prepared and different properties were characterized. Semi-interpenetrating polymer network (Semi-IPN) hydrogel films were prepared by crosslinking of chitosan with genipin and introducing sodium carboxymethyl cellulose (CMC) to this network via ionic interaction. The optimum weight ratio of Ch: CMC for electrostatic interaction was determined as 1:0.96 via potentiometric and conductometric titrations. The ratios of genipin/chitosan studied were 0.5, 1, 2 and 3% (w/w) with this constant Ch:CMC ratio.

The physical interactions between the Ch and CMC components of the prepared hydrogels were followed by FT-IR. The crosslinking degree could not be effectively followed by FT-IR spectroscopy. In order to show the presence of crosslinking within polymeric network, all samples were immersed in HCl solution and each film was tested to see if it would disintegrate or not. The results of this test showed that crosslinking of chitosan was achieved successfully and permanent hydrogel films were obtained. The formation of a blue color also confirmed that a crosslinked network has been obtained for samples Gnp1, Gnp2 and Gnp3.

The swelling degrees of the films in water decreased from 240 % to 91 % with increasing genipin content from 0.5 to 3 %, which indicates that cross-link density increased with increasing genipin content. Although cross-linking decreased the swelling degree of the hydrogel films in water, the cross-linked films still exhibited acceptable moisture absorbing capacity to be used in food packaging applications.

The char residue contents of the films at 800 °C as determined via TGA increased with increasing genipin content from 0.5 % to 3 % again indicating that crosslink density of the network hydrogel films increased with increasing cross-linker content. The hydrogel films in which chitosan was cross-linked with genipin exhibited one T_g as determined via DMA, which was also higher than the T_g of chitosan, indicating that there was no phase separation

between the Ch and CMC components of the covalently crosslinked permanent hydrogel films. Genipin cross-linking increased the tensile modulus, strength and thermal stability of the hydrogel films.

The biodegradation degrees of uncross-linked and genipin cross-linked Ch-CMC hydrogel films were determined in controlled compost at 58 °C according to ISO 14855-2 method. No phase lag was observed for uncross-linked and cross-linked hydrogel films and microcrystalline cellulose powder used as reference. All started to degrade within first day. A plateau phase was reached after 35 days, 35 days and 13 days for microcrystalline cellulose, uncross-linked film and cross-linked film, respectively. After 45 days, biodegradation degrees according to ISO 14855-2 method were 72 % and 47 % for the uncross-linked and cross-linked hydrogel films, respectively. The crosslinking of the Ch component of the system with genipin and the formation of a semi interpenetrating polymer network (SIPN) significantly decreased the biodegradation rate of the Ch-CMC hydrogel films as compared to the un-crosslinked physical Ch-CMC hydrogel film. The overall results indicate that the developed cross-linked hydrogel films based on chitosan and carboxymethyl cellulose have a great potential for food packaging applications.

In the second part of the study, performance of the hydrogel films on absorbing/regulating the excessive moisture inside packaging atmosphere was studied. As a first step, hydrogel films were incorporated in the Turkish coffee packaging in order to absorb the excess moisture in the headspace of the package which ingress during multiple opening of the lid as it is the case in real household consumption practice. The rationale behind this study was, as a dry food product, Turkish coffee gets stale and wasted due to moisture uptake which enters into the package headspace after each opening before usage at home consumption. Therefore, incorporation of hydrogel film inside the package as a moisture absorber would be a solution to avoid moisture build up inside the coffee and prolong the secondary shelf-life of the Turkish coffee. The results of this study showed that hydrogel films absorb effectively the moisture in the package headspace after opening. However, it was observed that the water absorption by the hydrogel was reversible.

As a consequence, the moisture trapped by the hydrogel after opening of the package desorbed when the lid of the package closed until it reached to moisture equilibrium with the coffee inside which has lower moisture content than the hydrogel. These findings

indicated that rather than a strict moisture absorber, hydrogel films might be more suitable for applications as a moisture regulator in food packages.

For this purpose, a second set of experiment was carried out on high moisture containing foods, namely, mushroom and broccoli florets. In these applications, hydrogel films were used as auxiliary packaging material for regulating the excess moisture in the package headspace. The main aim of this study was to slow down the moisture build up inside the package as a result of product transpiration when exposed to fluctuating temperatures and avoid the condensation of the moisture on the food which would otherwise accelerate the microbial growth and consequent spoilage. The results showed that the cross-linked Ch-CMC hydrogel film (Gnp1) effectively regulated the moisture inside the packages of both mushroom and broccoli and avoided water condensation upon exposure to fluctuating temperatures between 5 to 20 °C. The results of the quality analysis showed that compared to control samples which were packed without hydrogel, the mushrooms packed with hydrogel film had lower total bacterial load, were firmer in texture and lighter in color after being exposed to fluctuating temperatures during 24 h. Similar results were obtained for broccoli in terms of microbiological quality and color with the exception that broccoli florets packed with the hydrogel film were looser in texture than control samples.

It was concluded that the developed hydrogel films based on genipin crosslinked- chitosan and carboxymethyl cellulose have a great potential for food packaging applications and can be effectively used as auxiliary packaging materials for regulating the excessive moisture inside the packaging of high moisture containing foods which can help prolonging their shelflife by avoiding water condensation on the product upon temperature fluctuations.

8.2 RECOMMENDATIONS FOR FUTURE WORK

Several studies to continue this project can be recommended. In one such future study, ways to covalently bond CMC to Ch can be explored to prepare fully cross-linked interpenetrating polymeric networks of Ch and CMC and the effect of this structural change in the physical properties and applications in food packaging as compared to those of the semi-interpenetrating polymeric networks of Ch-CMC hydrogel films prepared in this study can be investigated.

Another recommendation to complete this study is to investigate the affect of hydrogel film on extending the shelf life of mushroom and broccoli florets by regulating the relative humidity of the packaging atmosphere. Hydrogel films can be coated inside trays which is generally used for packaging fruits and vegetable produces for absorbing the excess moisture and moisture absorbing performance of those trays can be investigated on high respiratory produces such as cheese, mushroom, broccoli florets. Additionally, reactivity of genipin with food can be evaluated. Migration risks of genipin from packaging material within food when they get in contact can be investigated.

Hydrogels have been getting importance in biomedical applications and increasingly studied in recent years. The newly developed hydrogel films might be very promising materials for applications in biomedical fields such as tissue engineering and wound healing due to their elastic and resistant structure and absorbing capacity. Therefore absorption capacity profiles of newly hydrogels films in biological medium could be determined instead of water in order to expose other possible medical applications. Additionally, genipin usage instead of glutaraldehyde to construct the network structure of films make them safe and biocompatible. The newly developed hydrogels films which are based on natural biocompatible polymers are quite attractive materials for medical applications.

The developed genipin cross-linked chitosan network posses a blue color resulting in a blue colored fluorescent hydrogel film. This property probably makes it attractive in drug delivery systems or tracking endesirable elements like heavy metals in tissues. The response of newly developed hydrogel films to different pH and temperatures might be determined in order to widen their applications areas for example as novel drug delivery systems or biosensors or in controlled release of fertilizers or water in agriculture.

REFERENCES

1. Global food losses and food waste – Extent, causes and prevention. Rome. 2011 [<http://www.fao.org/docrep/014/mb60e/mb60e.pdf>].
2. Ozdemir M, Floros JD. Active Food Packaging Technologies. *Critical Reviews in Food Science and Nutrition*. 2004;44(3):185-93.
3. Rux G, Mahajan P, Linke M, Saengerlaub S, Pant A, Caleb O, et al. Application of humidity-regulating trays for packaging of fresh strawberry and tomato. *iii International Conference on Fresh-Cut Produce: Maintaining Quality and Safety*. 2016;1141:263-7.
4. Peniche CA-M, W. Goycoolea , F. M. *Monomers, Polymers and Composites from Renewable Resources*. London: Elsevier; 2008.
5. Sung HW, Huang RN, Huang LLH, Tsai CC. In vitro evaluation of cytotoxicity of a naturally occurring cross-linking reagent for biological tissue fixation. *J Biomat Sci-Polym E*. 1999;10(1):63-78.
6. Mi FL , Sung HW, Shyu SS, Su CC, CK. P. Synthesis and characterization of biodegradable TPP/genipin co-crosslinked chitosan gel beads. *Polymer*. 2003;44(21):6521-30.
7. Braun D, Cherdron H, Rehahn M, Ritter H, Voit B. *Polymer Synthesis: Theory and Practice Fundamentals, Methods, Experiments*. Fourth ed. Germany: Springer; 2005.
8. L. RG. *Food Packaging Principles and Practice*. Third Edition ed: CRC Press; 2012.
9. Young RJ, Lovell eA. *Introduction to Polymers*. Third ed. United States of America: CRC Press; 2011.

10. Progelhof R, Throne JL. *Polymer Engineering Principles: Properties, Processes, Tests for Design*: Hanser; 1993.
11. M. WI, John S. *Mechanical Properties of Solid Polymers*. UK. 2013.
12. S. K, S.R. S. *Manufacturing Processes for Engineering Materials*. 5 ed: Pearson Education; 2008.
13. Hoffman AS. Hydrogels for biomedical applications. *Advanced Drug Delivery Reviews*. 2012;64, Supplement:18-23.
14. Rosiak JM, Yoshii F. Hydrogels and their medical applications. *Nuclear Instruments & Methods in Physics Research Section B-Beam Interactions with Materials and Atoms*. 1999;151(1-4):56-64.
15. Ahmed EM. Hydrogel: Preparation, characterization, and applications: A review. *Journal of Advanced Research*. 2015;6(2):105-21.
16. Vashist A, Gupta YK, Ahmad S. Interpenetrating biopolymer network based hydrogels for an effective drug delivery system. *Carbohydrate Polymers*. 2012;87(2):1433-9.
17. Yue Z, Wen F, Gao S, Ang MY, Pallathadka PK, Liu L, et al. Preparation of three-dimensional interconnected macroporous cellulosic hydrogels for soft tissue engineering. *Biomaterials*. 2010;31(32):8141-52.
18. Pereira R, Carvalho A, Vaz DC, Gil MH, Mendes A, Bártolo P. Development of novel alginate based hydrogel films for wound healing applications. *International Journal of Biological Macromolecules*. 2013;52:221-30.
19. Fernández E, López D, López-Cabarcos E, Mijangos C. Viscoelastic and swelling properties of glucose oxidase loaded polyacrylamide hydrogels and the evaluation of their properties as glucose sensors. *Polymer*. 2005;46(7):2211-7.

20. Oztop HN, Hepokur C, Saraydın D. Acrylamide–Sepiolite based composite hydrogels for immobilization of invertase. *Journal of Food Science*. 2009;74(7).
21. Altay A. Tarımda su tutucu olarak kullanılan hidrojelin farklı KNO₃ çözeltilerindeki fiziksel özelliklerinin belirlenmesi. *Tarım Bilimleri Araştırma Dergisi*. 2010;3(2):49-51.
22. Raafat AI, Eid M, El-Arnaouty MB. Radiation synthesis of superabsorbent CMC based hydrogels for agriculture applications. *Nuclear Instruments & Methods in Physics Research Section B-Beam Interactions with Materials and Atoms*. 2012;283:71-6.
23. Jing G, Wang L, Yu H, Amer WA, Zhang L. Recent progress on study of hybrid hydrogels for water treatment. *Colloids and Surfaces A: Physicochemical and Engineering Aspects*. 2013;416:86-94.
24. Kandile NG, Nasr AS. Hydrogels based on a three component system with potential for leaching metals. *Carbohydrate Polymers*. 2011;85(1):120-8.
25. Farris S, Schaich KM, Liu LS, Piergiorganni L, Yam KL. Development of polyion-complex hydrogels as an alternative approach for the production of bio-based polymers for food packaging applications: a review. *Trends in Food Science & Technology*. 2009;20(8):316-32.
26. Syed K. H. Gulrez SA-AaGOP, Carpi PA. Hydrogels: Methods of Preparation, Characterisation and Applications, *Progress in Molecular and Environmental Bioengineering - From Analysis and Modeling to Technology Applications*, Prof. Angelo Carpi (Ed.), InTech, DOI: 10.5772/24553. Available from: <http://www.intechopen.com/books/progress-in-molecular-and-environmental-bioengineering-from-analysis-and-modeling-to-technology-applications/hydrogels-methods-of-preparation-characterisation-and-applications>. InTech; 2011.
27. Caló E, Khutoryanskiy VV. Biomedical applications of hydrogels: A review of patents and commercial products. *European Polymer Journal*. 2015;65:252-67.

28. Van Vlierberghe S, Dubruel P, Schacht E. Biopolymer-Based Hydrogels As Scaffolds for Tissue Engineering Applications: A Review. *Biomacromolecules*. 2011;12(5):1387-408.
29. Utech S, Boccaccini AR. A review of hydrogel-based composites for biomedical applications: enhancement of hydrogel properties by addition of rigid inorganic fillers. *Journal of Materials Science*. 2016;51(1):271-310.
30. Xu X, Jha AK, Harrington DA, Farach-Carson MC, Jia X. Hyaluronic acid-based hydrogels: from a natural polysaccharide to complex networks. *Soft Matter*. 2012;8(12):3280-94.
31. L. BADaKK. Polysaccharide-Modified Synthetic Polymeric Biomaterials. *Biopolymers*. 2010;94(1):128-40.
32. Luo Y, Wang Q. Recent development of chitosan-based polyelectrolyte complexes with natural polysaccharides for drug delivery. *International Journal of Biological Macromolecules*. 2014;64:353-67.
33. Sundar S, Kundu J, Kundu SC. Biopolymeric nanoparticles. *Science and Technology of Advanced Materials*. 2010;11(1):014104.
34. Xiao W, He J, Nichol JW, Wang L, Hutson CB, Wang B, et al. Synthesis and characterization of photocrosslinkable gelatin and silk fibroin interpenetrating polymer network hydrogels. *Acta Biomaterialia*. 2011;7(6):2384-93.
35. Resmi R, Unnikrishnan S, Krishnan LK, Krishnan VK. Synthesis and characterization of silver nanoparticle incorporated gelatin-hydroxypropyl methacrylate hydrogels for wound dressing applications. *Journal of Applied Polymer Science*. 2017;134(10).

36. Lewandowska-Łańcucka J, Mystek K, Mignon A, Van Vlierberghe S, Łatkiewicz A, Nowakowska M. Alginate- and gelatin-based bioactive photocross-linkable hybrid materials for bone tissue engineering. *Carbohydrate Polymers*. 2017;157:1714-22.
37. Gennadios A, Hanna MA, Kurth LB. Application of edible coatings on meats, poultry and seafoods: A review. *Food Science and Technology-Lebensmittel-Wissenschaft & Technologie*. 1997;30(4):337-50.
38. Villegas R, O'Connor TP, Kerry JP, Buckley DJ. Effect of gelatin dip on the oxidative and colour stability of cooked ham and bacon pieces during frozen storage. *International Journal of Food Science and Technology*. 1999;34(4):385-9.
39. Gomez-Guillen MC, Perez-Mateos M, Gomez-Estaca J, Lopez-Caballero E, Gimenez B, Montero P. Fish gelatin: a renewable material for developing active biodegradable films. *Trends in Food Science & Technology*. 2009;20(1):3-16.
40. Lopes LC, Simas-Tosin FF, Cipriani TR, Marchesi LF, Vidotti M, Riegel-Vidotti IC. Effect of low and high methoxyl citrus pectin on the properties of polypyrrole based electroactive hydrogels. *Carbohydrate Polymers*. 2017;155:11-8.
41. Belgacem M.N. AG. Monomers, polymers and composites from renewable resources. France: Elsevier Ltd; 2008.
42. Zu Y, Zhang Y, Zhao X, Shan C, Zu S, Wang K, et al. Preparation and characterization of chitosan–polyvinyl alcohol blend hydrogels for the controlled release of nano-insulin. *International Journal of Biological Macromolecules*. 2012;50(1):82-7.
43. Nand Ashveen V. RDR, R. KJ. Characterization of Genipin Crosslinked Hydrogels Composed of Chitosan and Partially Hydrolyzed Poly(vinyl alcohol). *e-Polymers*. 2013;7(1):402-10.

44. Khurma J, Rohindra D, Nand A. Swelling and thermal characteristics of genipin crosslinked chitosan and poly(vinyl pyrrolidone) hydrogels. *Polymer Bulletin*. 2005;54(3):194-205.
45. Risbud MV, Hardikar AA, Bhat SV, Bhonde RR. pH-sensitive freeze-dried chitosan–polyvinyl pyrrolidone hydrogels as controlled release system for antibiotic delivery. *Journal of Controlled Release*. 2000;68(1):23-30.
46. Lih E, Lee JS, Park KM, Park KD. Rapidly curable chitosan–PEG hydrogels as tissue adhesives for hemostasis and wound healing. *Acta Biomaterialia*. 2012;8(9):3261-9.
47. Islam A, Yasin T. Controlled delivery of drug from pH sensitive chitosan/poly (vinyl alcohol) blend. *Carbohydrate Polymers*. 2012;88(3):1055-60.
48. Martinez-Ruvalcaba A, Chornet E, Rodrigue D. Viscoelastic properties of dispersed chitosan/xanthan hydrogels. *Carbohydrate Polymers*. 2007;67(4):586-95.
49. Zhong X, Ji C, L. AK, Kazarian SG, Ruys A, Deghani F. Fabrication of chitosan/poly(ϵ -caprolactone) composite hydrogels for tissue engineering applications. *J Mater Sci: Mater Med*. 2011;22(2):279-88.
50. Yang J, Chen J, Pan D, Wan Y, Wang Z. pH-sensitive interpenetrating network hydrogels based on chitosan derivatives and alginate for oral drug delivery. *Carbohydrate Polymers*. 2013;92(1):719-25.
51. Munjeri O, Collett JH, Fell JT. Hydrogel beads based on amidated pectins for colon-specific drug delivery: the role of chitosan in modifying drug release. *Journal of Controlled Release*. 1997;46(3):273-8.
52. Wang T, Zhu X-K, Xue X-T, Wu D-Y. Hydrogel sheets of chitosan, honey and gelatin as burn wound dressings. *Carbohydrate Polymers*. 2012;88(1):75-83.

53. Rosca C, Popa MI, Lisa G, Chitanu GC. Interaction of chitosan with natural or synthetic anionic polyelectrolytes. 1. The chitosan–carboxymethylcellulose complex. *Carbohydrate Polymers*. 2005;62(1):35-41.
54. Bajpai AK, Giri A. Water sorption behaviour of highly swelling (carboxy methylcellulose-g-polyacrylamide) hydrogels and release of potassium nitrate as agrochemical. *Carbohydrate Polymers*. 2003;53(3):271-9.
55. Gulsonbi M, Parthasarathy S, Raj KB, Jaisankar V. Green synthesis, characterization and drug delivery applications of a novel silver/carboxymethylcellulose - poly(acrylamide) hydrogel nanocomposite. *Ecotoxicology and Environmental Safety*. 2016;134:421-6.
56. Asma C, Meriem E, Mahmoud B, Djaifer B. Physicochemical characterization of gelatin-cmc composite edibles films from polyion-complex hydrogels. *Journal of the Chilean Chemical Society*. 2014;59(1):2279-83.
57. Ma JH, Xu YJ, Fan B, Liang BR. Preparation and characterization of sodium carboxymethylcellulose/poly(N-isopropylacrylamide)/clay semi-IPN nanocomposite hydrogels. *European Polymer Journal*. 2007;43(6):2221-8.
58. Chen HQ, Fan MW. Chitosan/carboxymethyl cellulose polyelectrolyte complex scaffolds for pulp cells regeneration. *Journal of Bioactive and Compatible Polymers*. 2007;22(5):475-91.
59. Zhao Q, Qian J, An Q, Gao C, Gui Z, Jin H. Synthesis and characterization of soluble chitosan/sodium carboxymethyl cellulose polyelectrolyte complexes and the pervaporation dehydration of their homogeneous membranes. *Journal of Membrane Science*. 2009;333(1–2):68-78.
60. Mitsumata T, Suemitsu Y, Fujii K, Fujii T, Taniguchi T, Koyama K. pH-response of chitosan, κ -carrageenan, carboxymethyl cellulose sodium salt complex hydrogels. *Polymer*. 2003;44(23):7103-11.

61. Bigucci F, Abruzzo A, Vitali B, Saladini B, Cerchiara T, Gallucci MC, et al. Vaginal inserts based on chitosan and carboxymethylcellulose complexes for local delivery of chlorhexidine: Preparation, characterization and antimicrobial activity. *International Journal of Pharmaceutics*. 2015;478(2):456-63.
62. Cerchiara T, Abruzzo A, Parolin C, Vitali B, Bigucci F, Gallucci MC, et al. Microparticles based on chitosan/carboxymethylcellulose polyelectrolyte complexes for colon delivery of vancomycin. *Carbohydrate Polymers*. 2016;143:124-30.
63. Lai WF, Shum HC. Hypromellose-graft-chitosan and Its Polyelectrolyte Complex as Novel Systems for Sustained Drug Delivery. *Acs Applied Materials & Interfaces*. 2015;7(19):10501-10.
64. Nakagawa K, Sowasod N, Tanthapanichakoon W, Charinpanitkul T. Hydrogel based oil encapsulation for controlled release of curcumin by using a ternary system of chitosan, kappa-carrageenan, and carboxymethylcellulose sodium salt. *Lwt-Food Science and Technology*. 2013;54(2):600-5.
65. Kaihara S, Suzuki Y, Fujimoto K. In situ synthesis of polysaccharide nanoparticles via polyion complex of carboxymethyl cellulose and chitosan. *Colloids and Surfaces B: Biointerfaces*. 2011;85(2):343-8.
66. Feng ZC, Shao ZZ, Yao JR, Chen X. Protein adsorption and separation on amphoteric chitosan/carboxymethylcellulose membranes. *Journal of Biomedical Materials Research Part A*. 2008;86A(3):694-700.
67. Municipal Solid Waste Generation, Recycling, and Disposal in the United States: Facts and Figures for 2012 2012 [https://www.epa.gov/sites/production/files/2015-09/documents/2_msw_fs.pdf].
68. Cezmi N. Türkiye'de Eysel Nitelikli Katı Atıklar Available fom: https://www.tubitak.gov.tr/tubitak_content_files/vizyon2023/csk/EK-4.pdf.

69. Cox J, Downing P. Food Behaviour Consumer Research: Quantitative Phase. wrap, Banbury UK. 2007 [Available from: http://www.wrap.org.uk/downloads/Food_behaviour_consumer_research_quantitative_jun_2007.0a80ed7d.6393.pdf].
70. We Don't Waste Food! a Householder Survey Banbury, UK. 2007 [http://www.wrap.org.uk/sites/files/wrap/We_don_t_waste_food_A_household_survey_mar_07.db6802f9.397.pdf].
71. Williams H, Wikström F, Löfgren M. A life cycle perspective on environmental effects of customer focused packaging development. *Journal of Cleaner Production*. 2008;16(7):853-9.
72. L. RG. *Food Packaging Principles and Practice*. Second Edition ed. USA: CRC Press; 2006.
73. Saha N, Benlikaya R, Slobodian P, Saha P. Breathable and Polyol Based Hydrogel Food Packaging. *Journal of Biobased Materials and Bioenergy*. 2015;9(2):136-44.
74. Marsh K, Bugusu B. *Food Packaging—Roles, Materials, and Environmental Issues*. *Journal of Food Science*. 2007;72(3):39-55.
75. L.W. M. *Plastic Films in Food Packaging Materials, Technology and Applications*. Oxford: Elsevier; 2013.
76. Brown WE. *Plastics in Food Packaging Properties, Design and Fabrications*: Marcel Dekker, Inc.; 1992.
77. Gregorova A, Saha N, Kitano T, Saha P. Hydrothermal effect and mechanical stress properties of carboxymethylcellulose based hydrogel food packaging. *Carbohydrate Polymers*. 2015;117:559-68.

78. Müller CMO, Laurindo JB, Yamashita F. Effect of cellulose fibers addition on the mechanical properties and water vapor barrier of starch-based films. *Food Hydrocolloids*. 2009;23(5):1328-33.
79. Liu L, Kerry JF, Kerry JP. Application and assessment of extruded edible casings manufactured from pectin and gelatin/sodium alginate blends for use with breakfast pork sausage. *Meat Science*. 2007;75(2):196-202.
80. Lee KY, Shim J, Lee HG. Mechanical properties of gellan and gelatin composite films. *Carbohydrate Polymers*. 2004;56(2):251-4.
81. Ryu SY, Rhim JW, Roh HJ, Kim SS. Preparation and Physical Properties of Zein-Coated High-Amylose Corn Starch Film. *LWT - Food Science and Technology*. 2002;35(8):680-6.
82. Rhim JW, Wang LF. Mechanical and water barrier properties of agar/kappa-carrageenan/konjac glucomannan ternary blend biohydrogel films. *Carbohydrate Polymers*. 2013;96(1):71-81.
83. Wang LF, Rhim JW. Preparation and application of agar/alginate/collagen ternary blend functional food packaging films. *International Journal of Biological Macromolecules*. 2015;80:460-8.
84. Yam KL, Lee DS. Design of modified atmosphere packaging for fresh produce In *Active Food Packaging* Design of modified atmosphere packaging for fresh produce In *Active Food Packaging*. Glasgow: Blackie Academic & Professional; 1995.
85. Yam KL, Takhistov PT, Miltz J. Intelligent Packaging: Concepts and Applications. *Journal of Food Science*. 2005;70(1).
86. Su Y, Mo X. Genipin crosslinked gelatin nanofibers for tissue engineering. *Journal of Controlled Release*. 2011;152:e230-e2.

87. Feng H, Zhang L, Zhu C. Genipin crosslinked ethyl cellulose–chitosan complex microspheres for anti-tuberculosis delivery. *Colloids and Surfaces B: Biointerfaces*. 2012;103:530-7.
88. Fourier Transform Infrared Spectroscopy (FT-IR) 2017 [Available from: <http://www.nuance.northwestern.edu/keck-ii/keck-ii-instruments/ftir-spectroscopy/>].
89. Brown ME. *Introduction to Thermal Analysis*. Second ed: Springer Netherlands; 2001.
90. Menard KP. *Dynamic Mechanical Analysis A Practical Introduction*, CRC Press. Second Edition ed: CRC Press; 2008.
91. Bottom R. *Principles and Applications of Thermal Analysis*. Singapore: Wiley-Blackwell; 2008. 480 p.
92. Description about MODA Available from: http://saidagroup.jp/fds_en/products/description-moda.
93. ISO 3972 Sensory analysis - Methodology - Method of investigating sensitivity of taste. International Organization for Standardization. Switzerland.2011.
94. ISO 5496 Sensory analysis —Methodology — Initiation and training of assessors in the detection and recognition of odours. International Organization for Standardization. Switzerland.2006.
95. ISO 4121 Sensory analysis — Guidelines for the use of quantitative response scales. International Organization for Standardization. Switzerland2003.
96. Jacxsens L, Devlieghere Fa, Debevere J. *International Journal of Food Microbiology*. 2002;73(2-3):331-41.

97. Molino JA, Kennedy JF, Beuse PA, Miller CC, Davis W, Andersen CK. Daytime Color Appearance of Retroreflective Traffic Control Sign Materials. 2013.
98. Van de Velde K, Kiekens P. Structure analysis and degree of substitution of chitin, chitosan and dibutrylchitin by FT-IR spectroscopy and solid state ^{13}C NMR. *Carbohydrate Polymers*. 2004;58(4):409-16.
99. Jiang H, GA, Zuo Y., Li, Y. Cheng, Wang, L. H. A homogenous CS/NaCMC/n-HA polyelectrolyte complex membrane prepared by gradual electrostatic assembling. *J Mater Sci: Mater Med* 2011;22:289-97.
100. Liuyun J. YL, Z. Li, Jianguo, L. Preparation and properties of a novel bone repair composite:nano-hydroxyapatite/chitosan/carboxymethyl cellulose. *J Mater Sci: Mater Med*. 2008;9:981-7.
101. Liu XG, Y. L. Yang, D. , Li, Z. Z. Yao, K. D. Antibacterial Action of Chitosan and Carboxymethylated Chitosan. *J Appl Polym Sci*,. 2001;79:1324-35.
102. Aldana AAG, A. Strumia, M.C. Martinelli, M. Preparation and characterization of chitosan/genipin/poly(N-vinyl-2-pyrrolidone) films for controlled release drugs. *Mater Chem Phys*.134.
103. Butler MF, Ng Y, Pudney PDA. Mechanism and kinetics of the crosslinking reaction between biopolymers containing primary amine groups and genipin. *Journal of Polymer Science:Part A Polymer Chemistry*. 2003;41
104. Touyama R, Takade Y, Inoue K, Kawamura I, Yatsuzuka M, Ikumoto T, et al. Studies on blue pigments produced from genipin and methylamine. I. Structures of the brownish red pigments , intermediates leading to the blue pigments. *Chem Pharm Bull*. 1994;42.
105. Fujikawa S, Fukui Y, Koga K. Structure of genipocyanin G1, a spontaneous reaction between genipin and glycine,. *Tetrahedron Lettres*,.28(40).

106. Rohindra DR, Nand AV, Khurma JR. Swelling properties of chitosan hydrogels. *The South Pacific Journal of Natural Sciences*. 2004;22(1):32-5.
107. Liu Y, Chen W, Kim H-I. Mechanical and Antimicrobial Properties of Genipin-Crosslinked Chitosan/Poly(Ethylene Glycol) IPN. *Journal of Macromolecular Science, Part B*. 2012;51(6):1069-79.
108. Cui L, Jia J, Guo Y, Liu Y, Zhu P. Preparation and characterization of IPN hydrogels composed of chitosan and gelatin cross-linked by genipin. *Carbohydrate Polymers*. 2014;99:31-8.
109. Siqueira EJ, Brochier Salon MC, Mauret E. The effects of sodium chloride (NaCl) and residues of cellulosic fibres derived from sodium carboxymethylcellulose (NaCMC) synthesis on thermal and mechanical properties of CMC films. *Industrial Crops and Products*. 2015;72:87-96.
110. Tripathi S, Mehrotra GK, Dutta PK. Physicochemical and bioactivity of cross-linked chitosan–PVA film for food packaging applications. *International Journal of Biological Macromolecules*. 2009;45(4):372-6.
111. Bonilla J, Fortunati E, Atarés L, Chiralt A, Kenny JM. Physical, structural and antimicrobial properties of poly vinyl alcohol–chitosan biodegradable films. *Food Hydrocolloids*. 2014;35:463-70.
112. Kittur FS, Harish Prashanth KV, Udaya Sankar K, Tharanathan RN. Characterization of chitin, chitosan and their carboxymethyl derivatives by differential scanning calorimetry. *Carbohydrate Polymers*. 2002;49(2):185-93.
113. Sakurai K, Maegawa T, Takahashi T. Glass transition temperature of chitosan and miscibility of chitosan/poly(N-vinyl pyrrolidone) blends. *Polymer*. 2000;41(19):7051-6.


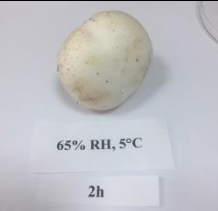












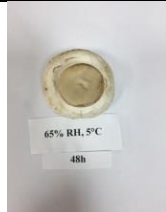









114. El-Sayed S, Mahmoud KH, Fatah AA, Hassen A. DSC, TGA and dielectric properties of carboxymethyl cellulose/polyvinyl alcohol blends. *Physica B: Condensed Matter*. 2011;406(21):4068-76.
115. Pieróg M, Ostrowska-Czubenko J, Gierszewska-Drużyńska M. Thermal degradation of double crosslinked hydrogel chitosan membranes. *Progr Chem Appl Chitin Deriv*. 2012;17:67-74.
116. Acharyulu R, Gomathi T, N. SP. Synthesis and characterization of cross linked chitosan-polystyrene polymer blends. *Der Pharmacia Lettre*, . 2013;5: 74-83.
117. Oun AA, Rhim J-W. Preparation and characterization of sodium carboxymethyl cellulose/cotton linter cellulose nanofibril composite films. *Carbohydrate Polymers*. 2015;127:101-9.
118. Anese M., Manzocco L., M.C. N. Modeling secondary shelf-life of ground roasted coffee. *J Agric Food Chem*. 2006;54.
119. Makri E, Tsimogiannis D, Dermesonluoglu EK, Taoukisa PS. Modeling of Greek coffee aroma loss during storage at different temperatures and water activities. *Procedia Food Science*. 2011;1:1111-7.
120. Mahajan PV, Rodrigues FAS, Motel A, Leonhard A. Development of a moisture absorber for packaging of fresh mushrooms (*Agaricus bisporus*). *Postharvest Biology and Technology*. 2008;48(3):408-14.
121. Rux G, Mahajan PV, Geyer M, Linke M, Pant A, Saengerlaub S, et al. Application of humidity-regulating tray for packaging of mushrooms. *Postharvest Biology and Technology*. 2015;108:102-10.
122. Akram M, Jansen KMB, Bhowmik S, Ernst LJ. Moisture absorption analysis of high performance polyimide adhesive. *SAMPE*; 2011.

123. Gao D, Heimann RB, Lerchner J, Seidel J, Wolf G. Development of a novel moisture sensor based on superabsorbent poly(acrylamide)-montmorillonite composite hydrogels. *Journal of Materials Science*. 2001;36(18):4567-71.
124. Aaron L. Brody EPS, Lauri R. Kline. *Active Packaging for Food Applications*: CRC Press; 2001.
125. Burton KS, Partis MD, Wood DA, Thurston CF. Accumulation of serine proteinase in senescent sporophores of the cultivated mushroom, *Agaricus bisporus*. *Mycological Research*. 1997;101(2):146-52.
126. Singh P, Langowski H-C, Wani AA, Saengerlaub S. Recent advances in extending the shelf life of fresh *Agaricus* mushrooms: a review. Recent advances in extending the shelf life of fresh *Agaricus* mushrooms: a review. *J Sci Food Agric*. 2010;90:1393-402.
127. McGarry A, Burton KS. Mechanical properties of the mushroom, *Agaricus bisporus*. *Mycological Research*. 1994;98(2):241-5.
128. Martinez MV, Whitaker JR. The biochemistry and control of enzymatic browning. *Trends in Food Science & Technology*. 1995;6(6):195-200.
129. Moquet F, Mamoun M, Olivier JM. *Pseudomonas tolaasii* and tolaasin: comparison of symptom induction on a wide range of *Agaricus bisporus* strains. *Pseudomonas tolaasii* and tolaasin: comparison of symptom induction on a wide range of *Agaricus bisporus* strains. *FEMS Microbiology Letters*. 1996;142:99-103.
130. Wells J, Sapers G, Fett W, Butterfield J, Jones J, Bouzar H. Postharvest discoloration of the cultivated mushroom *Agaricus bisporus* caused by *Pseudomonas tolaasii*, 'P. reactans', and 'P. gingeri'. *Phytopathology* 1996;86:1098-104.
131. Doores S, Kramer M, Beelman R. Evaluation and Bacterial Populations Associated with Fresh Mushrooms (*Agaricus Bisporus*). *Developments in Crop Science*. 1987;10:283-94.

132. Chikthimmah N, Beelman R. Microbial Spoilage of Fresh Mushrooms. *Microbiology of Fruits and Vegetables*: CRC Press; 2005. p. 135-58.
133. Chikthimmah N, McMillen J, LaBorde L, Demirci A, Beelman R. Irrigation with electrolyzed oxidizing water to reduce bacterial populations on fresh mushrooms. Institute of Food Technologists Annual Meeting; Chicago, IL 2003.
134. Florkowski WJ, Brückner B, Schonhof I. Consumer preferences for broccoli quality attributes and packaging. XIII International Symposium on Horticultural Economics; New Jersey, USA. p. 453-8.

APPENDIX A: THE DETAILED PICTURES OF MUSHROOM RECORDED AT EACH TIME INTERVAL

Table A.1. Appearance of mushroom stored in dessicator with 65, 85 and 100 %RH at 25°C

RH (%)	Initial	t=2h	t=4h	t=6h	t=24h	t=26h	t=28h	t=30h	t=48h
65	 65% RH, 5°C Initial	 65% RH, 5°C 2h	 65% RH, 5°C 4h	 65% RH, 5°C 6h	 65% RH, 5°C 24h	 65% RH, 5°C 26h	 65% RH, 5°C 28h	 65% RH, 5°C 30h	 65% RH, 5°C 48h
				 65% RH, 5°C 6h	 65% RH, 5°C 24h	 65% RH, 5°C 26h	 65% RH, 5°C 28h	 65% RH, 5°C 30h	 65% RH, 5°C 48h
85	 85% RH, 5°C Initial	 85% RH, 5°C 2h	 85% RH, 5°C 4h	 85% RH, 5°C 6h	 85% RH, 5°C 24h	 85% RH, 5°C 26h	 85% RH, 5°C 28h	 85% RH, 5°C 30h	 85% RH, 5°C 48h






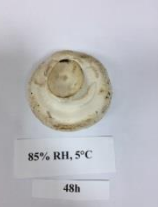


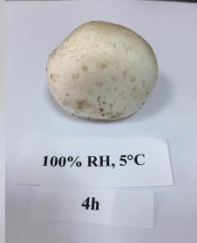
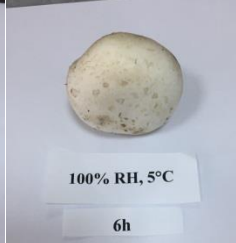

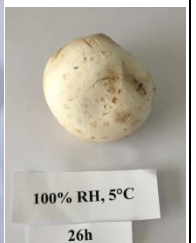







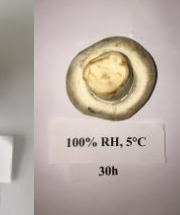
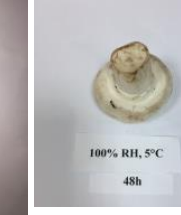



































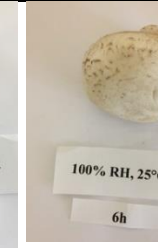












RH (%)	Initial	t=2h	t=4h	t=6h	t=24h	t=26h	t=28h	t=30h	t=48h
				 85% RH, 5°C 6h	 85% RH, 5°C 24h	 85% RH, 5°C 26h	 85% RH, 5°C 28h	 85% RH, 5°C 30h	 85% RH, 5°C 48h
100	 100% RH, 5°C Initial	 100% RH, 5°C 2h	 100% RH, 5°C 4h	 100% RH, 5°C 6h	 100% RH, 5°C 24h	 100% RH, 5°C 26h	 100% RH, 5°C 28h	 100% RH, 5°C 30h	 100% RH, 5°C 48h
				 100% RH, 5°C 6h	 100% RH, 5°C 24h	 65% RH, 5°C 26h	 100% RH, 5°C 28h	 100% RH, 5°C 30h	 100% RH, 5°C 48h


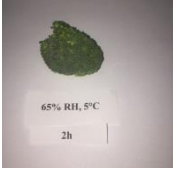






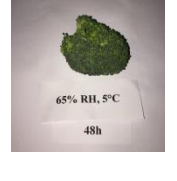












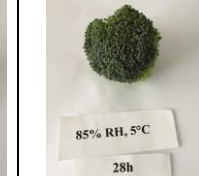


Table A.2. Appearance of mushroom stored in dessicator with 65, 85 and 100 %RH at 25 °C

RH (%)	Initial	t=2h	t=4h	t=6h	t=24h	t=26h	t=28h	t=30h	t=48h
65	 65% RH, 25°C Initial	 65% RH, 25°C 2h	 65% RH, 25°C 4h	 65% RH, 5°C 6h	 65% RH, 25°C 24h	 65% RH, 25°C 26h	 65% RH, 25°C 28h	 65% RH, 25°C 30h	 65% RH, 25°C 30h
		 65% RH, 5°C 6h		 65% RH, 5°C 6h	 65% RH, 25°C 24h	 65% RH, 25°C 26h	 65% RH, 25°C 28h	 65% RH, 25°C 30h	 65% RH, 25°C 48h
85	 85% RH, 25°C Initial	 85% RH, 25°C 2h	 85% RH, 5°C 4h	 85% RH, 25°C 6h	 85% RH, 25°C 24h	 85% RH, 25°C 26h	 85% RH, 25°C 28h	 85% RH, 25°C 30h	 85% RH, 25°C 48h

RH (%)	Initial	t=2h	t=4h	t=6h	t=24h	t=26h	t=28h	t=30h	t=48h
		 85% RH, 25°C 0h		 85% RH, 25°C 6h	 85% RH, 25°C 24h	 85% RH, 25°C 26h	 85% RH, 25°C 28h	 85% RH, 25°C 30h	 85% RH, 25°C 48h
100	 100% RH, 25°C Initial	 100% RH, 5°C 2h	 100% RH, 25°C 4h	 100% RH, 25°C 6h	 100% RH, 25°C 24h	 100% RH, 25°C 26h	 100% RH, 25°C 28h	 100% RH, 25°C 30h	 100% RH, 25°C 48h
		 100% RH, 25°C 6h		 100% RH, 25°C 6h	 100% RH, 25°C 24h	 100% RH, 25°C 26h	 100% RH, 25°C 28h	 100% RH, 25°C 30h	 100% RH, 25°C 48h

APPENDIX B: THE DETAILED PICTURES OF BROCCOLI FLORETS RECORDED AT EACH TIME INTERVAL

Table B.1. Appearance of broccoli stored in dessicator with 65, 85 and 100 %RH at 5 °C

RH (%)	Initial	t=2h	t=4h	t=6h	t=24h	t=26h	t=28h	t=30h	t=48h
65	 65% RH, 5°C Initial	 65% RH, 5°C 2h	 65% RH, 5°C 4h	 65% RH, 5°C 6h	 65% RH, 5°C 24h	 65% RH, 5°C 26h	 65% RH, 5°C 28h	 65% RH, 5°C 30h	 65% RH, 5°C 48h
				 65% RH, 5°C 6h	 65% RH, 5°C 24h	 65% RH, 5°C 26h	 65% RH, 5°C 28h	 65% RH, 5°C 30h	 65% RH, 5°C 48h
85	 85% RH, 5°C Initial	 85% RH, 5°C 2h	 85% RH, 5°C 4h	 85% RH, 5°C 6h	 85% RH, 5°C 24h	 85% RH, 5°C 26h	 85% RH, 5°C 28h	 85% RH, 5°C 30h	 85% RH, 5°C 48h























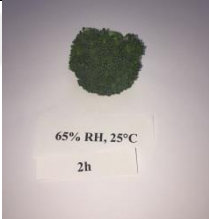





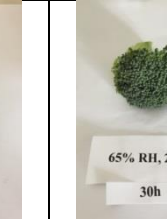





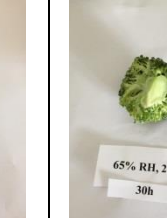



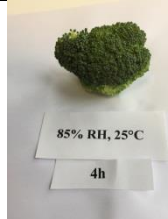

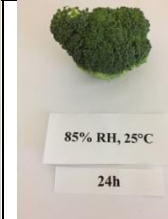





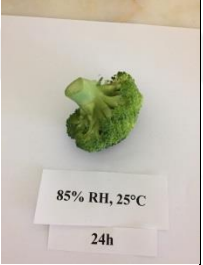


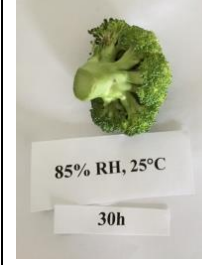
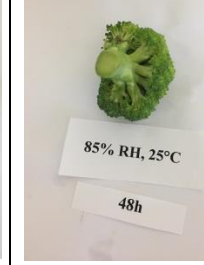














RH (%)	Initial	t=2h	t=4h	t=6h	t=24h	t=26h	t=28h	t=30h	t=48h
				 85% RH, 5°C 6h	 85% RH, 5°C 24h	 85% RH, 5°C 26h	 85% RH, 5°C 28h	 85% RH, 5°C 30h	 85% RH, 5°C 48h
100	 100% RH, 5°C Initial	 100% RH, 5°C 2h	 100% RH, 5°C 4h	 100% RH, 5°C 6h	 100% RH, 5°C 6h	 100% RH, 5°C 26h	 100% RH, 5°C 28h	 100% RH, 5°C 30h	 100% RH, 5°C 48h
				 100% RH, 5°C 6h	 100% RH, 5°C 6h	 100% RH, 5°C 26h	 100% RH, 5°C 28h	 100% RH, 5°C 30h	 100% RH, 5°C 48h

Table B.2. Appearance of broccoli stored in dessicator with 65, 85 and 100 %RH at 25 °C

RH (%)	Initial	t=2h	t=4h	t=6h	t=24h	t=26h	t=28h	t=30h	t=48h
65	 65% RH, 25°C Initial	 65% RH, 25°C 2h	 65% RH, 25°C 4h	 65% RH, 25°C 6h	 65% RH, 25°C 24h	 65% RH, 25°C 26h	 65% RH, 25°C 28h	 65% RH, 25°C 30h	 65% RH, 25°C 48h
				 65% RH, 25°C 6h	 65% RH, 25°C 24h	 65% RH, 25°C 26h	 65% RH, 25°C 28h	 65% RH, 25°C 30h	 65% RH, 25°C 48h
85	 85% RH, 25°C Initial	 85% RH, 25°C 2h	 85% RH, 25°C 4h	 85% RH, 25°C 6h	 85% RH, 25°C 24h	 85% RH, 25°C 26h	 85% RH, 25°C 28h	 85% RH, 25°C 30h	 85% RH, 25°C 48h

RH (%)	Initial	t=2h	t=4h	t=6h	t=24h	t=26h	t=28h	t=30h	t=48h
				 85% RH, 25°C 6h	 85% RH, 25°C 24h	 85% RH, 25°C 26h	 85% RH, 25°C 28h	 85% RH, 25°C 30h	 85% RH, 25°C 48h
100	 100% RH, 25°C Initial		 100% RH, 25°C 4h	 100% RH, 25°C 6h	 100% RH, 25°C 24h	 100% RH, 25°C 26h	 100% RH, 25°C 28h	 100% RH, 25°C 30h	 100% RH, 25°C 48h
				 100% RH, 25°C 6h	 100% RH, 25°C 24h	 100% RH, 25°C 26h	 100% RH, 25°C 28h	 100% RH, 25°C 30h	 100% RH, 25°C 48h

APPENDIX C: THE DETAILED PICTURES OF SILICA GELS AND HYDROGEL FILMS RECORDED AT EACH TIME INTERVAL

Table C.1. Appearance of silica gel stored in dessicator with 65, 85 and 100 %RH at 5 °C




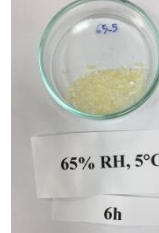
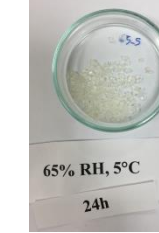






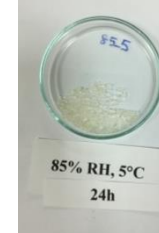


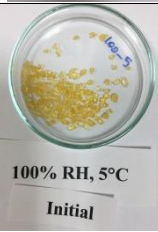
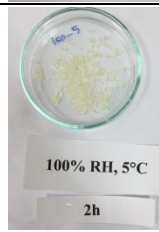
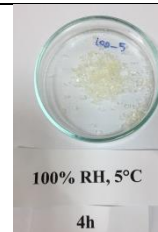


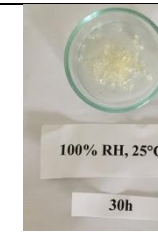
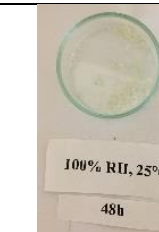
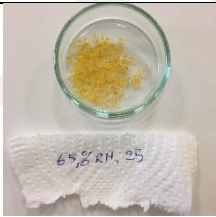
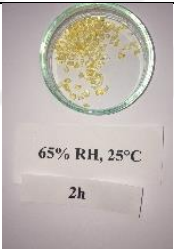
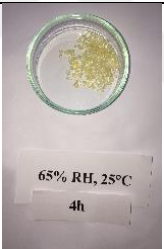

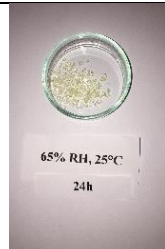
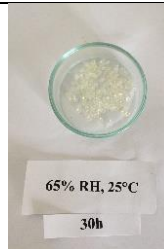


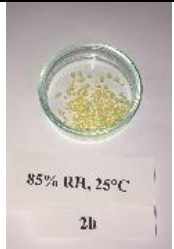


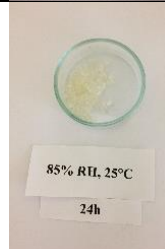




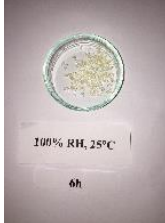

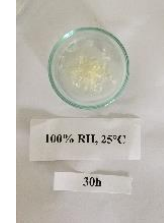
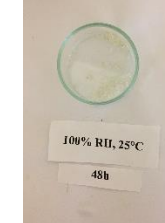
RH (%)	Initial	t=2h	t=4h	t=6h	t=24h	t=30h	t=48h
65	 65% RH, 5°C Initial	 65% RH, 5°C 2h	 65% RH, 5°C 4h	 65% RH, 5°C 6h	 65% RH, 5°C 24h	 65% RH, 5°C 30h	 65% RH, 5°C 48h
85	 85% RH, 5°C Initial	 85% RH, 5°C 2h	 85% RH, 5°C 4h	 85% RH, 5°C 6h	 85% RH, 5°C 24h	 85% RH, 5°C 30h	 85% RH, 5°C 48h
100	 100% RH, 5°C Initial	 100% RH, 5°C 2h	 100% RH, 5°C 4h	 100% RH, 5°C 6h	 100% RH, 5°C 24h	 100% RH, 25°C 30h	 100% RH, 25°C 48h

Table C.2. Appearance of silica gel stored in dessicator with 65, 85 and 100 %RH at 25 °C

RH (%)	Initial	t=2h	t=4h	t=6h	t=24h	t=30h	t=48h
65							
85							
100							

C.3. Appearance of hydrogel film stored in dessicator with 65, 85 and 100 %RH at 5 °C


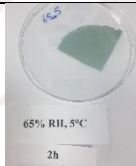
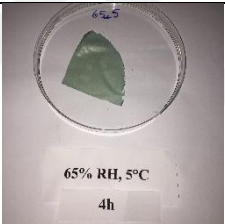
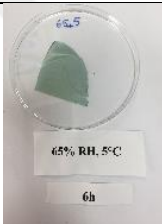
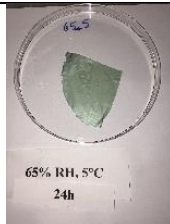
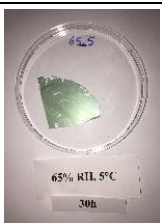


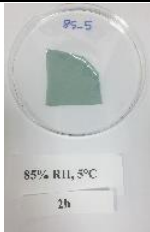
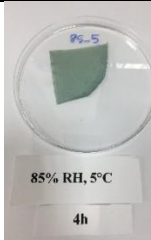
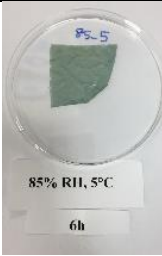



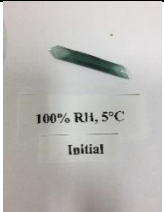
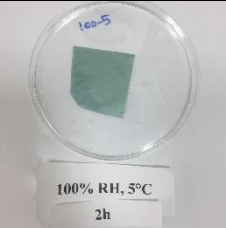
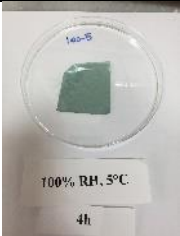
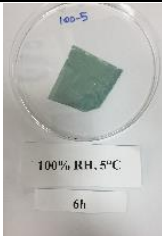
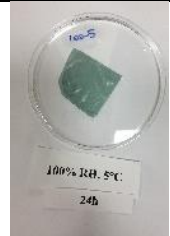
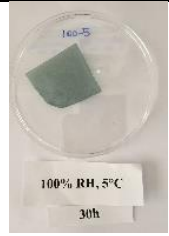

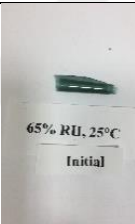
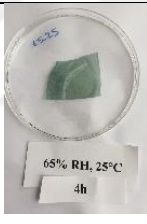
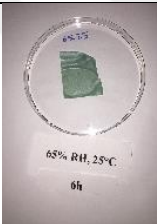

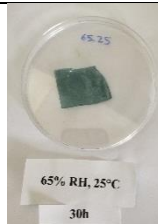
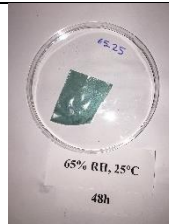

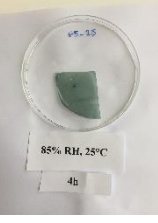
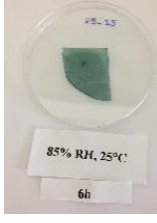
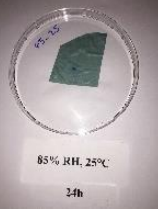



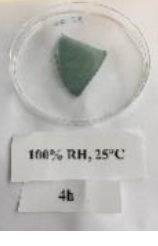

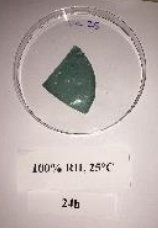


RH (%)	Initial	t=2h	t=4h	t=6h	t=24h	t=30h	t=48h
65	 65% RH, 5°C Initial	 65% RH, 5°C 2h	 65% RH, 5°C 4h	 65% RH, 5°C 6h	 65% RH, 5°C 24h	 65% RH, 5°C 30h	 65% RH, 5°C 48h
85	 85% RH, 5°C Initial	 85% RH, 5°C 2h	 85% RH, 5°C 4h	 85% RH, 5°C 6h	 85% RH, 5°C 24h	 85% RH, 5°C 30h	 85% RH, 5°C 48h
100	 100% RH, 5°C Initial	 100% RH, 5°C 2h	 100% RH, 5°C 4h	 100% RH, 5°C 6h	 100% RH, 5°C 24h	 100% RH, 5°C 30h	 100% RH, 5°C 48h

Table C.4. Appearance of silica gel stored in dessicator with 65, 85 and 100 %RH at 25 °C

RH (%)	Initial	t=4h	t=6h	t=24h	t=30h	t=48h
65	 65% RH, 25°C Initial	 65% RH, 25°C 4h	 65% RH, 25°C 6h	 65% RH, 25°C 24h	 65% RH, 25°C 30h	 65% RH, 25°C 48h
85	 85% RH, 25°C Initial	 85% RH, 25°C 4h	 85% RH, 25°C 6h	 85% RH, 25°C 24h	 85% RH, 25°C 30h	 85% RH, 25°C 48h
100	 100% RH, 25°C Initial	 100% RH, 25°C 4h	 100% RH, 25°C 6h	 100% RH, 25°C 24h	 100% RH, 25°C 30h	 100% RH, 25°C 48h

APPENDIX D: THE DETAILED PICTURES OF MUSHROOM AND BROCCOLI FLORETS RECORDED AT EACH TIME INTERVAL

Table D.1. Appearance of mushroom at each time interval during humidity regulating cycle study


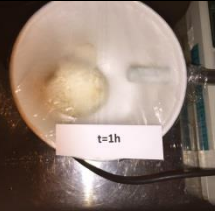

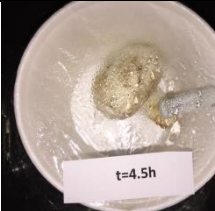
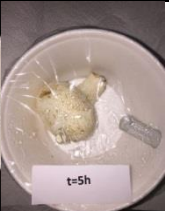

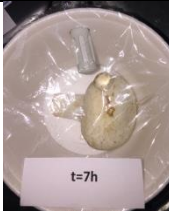
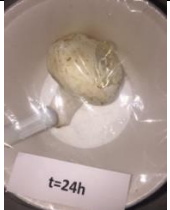

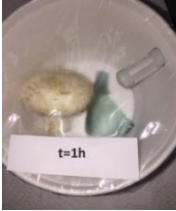


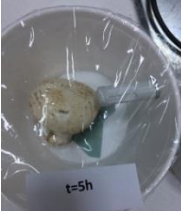


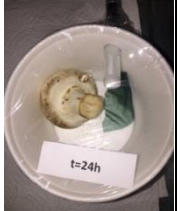








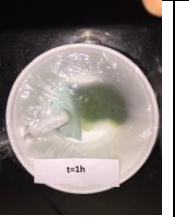

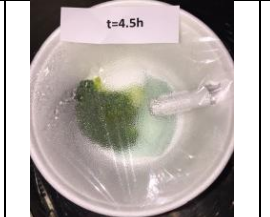



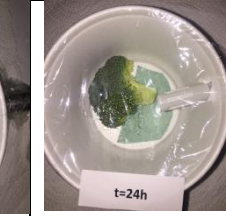
	Initial	t=1h	t=3.5h	t=4.5h	t=5h	t=6h	t=7h	t=24h
Control								
Hydrogel film								

Table D.2. Appearance of broccoli florets at each time interval during humidity regulating cycle study

	Initial	t=1h	t=3.5h	t=4.5h	t=5h	t=6h	t=7h	t=24h
Control								
Hydrogel film								

APPENDIX E: STATISTICAL ANALYSIS RESULTS FOR FIRMNESS ANALYSIS

Table E.1. Analysis of variance of firmness for mushroom

Source	DF	Sum of squares	Mean squares	F	Pr > F
Model	2	55451.012	27725.506	5.048	0.052
Error	6	32951.298	5491.883	-	-
Corrected Total	8	88402.311	-	-	-
<i>Computed against model $Y=Mean(Y)$</i>				-	-

Table E.2. Analysis of variance of firmness for broccoli

Source	DF	Sum of squares	Mean squares	F	Pr > F
Model	2	34715.223	17357.612	4.319	0.069
Error	6	24116.074	4019.346	-	-
Corrected Total	8	58831.297	-	-	-
<i>Computed against model $Y=Mean(Y)$</i>				-	-

Table E.3. Q1 / Tukey (HSD) / Analysis of the differences between the categories with a confidence interval of 95% for firmness of mushroom

Category	LS means	Standard error	Lower bound (95%)	Upper bound (95%)	Groups
Hydrogel	420.110	42.786	315.388	524.832	A
Initial	280.074	42.786	175.351	384.796	A
Control	235.996	42.786	131.274	340.718	A

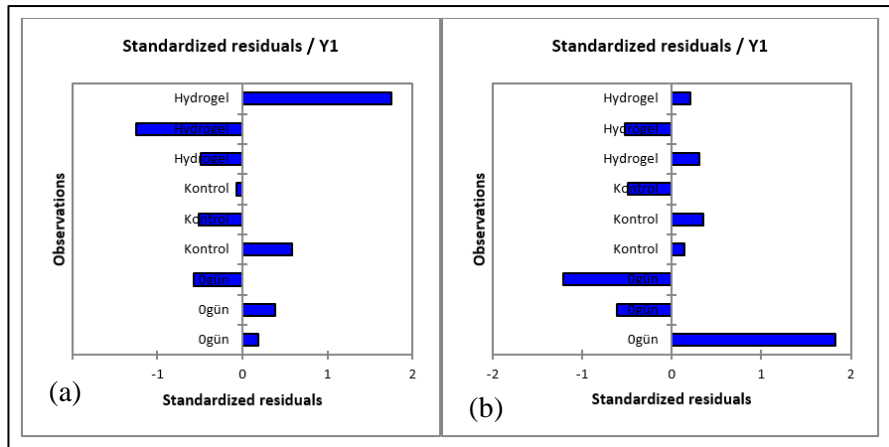


Figure G.1. Standardized residual of firmness (a) mushroom, (b) broccoli

Table E.4. Q1 / Tukey (HSD) / Analysis of the differences between the categories with a confidence interval of 95% for firmness of broccoli

Category	LS means	Standard error	Lower bound (95%)	Upper bound (95%)	Groups
Initial	370.983	36.603	281.394	460.572	A
Control	259.871	36.603	170.282	349.461	A
Hydrogel	225.436	36.603	135.847	315.025	A

APPENDIX F: STATISTICAL ANALYSIS RESULTS FOR COLOR MEASUREMENT

Table F.1. Analysis of variance of Variable L* for color measurement of mushroom

Source	DF	Sum of squares	Mean squares	F	Pr > F
Model	2	11.796	5.898	1.552	0.286
Error	6	22.801	3.800	-	-
Corrected Total	8	34.596	-	-	-
<i>Computed against model $Y=Mean(Y)$</i>				-	-

Table F.2. Analysis of variance of Variable a* for color measurement of mushroom

Source	DF	Sum of squares	Mean squares	F	Pr > F
Model	2	4.210	2.105	1.400	0.317
Error	6	9.020	1.503	-	-
Corrected Total	8	13.231	-	-	-
<i>Computed against model $Y=Mean(Y)$</i>					

Table F.3. Analysis of variance of Variable b* for color measurement of mushroom

Source	DF	Sum of squares	Mean squares	F	Pr > F
Model	2	13.716	6.858	1.360	0.326
Error	6	30.259	5.043	-	-
Corrected Total	8	43.975	-	-	-
<i>Computed against model $Y=Mean(Y)$</i>				-	-

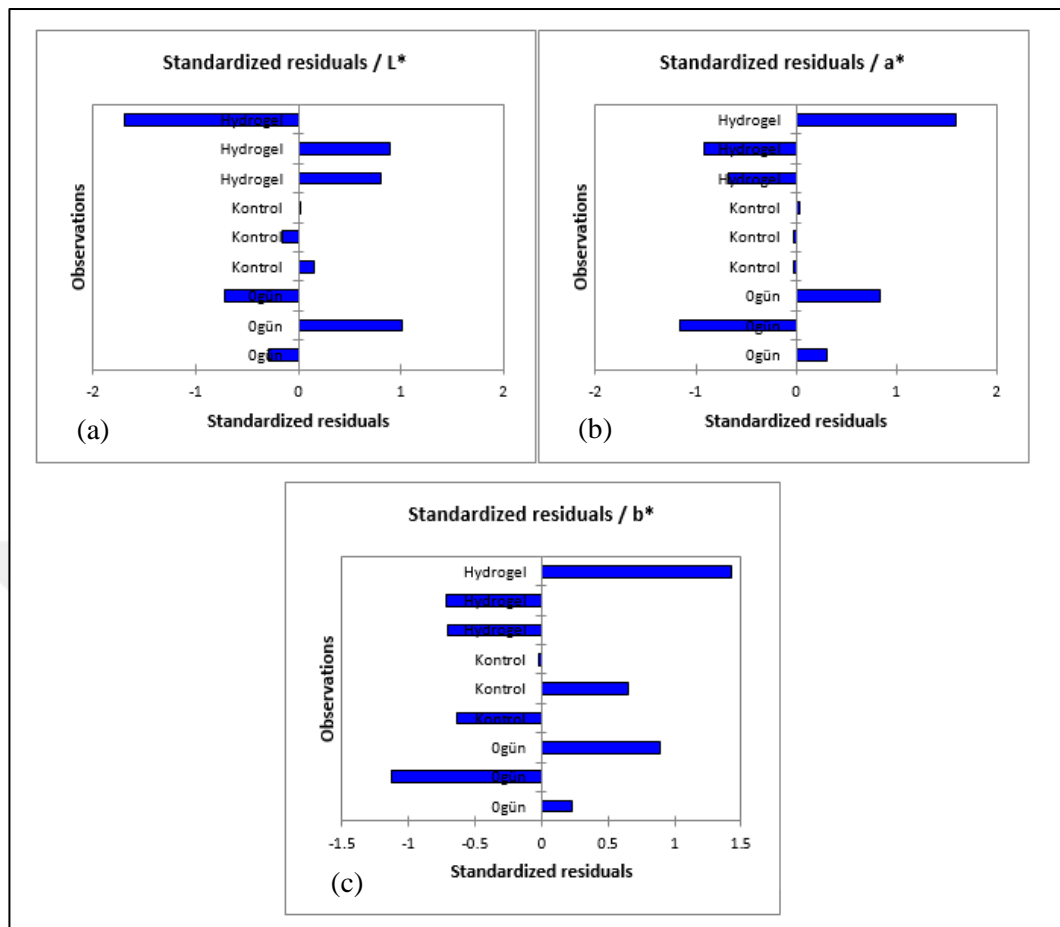


Figure F.1. Standardized residual of (a) Variable L*, (b) Variable a*, (c) Variable b* of mushroom

Table F.4. Q1 / Tukey (HSD) / Analysis of the differences between the categories with a confidence interval of 95% for Variable L* of mushroom

Category	LS means	Standard error	Lower bound (95%)	Upper bound (95%)	Groups
Hydrogel	89.753	1.125	86.999	92.508	A
Initial	89.717	1.125	86.962	92.471	A
Control	87.307	1.125	84.552	90.061	A

Table F.5. Q1 / Tukey (HSD) / Analysis of the differences between the categories with a confidence interval of 95% for Variable a* of mushroom

Category	LS means	Standard error	Lower bound (95%)	Upper bound (95%)	Groups
Control	3.043	0.708	1.311	4.776	A
Hydrogel	1.967	0.708	0.234	3.699	A
Initial	1.393	0.708	-0.339	3.126	A

Table F.6. Q1 / Tukey (HSD) / Analysis of the differences between the categories with a confidence interval of 95% for Variable b* of mushroom

Category	LS means	Standard error	Lower bound (95%)	Upper bound (95%)	Groups
Control	16.893	1.297	13.720	20.067	A
Hydrogel	15.517	1.297	12.343	18.690	A
Initial	13.873	1.297	10.700	17.047	A

Table F.7. Analysis of variance of Variable L* for color measurement of broccoli

Source	DF	Sum of squares	Mean squares	F	Pr > F
Model	2	47.185	23.592	5.362	0.046
Error	6	26.400	4.400	-	-
Corrected Total	8	73.585	-	-	-
<i>Computed against model $Y = \text{Mean}(Y)$</i>				-	-

Table F.8. Analysis of variance of Variable a* for color measurement of broccoli

Source	DF	Sum of squares	Mean squares	F	Pr > F
Model	2	26.191	13.096	3.554	0.096
Error	6	22.112	3.685	-	-
Corrected Total	8	48.303	-	-	-
<i>Computed against model $Y=Mean(Y)$</i>				-	-

Table F.9. Analysis of variance of Variable b* for color measurement of broccoli

Source	DF	Sum of squares	Mean squares	F	Pr > F
Model	2	50.305	25.153	2.241	0.188
Error	6	67.354	11.226	-	-
Corrected Total	8	117.659	-	-	-
<i>Computed against model $Y=Mean(Y)$</i>				-	-

Table F.10. Q1 / Tukey (HSD) / Analysis of the differences between the categories with a confidence interval of 95% for Variable L* of broccoli

Category	LS means	Standard error	Lower bound (95%)	Upper bound (95%)	Groups	
Hydrogel	40.073	1.211	37.109	43.038	A	-
Control	38.790	1.211	35.826	41.754	A	B
Initial	34.703	1.211	31.739	37.668	-	B

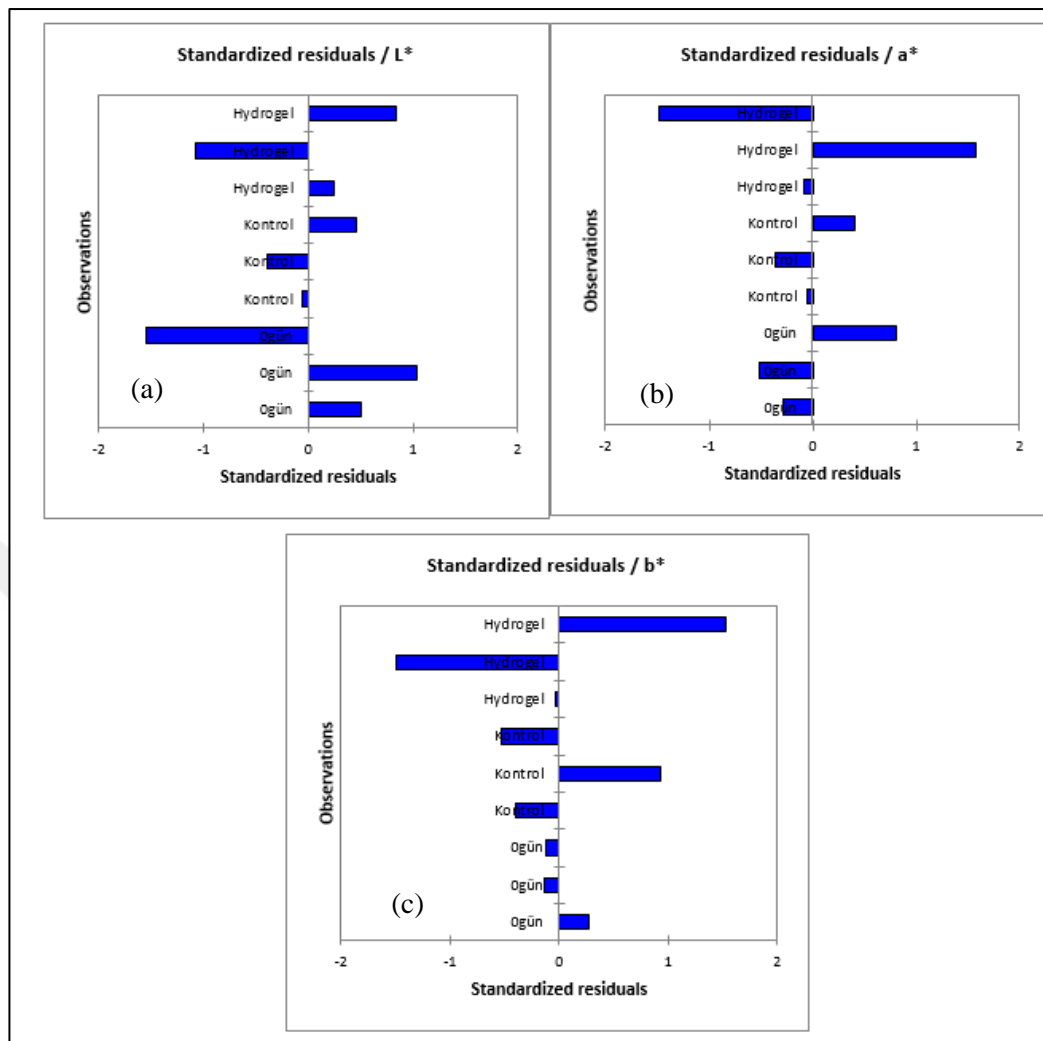


Figure E.2. Standardized residual of (a) Variable L^* , (b) Variable a^* , (c) Variable b^* of broccoli

Table F.11. Q1 / Tukey (HSD) / Analysis of the differences between the categories with a confidence interval of 95% for Variable a^* of broccoli

Category	LS means	Standard error	Lower bound (95%)	Upper bound (95%)	Groups
Initial	-4.437	1.108	-7.149	-1.724	A
Hydrogel	-7.650	1.108	-10.363	-4.937	A
Control	-8.357	1.108	-11.069	-5.644	A

Table F.12. Q1 / Tukey (HSD) / Analysis of the differences between the categories with a confidence interval of 95% for Variable b* of broccoli

Category	LS means	Standard error	Lower bound (95%)	Upper bound (95%)	Groups
Control	16.597	1.934	11.862	21.331	A
Hydrogel	14.500	1.934	9.765	19.235	A
Initial	10.873	1.934	6.139	15.608	A



APPENDIX F: STATISTICAL ANALYSIS RESULTS FOR MICROBIOLOGICAL ANALYSIS

Table G.1. Analysis of variance of TBC for mushroom

Source	DF	Sum of squares	Mean squares	F	Pr > F
Model	2	1.004	0.502	1.918	0.227
Error	6	1.570	0.262	-	-
Corrected Total	8	2.574	-	-	-
<i>Computed against model $Y=Mean(Y)$</i>				-	-

Table G.2. Analysis of variance of yeast for mushroom

Source	DF	Sum of squares	Mean squares	F	Pr > F
Model	2	1.408	0.704	14.031	0.005
Error	6	0.301	0.050	-	-
Corrected Total	8	1.709	-	-	-
<i>Computed against model $Y=Mean(Y)$</i>				-	-

Table G.3. Analysis of variance of mold for mushroom

Source	DF	Sum of squares	Mean squares	F	Pr > F
Model	2	0.162	0.081	0.133	0.878
Error	6	3.654	0.609	-	-
Corrected Total	8	3.815	-	-	-
<i>Computed against model $Y=Mean(Y)$</i>				-	-

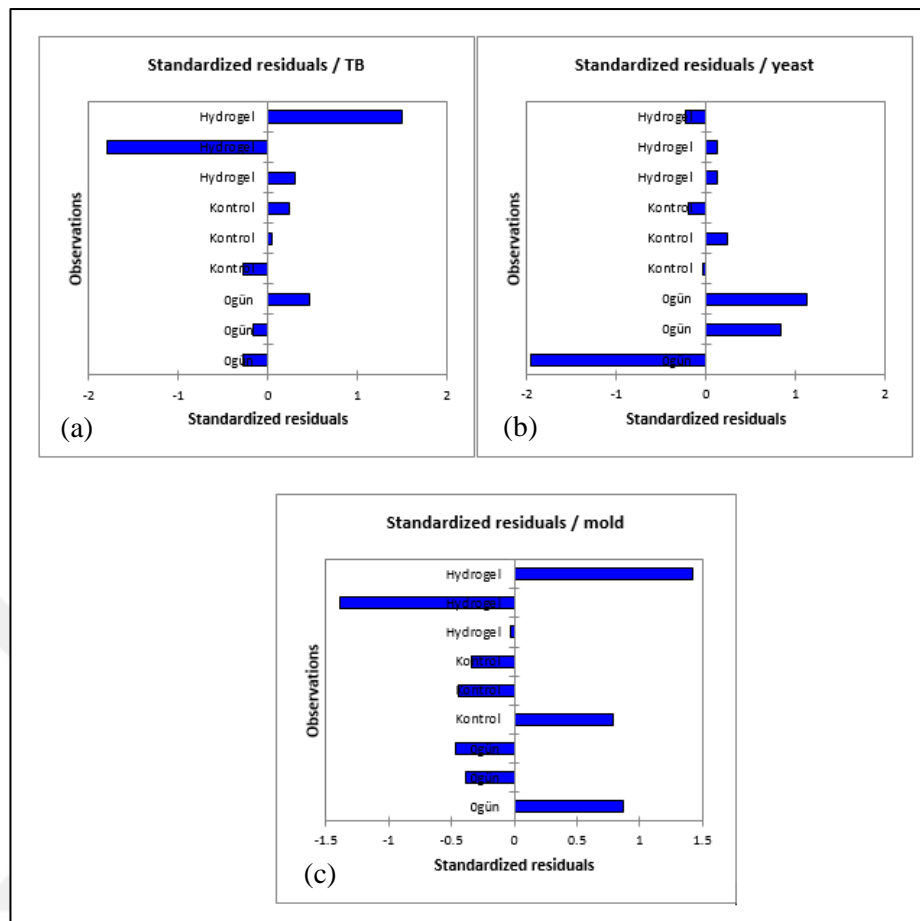


Figure G.1. Standardized residual of (a) TBC, (b) yeast, (c) mold of mushroom

Table G.4. Q1 / Tukey (HSD) / Analysis of the differences between the categories with a confidence interval of 95% for TBC of mushroom

Category	LS means	Standard error	Lower bound (95%)	Upper bound (95%)	Groups
Control	6.921	0.295	6.198	7.644	A
Hydrogel	6.350	0.295	5.627	7.073	A
Initial	6.128	0.295	5.406	6.851	A

Table G.5. Q1 / Tukey (HSD) / Analysis of the differences between the categories with a confidence interval of 95% for yeast of mushroom

Category	LS means	Standard error	Lower bound (95%)	Upper bound (95%)	Groups	
Control	6.883	0.129	6.566	7.199	A	
Initial	6.291	0.129	5.974	6.607	-	B
Hydrogel	5.923	0.129	5.606	6.239	-	B

Table G.6. Q1 / Tukey (HSD) / Analysis of the differences between the categories with a confidence interval of 95% for mold of mushroom

Category	LS means	Standard error	Lower bound (95%)	Upper bound (95%)	Groups
Control	4.686	0.451	3.583	5.789	A
Initial	4.648	0.451	3.545	5.751	A
Hydrogel	4.385	0.451	3.282	5.487	A

Table G.7. Analysis of variance of TBC for broccoli

Source	DF	Sum of squares	Mean squares	F	Pr > F
Model	2	2.192	1.096	6.721	0.029
Error	6	0.979	0.163	-	-
Corrected Total	8	3.171	-	-	-
<i>Computed against model $Y = \text{Mean}(Y)$</i>				-	-

Table G.8. Analysis of variance of yeast for broccoli

Source	DF	Sum of squares	Mean squares	F	Pr > F
Model	2	0.147	0.074	0.306	0.747
Error	6	1.444	0.241	-	-
Corrected Total	8	1.592	-	-	-
<i>Computed against model $Y=Mean(Y)$</i>				-	-

Table G.9. Analysis of variance of mold for broccoli

Source	DF	Sum of squares	Mean squares	F	Pr > F
Model	2	0.504	0.252	1.354	0.327
Error	6	1.117	0.186	-	-
Corrected Total	8	1.622	-	-	-
<i>Computed against model $Y=Mean(Y)$</i>				-	-

Table G.10. Q1 / Tukey (HSD) / Analysis of the differences between the categories with a confidence interval of 95% for TBC of broccoli

Category	LS means	Standard error	Lower bound (95%)	Upper bound (95%)	Groups	
Control	7.737	0.233	7.167	8.308	A	-
Hydrogel	6.825	0.233	6.254	7.396	A	B
Initial	6.594	0.233	6.023	7.165	-	B

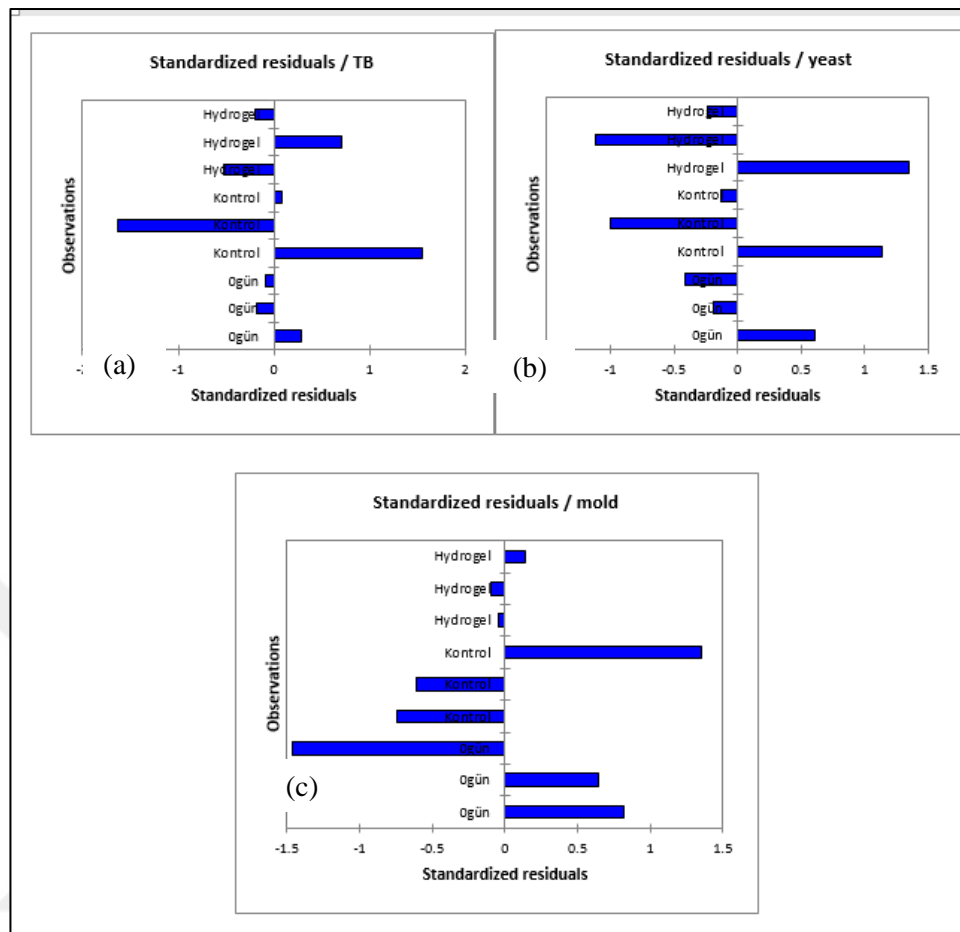


Figure G.2. Standardized residual of (a) TBC, (b) yeast, (c) mold of broccoli

Table G.11. Q1 / Tukey (HSD) / Analysis of the differences between the categories with a confidence interval of 95% for yeast of broccoli

Category	LS means	Standard error	Lower bound (95%)	Upper bound (95%)	Groups
Control	6.296	0.283	5.603	6.989	A
Hydrogel	6.054	0.283	5.360	6.747	A
Initial	6.003	0.283	5.310	6.696	A

Table G.12. Q1 / Tukey (HSD) / Analysis of the differences between the categories with a confidence interval of 95% for mold of broccoli

Category	LS means	Standard error	Lower bound (95%)	Upper bound (95%)	Groups
Initial	4.045	0.249	3.435	4.655	A
Hydrogel	3.610	0.249	3.001	4.220	A
Control	3.495	0.249	2.885	4.105	A